UNIVERSITY OF CALIFORNIA
RIVERSIDE

Photo- Responsive Adhesion and De-Adhesion of Polymers and Nanoparticles

A Dissertation submitted in partial satisfaction
of the requirements for the degree of

Doctor of Philosophy

in

Bioengineering

by

Seyed Hossein Mostafavi

December 2019

Dissertation Committee:
Dr. Christopher J Bardeen, Chairperson
Dr. Victor Rodgers
Dr. Valentine Vullev

The Dissertation of Seyed Hossein Mostafavi is approved:

_____

_____

_____

Committee Chairperson

University of California, Riverside

Acknowledgments

I would like to first express gratitude to my advisor, Christopher Bardeen, for his tireless support and supervision. He has taught me not only science and systematic approach for solving problems, but I learn how to be kind and giving.

There were numerous times that I went to his office hopelessly and broken, come out full of hope and motivated. There were multiple times that I expected he give up on me, he supported me even more. There were times that I felt disappointed and he reached out and gave me a reason to continue my path.

Dr Bardeen with any doubts is the greatest scientist I met in my life and for sure one of the kindest one.

Chris, thank you for your all your supports that you offered me. It has been an honor to work and learn with you and I will be forever in your debts.

I need to thank the love of my life, Shabnam. She was with me during the last 7 years, and endured the hardship of being and living with a grad students. She left her family for me and never stopped supporting me in my course works, research and life. she made my life colorful and gave me a reason to be happy all the time. I probably couldn't be at this point of my life without her sacrifices.

Shabnam, it was always an honor for me to be with you and I can not thank you as you deserve.

I cannot thank my beloved father and mother enough. They both worked hard and provided a peaceful environment for my growth and development and I can't remember anytime that they prioritized themselves over me. They both sacrificed whatever they had for me and the only thing that they asked was that I continue my education and become a successful and useful person in my life. I wish my father was with us at this moment of life and could see my graduation and I wish my mother could attend my defense.
Mom, I didn't see anyone as kind as you are in my whole life. I love you and I will love you forever.

I also want to thank Mohamad, Ali, Fatemeh. I am always thankful to have the loveliest siblings.
You are always having a special place in my heart.

I need to specially thank Dr. Kerry Hanson and all other mentors, lab mates and students that helped me on this journey.

تشکر میکنم از پدر عزیزم که علاقه به علم اندوزی را در دلم گذاشت، از مادر فداکارم که با مهربانی و دلسوزی همیشگی انسانیت را به من آموخت و همسر خوش قلبم که چون یار کنارم ایستاد و حمایتم کرد. از

فاطمه مهربان، علی پر تلاش و محمد خوش فکر تشکر میکنم که همیشه محبتشان را نثارم کردند.

Acknowledgement of Previously Published Material

1: Mostafavi, Seyed Hossein, et al. "Photoinduced Deadhesion of a Polymer Film Using a Photochromic Donor–Acceptor Stenhouse Adduct." Macromolecules 52.16 (2019): 6311-6317.

2: Mostafavi, Seyed Hossein, et al. "Noncovalent Photochromic Polymer Adhesion." Macromolecules 51.6 (2018): 2388-2394.

ABSTRACT OF THE DISSERTATION

Photo- Responsive Adhesion and De-Adhesion of Polymers and Nanoparticles

by

Seyed Hossein Mostafavi

Doctor of Philosophy, Graduate Program in Bioengineering
University of California, Riverside, December 2019
Dr. Christopher Bardeen, Chairperson

Photochromic behavior is not a new concept in chemistry and was mentioned for the first time in literature more than a century ago. This dissertation focused on using photochromic molecules to innovate and develop methods to remotely modify adhesion of thin films to substrates. We explored both photo-induced covalent and non-covalent adhesion.

To induce non-covalent adhesion, we hypothesized that if photochromic molecules embedded in a polymer were exposed to light, this could change the properties of the molecule which might lead to the change of polymer adhesion to substrate. We investigated

the effect of ultraviolet (UV) and visible light exposure on the adhesion of polystyrene (**PS**) for a range of photochromic molecules such as, donor-acceptor Stenhouse adducts (**DASA**), diarylethene derivatives (**DAE**) and spiropyrans (**SP**) to glass substrate. We utilized adhesion measurement methods like water detachment, pull-off and the lap shear tests, which were used to detect the increase and decrease of adhesion to the glass surface after light exposure. We also investigated the effects of photochrome concentration, light wavelength, substrate properties, and polymer structure on adhesion and de-adhesion.

The innovative part of our final project was to engineer multi-functional nanoparticles and substrates with light-switchable covalent adhesion. Nanoparticles with surface-bound anthracene (**AN**) were able to undergo [4+4] photocycloaddition reactions to form covalent adhesion. In theory this reaction could help nanoparticles to selectively assemble and make a predesigned structure after being activated by light. Our results demonstrated that under ultraviolet (365 nm) illumination, both unimolecular and bimolecular photochemical reactions led to the loss of surface-bound **AN** absorbance. These competing reaction pathways decreased the efficiency of the cross-linking dimerization reaction.

Table of Contents

Table of Figures

Table of Tables

1- Chapter 1 Introduction

1-1 Motivation

For centuries nature has been using light as a source of energy. Some plants, organisms, and cells directly respond to light, and as a response they change their shape and properties. In the human body, exposure to light releases enzymes and initiates biological pathways. Observing these light sensitive motions in nature has inspired scientists, to mimic them and fully control the various processes using optical stimulus. Remote control of processes is not the only benefit of lights; light can also be highly selective, cheap to use, produces no chemical contamination or mechanical wear, is harmless to use, and is more precise than mechanical devises.[1–3].

Inspired by nature, the goal of our group and current research is to enlist light for the sake of humans and particularly we want to engineer light responsive adhesion. We plan to design multi-functional nanoparticles and films with switchable adhesion. Reversible adhesives enable us to temporarily glue two surfaces together and detach them remotely by light irradiation. This technology may be used to protect/deprotect silicon dioxide surfaces in semiconductor manufacturing where residual adhesives must be avoided, or help us to engineer light responsive nail polish as a clean substitute for the current method of removing nail polishes with acetone. Light responsive nanoparticles can assemble and make predesigned structures, perform a task and then be disassembled by another stimulus when their job is finished. This technology is not only beneficial for

making microstructures, but also provides a platform to deliver and release molecules near their target. In drug delivery, nanoparticles can attach to a drug with the first stimulus and release drug molecules into the target with second one. This attachment and release is achieved through light responsive adhesion and can open and close a gate, releasing drugs or other substances (Figure 1-1). In microfluidics, light exposure to these nanoparticles can stop the flow of liquid by light in one direction and force the current to follow another path.

A key feature of this project is to use photochromic molecules. The term "photo chromic material" is used for a molecule that undergo reversible photo stimulated transformation between two different isomers. The unique properties of photochromic molecules encouraged us to take advantage of them to regulate adhesion[4].

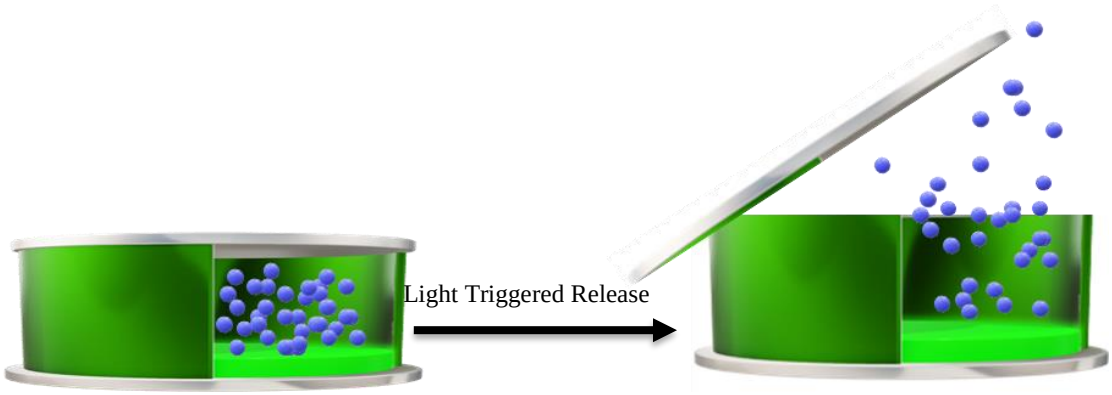

Figure 1- 1: Potential application of photo-triggered light response. The reservoir can encapsulate one or more types of chemical substance. Opening and closing the gate sealed with a light responsive polymer release a controlled amount of drug into the external media

1-2 Photochromic molecules:

Photochromic behavior was first reported by Fritsche in year 1867 when he noticed sunlight exposure can bleach tetracene and lack of exposure will reverse the reaction. [5]

Later, in 1899, Markwald observed the reversible color change of 2,3,4,4-tetrachloronapthalen-1(4H)-one 2 in the solid state and in 1950, Hirshberg invented the term photochromism [originated from two Greek words: "phos" (light) and "chroma" (color)], which, from that date forward, used to describe this process[6,7]. During this procedure some properties of the molecule including: absorbance spectra, fluorescence emission, electron conductivity, refractive index, geometrical structure, volume, *etc*. might significantly change. And more interestingly, these properties are able to switch back again to the initial status by irradiating with different wavelengths of lights or by increasing the temperature. Although photochromism itself is a non-destructive reaction, loss of performances occurs over repeated cycles due to side reactions, including oxidation, which can cause chemical degradation.[8–11] In the 1980s there were discoveries of new photochromic molecules that showed high resistance to these degradation process. These molecules include dchromenes, diarylethenes, and spirooxazines, and their resilience was the reason several commercial applications were developed, including optical filters, optical recording and photochromic lenses.[11,12] Some of the photo chromic compounds are illustrated in Figure 1-2:

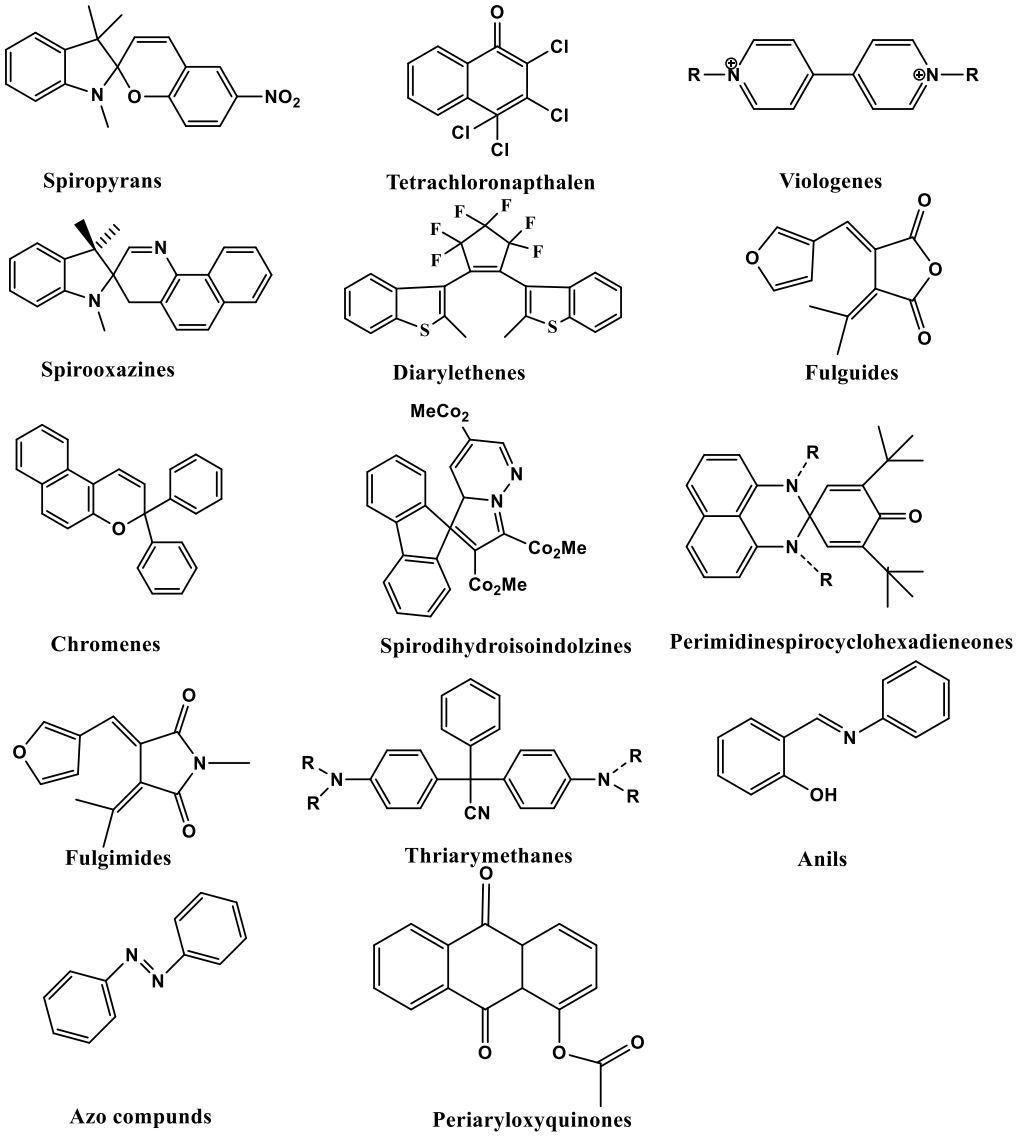

Figure 1- 2: Illustration of some photochromic molecules that undergoes photo-switching by light irradiation[11]

1-3 Different types of photochromism:

Molecular photo-switch reactions are reversible transformations and, based on the type of stimulus that induces back the reaction, they can be categorized into two classes[13]:

1-3-1 Classification based on types of reversibility stimulant:

1-3-1-1 Type P photochromism:

This kind can be switched in both (forward and backward) directions with different wavelengths of light. In P-type photochromes, the color change can be observed after irradiation with a specific wavelength of light, and it will not go back even after removal of the light. The return process initiates after irradiation with another wavelength of light.[11]

1-3-1-2 Type T photochromism:

In contrast to type P, light is only able to drive the reaction in one direction in T-type photochromes. These photochromic molecules will go back to their original state, by a thermal stimulus, after removing the light.[11]

Reversibility of response is a very important aspect of photochromes and we cannot describe light-sensitive materials that do not undergo a back reaction as photochromic.
Photochromic systems are also divided into two other big classes of molecules based on their color change:

1-3-2 Classification based on types of Color change:

1-3-2-1 Positive photochromes:

In positive photochromes, the original state is colorless and upon light irradiation the absorbance increases. The major problem with these types of molecules is that after light irradiation the formation of color will act as a hinderance for light to penetrate deep into the films and it becomes hard to get to 100% transformation.

1-3-2-2 Negative photochromes:

In contrast, the negative photochromes (inverse or reverse photochrome) initially have color and then their absorption decreases after light irradiation. [11,14,15]

The majority of organic photochromic molecules are positive photochromes.

1-4 Overview of Some Photochromic Molecules:

1-4-1 Spiropyran (SP):

This molecule is one of the most studied among photochromic molecules. it can undergo structural isomerization in response to a range of different stimuli like: light, metal ions, temperature, redox potential, and mechanical stress.

We decided to use this molecule in our experiment since it can isomerize to the Merocyanine (**MC**) form using UV light. **MC** has a strong absorption between 550–600

nm, a deep blue color. The electric dipole moment -which we need for a reversible adhesion- is higher in **MC** (14–18 D) than in **SP** (4–6 D). In our experiments, we made a thin film of polystyrene containing SP. Initially, we investigated The **SP** transformation to **MC** and it's reversibility. In polar solvents and environments like cells, **MC** is the preferred form. In non-polar solvents like hexane, the **SP** form is favored. [14,16–19]

1-4-2 Donor–acceptor Stenhouse adducts

A new class of negative photochromes was introduced in 2014 by Read de Alaniz et al from the University of California, Santa Barbara. They have used the term donor–acceptor Stenhouse adducts (**DASA**s) in recognition of John Stenhouse. The second generation of **DASA**s was developed in 2016. Recently, the 3rd generation has been developed. [8]

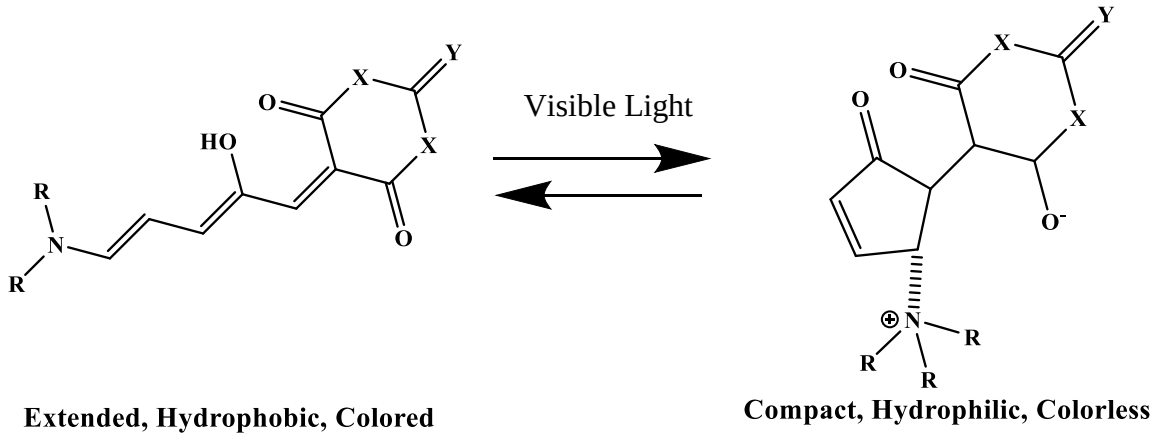

Figure 1- 3: DASA is relatively a new photo switch organic molecule which is a negative photochrome and the molecules volume reduces after light exposure [8]

These molecules initially are colored, conjugated, hydrophobic and extended. After exposure to light they will turn to colorless, ring-closed and hydrophilic zwitterionic structure. These molecules have very high fatigue resistance. These molecules show promising applications in drug release as well. [8,20]

1-4-3 DASA vs Spiropyran

There are few significant differences between spiropyran and **DASA** which we tried to employ to understand different aspects of light induced adhesion and the role of photochromic molecule in increasing and decreasing adhesion.

The most important similarity is that in both molecules the polarity of the molecules increases after light irradiation.

But these molecules have two big differences. 1- The DASA molecule extends after light irradiation; in contrast, SP transforms to a more compact form after light irradiation. 2- DASA is a negative photochrom but SP is positive.

Using these two different photochromes not only helped us to identify and get closer to finding the mechanism of adhesion.

1-5 Substrate:

The substrate plays an important role in adhesion. In general, the surface of the substrate will bond to the deposited film if we have a good adhesion. Thin films (<1um) have been used for variety of purposes like generating resistance to corrosion, erosion, abrasion, tarnish, wear or high temperature oxidation; to reduce electrical resistance,

provide lubrication and so on. The interesting part is that no matter what the application is, the thin films are not functional without proper adhesion to substrate. Thin films structure, and properties have a direct relation to its adhesion to the substrate.[21,22]

1-5-1 Glass Types:

We have used different types of glass slides in these experiments. Glass is non-crystalline and has many applications in industry and science. Silicon dioxide (SiO_2) is a common fundamental constituent of glass. There are two main reasons for the selection of glass. First of all, glass is transparent which makes it a very good substrate for photo modulation of adhesion, and this will enable us to irradiate the polymer- glass interface directly. The surface hydrophilicity of glass can be easily tuned using plasma, piranha wash or extreme heat; also, these substrates are very cheap to use and easily cut in to any shapes that we need.

Contact angle measurements show that after piranha wash, the wettability of glass increases, which indicates that washing does indeed make the SiO_2 surfaces more hydrophilic by the formation of silanols. Upon heating (over 150º C), there is a steady decrease in the wettability of a glass surface, which is an indication of surface dehydration (evaporation and condensation of silanol groups). The loss of water occurs gradually to give a surface that is relatively hydrophobic.[23]

We have used three types of glass slides in our experiments.

1-5-1-1 Quartz:

Quarts is almost pure silica (99%, SiO_2). It has very low thermal expansion, it is very hard and relatively expensive compare to other types of glass.[24]

1-5-1-2 Soda-lime-silica glass:

The most common commercial glass in industry is soda-lime-silica glass. It is cheaper than other kinds of glasses and easy to recycle. The main compositions of soda-lime glass is 70–75 wt% Silica (SiO_2), 12–16 wt% Sodium Oxide (Na_2O), and 10–15 wt% lime (CaO) .[24]

1-5-1-3 Borosilicate Glass:

Borosilicate glass contains 8% wt boron oxide (B_2O_3). Borosilicate glass is composed of 70–80 wt% Silica (SiO_2), 7–13 wt% of Borosilicate B_2O_3 4–8 wt% Sodium oxide (Na_2O) or K_2O, and 2–8 wt% of Aluminum oxide (Al_2O_3).[24]

1-6 Adhesion, Adhesion Technology and Definitions

Humankind has been using different types of materials for gluing two different surfaces together for centuries. Scientists felt the need for improving this technology significantly after the 1940s because synthetic polymer technology developed significantly in this decade and adhesion was a requirement for almost every application of these polymers. Although decades of research and development have passed, and scientists

invented many solutions in response to industry desires, there is still room for developments like adhesion in wet conditions and remotely controlled adhesion modulation. [25]

1-6-1 Adhesion bonding and mechanical properties:

Adhesion is any form of attraction between unlike molecular species that have been connected directly, such as interactions between thin films and substrates. The work of adhesion is the energy required to separate unit areas of two different surfaces. The term cohesion is the attraction between two identical materials. The adhesion between two surfaces can originate from intermolecular or mechanical forces, or both. These interactions can be repulsive or attractive, and their range of action and magnitude can vary based on the operating forces between two surfaces, which depends on the nature of the interacting surfaces and medium between them. The strength of the adhesion between two materials depends on the interactions between the two materials and the surface area over which the two materials are in contact.

1-6-2 Types of Adhesion:

There are 5 proposed mechanism for adhesion:

1-6-2-1 Mechanical interlocking:

Mechanical interlocking happens when the adhesive flows into substrate pores and irregularities. A very good example of this kind of adhesion is filling pores of teeth using mercury amalgam. In order to develop strong mechanical adhesion, special surface treatment is needed.

1-6-2-2 Diffusion theory:

When we have 2 types of polymers that can diffuse into each other, we will have an adhesion based on diffusion.

1-6-2-3 Electrostatic adhesion:

Differences in electrical charge may result in another type of adhesion that is called electrostatic adhesion. This mechanism is the most reversible type of adhesion mechanism. Also, in many cases, we can remotely increase and decrease electrical charge and induce adhesion.

1-6-2-4 Dispersive adhesion:

The main force in this type of adhesion is van der Waals forces, and it happens when two surfaces have induced polarization.

1-6-2-5 Chemical adhesion:

Substrate and adhesives may form a chemical bond. Ionic bonds and covalent bonds make the strongest adhesion. The hydrogen bond is in the next level in case of strength.

Chemical bonds make a very strong adhesion, but these forces are only effective when distances between two surfaces is less than a quarter of nanometer (Figure 1-4).[26] The key types of intermolecular and surface forces are listed in Table 1-1

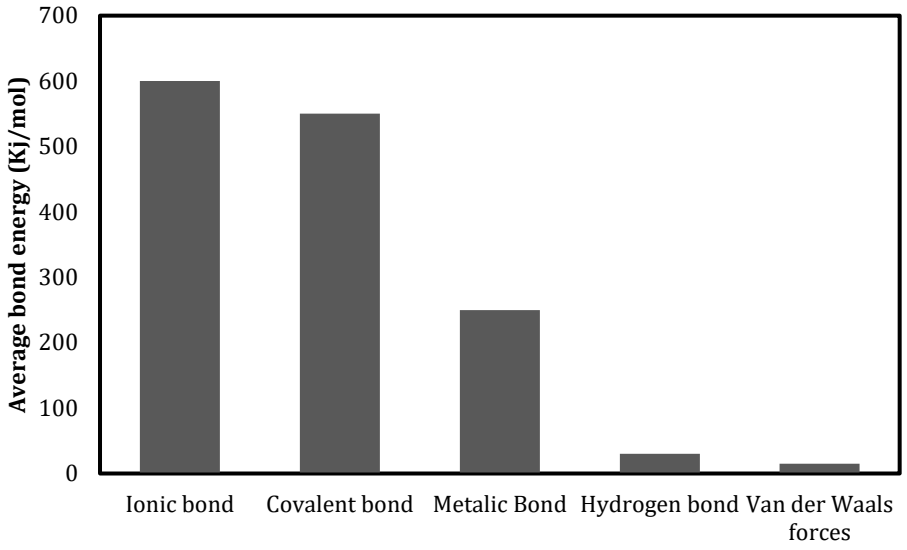

Figure 1- 4: The strength of chemical adhesive interactions.[26]

Table 1- 1: **Different types of adhesion forces and their main features are listed in this table.**[27]

Type of interactions		Main features
Intermolecular forces	Dispersive	Weak interactions /dispersion forces A force existing between all bodies. Usually attractive and can be repulsive.
	Electrostatic	Dipole-dipole, Ion dipole or hydrogen bonds
	Chemical	Ionic and covalent interactions
Mechanical Forces	Mechanical	Films fill the voids or pores of the surfaces /interlocking.
	Diffusive	Merge or intermingle at the bonding interface by diffusion

1-6-3 Effect of surface conditions on adhesion:

Requirements to generate an ideal adhesion will be explained below:

1-6-3-1 Clean surfaces:

Many factors, including surface roughness, contamination, and applied force on both surfaces can alter adhesion. For instance, dust particles severely decrease adhesion by stopping a direct contact between the surfaces, so washing a substrate properly is a critical step in forming a strong adhesive bond.[28,29] Williamson et al in their studies on the effect of contamination and roughness on adhesion, proposed that if the dust particles are larger than the surface roughness, then the adhesion will be reduced; otherwise, the dust has small effect on adhesion. Adhesion also depends upon the vapor density in the nearby environments. So, it is important to control the surface and environment to reach the preferred results.[24,29–32]

In order to have an effective adhesion, a clean surface is necessary. Some chemical groups such as –OH, –SH, –COOH, and $–NH_2$ will increase wettability of surface, and washing the surface is the first step to expose these groups. Contamination of surface is one important reason for malfunction of adhesion, and cleaning processes minimize this effect. In our experiment, we used piranha solution for cleaning the surface.[33–35]

1-6-3-2 Adhesion and roughness

Surface roughness is one of the most important factors in developing adhesion between two unlike surfaces. In general, for elastic surfaces, the roughness and adhesion are inversely related.[29,36–39] The reduction of adhesion in rough surfaces is mainly because roughness in elastic surfaces reduces the likelihood of intimate contact between the surfaces. [25,40]

1-6-3-3 Proper contact angle and good wetting

For developing an adhesion system, we need to have knowledge of surface and interfaces. To have strong adhesion, the adhesive should be able to wet the substrate. For measuring the wettability, an internal angle of a droplet of liquid on substrate will be calculated. This method is called contact angle measurement. For a solid and liquid at fixed temperature and pressure, there is always an equilibrium in contact angle. Measuring the contact angle between a liquid drop and solid surface is one of the easiest ways to find the wettability of a surface. This angle is affected by properties of both surfaces (solid and liquid) and their interactions, pressure, temperature and surface roughness. [39] Figure 1-5 shows 3 different type of contact angle.

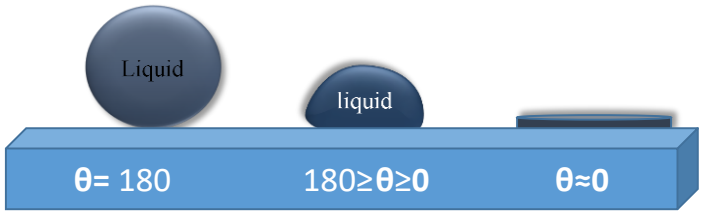

Figure 1- 5: On super hydrophobic surfaces θ is close to 180º. When water spreads on a surface, it means that surface is super hydrophobic and θ will be close to zero. In most cases the θ is between 0 and 180.

In this study, contact angles of the polymer films were measured using a Kruss DO4010 Easy drop instrument. When θ is about zero, it means that the liquid wets the surface and spreads on it. On the other hand, no wetting will occur at θ= 180º .

1-6-3-4 Low viscosity adhesives and adequate flow

Another factor that we need to consider is the viscosity of adhesive. The adhesive should be able to flow on surface and cover it. In mechanical interlocution, the adhesive should flow inside the pores and fill that up.[41]

1-6-3-5 Air entrapment:

Studies of the interfaces of glass and adhesive using optical microscopy reveals that there is a layer of air between them. As temperature rises this air will find a way into the adhesive and be trapped there as bubbles. A complete depletion of entrapped air will happen when we have zero contact angle or liquefy the adhesive during heat cure.[42]

1-6-4 Adhesion measurement:

As it discussed before, an adhesion forms when two different materials stick together, so we can define the adhesion measurement as the force needed to separate them.

1-6-4-1 Methods for characterization:

The methods of measurement of thin film adhesion can be categorized in several ways:

1) Qualitative and quantitative methods.

2) Destructive and non-destructive methods.

3) Mechanical and non-mechanical methods.

Adhesion measurement method can be categorized into two different classes:

1-6-4-1-1 Destructive and non-destructive measurements

Most of the adhesion tests fall into thee destructive group. In these tests, force is applied to the coated films and then the percent of damage is detected or observed. Adhesion can also be measured by applying a pulse of energy to the substrate/coating class, after which a loading force is applied to the coating in some specified manner and the resulting damage subsequently observed. Nondestructive methods includes observation, tap test, ultrasonic testing, x ray test and Infrared Thermography.

1-6-4-2 Mechanical method for adhesion measurement:

All mechanical methods are destructive, and this means that we need to destroy the thin films in order to measure adhesion. Mechanical methods can be classified into two different typed:

a) Methods that measure detachment normal to surface
b) Methods that measure detachment lateral to interface

1-6-4-2-1 Scotch tape:

This method is a qualitative method and works by pressing a scotch tape to the film and then stripping it in an abrupt move, and in the process, three things might happen: 1- The film completely detaches 2- The film partially detaches 3- The film stays attached.

The advantages of this methods are:

1- This test is reasonably low-cost.
2- This test can be executed very quickly and easily.
3- This method is able to provide valuable data for exploratory research.

This method has some disadvantages, such as:

1- It’s highly qualitative, and unfortunately, it does not provide any numbers to compare results.

2- The results depend on many factors, such as the type of tape the pressure, and strength of interaction of tape and thin films
3- It is only applicable when the adhesion between substrate and film is less than the film and tape

1-6-4-2-2 Lap Shear Test:

The lap shear test is a method to measure stresses across the bond area. There are some different types of shear tests, including Single lap, Double lap, Double-sided bonded and single sided bonded. In our experiments, we have used the single lap test to compare adhesion between various surfaces. This measurement was done using Instron instrument and the instrument report the results in Newton. This test measures lateral force that need to break the adhesion.

1-6-4-2-3 Water Detachment:

This method was developed and used for the first time in our group. This method is cheap and easy to perform and can provide a reliable method for comparing adhesion. In this method, we monitor delamination of a polymer in the presence of water over time. We will go over this method thoroughly in next chapter.[44]

1-6-4-2-4 Pull-off adhesion test:

This method is based on gluing together two surfaces (one can be a pulling device) using the adhesive. In this method, the amount of force required to break the adhesion was applied perpendicular to the film. This test was performed by using the photochrome/polymer mixture as glue and attaching one microscopic slide as a bridge to two other slides. Adhesion was measured by adding weights incrementally on the bridging slide until the adhesion failed.

1-6-5 Remotely-Modified Adhesion

Photo-induced adhesion and de-adhesion have attracted much attention recently, and many scientists are working to develop this technology. [45]

1-6-5-1 Reversible Adhesion

The importance of adhesion was discussed widely in this report. However, in many situations, we need to remotely modify adhesion. Remote modification refers to reducing/increasing adhesion without physical contact. Some remotely induced adhesives are sensitive to temperature [46] and pressure[47], but the majority of remotely induced adhesives are light sensitive. Light is the best resource to utilize for adhesion modification. Unlike the methods described in this thesis, previous methods of light-controlled adhesion are very time consuming and hard to achieve because they require either (a) specially designed custom polymers, or (b) chemically modified glass surfaces. Gelmi et al. explored

the reversible adhesion of a chemically activated AFM tip with fibronectin and a spiropyran-modified surface, and they found that UV irradiation can potentially change the adhesion. [48] Blass et al. similarly used modified AFM tip to measure switchable adhesion but instead, they used β-cyclodextrin functionalized surfaces and Azobenzene functionalized AFM tip.[49]

Kaiser et al, used anthracene derivatives to switch adhesion on and off. UV light induced dimerization of anthracene between two surfaces and heat, reversing this reaction.[50] Trying to develop photo-induced de-adhesion, Asadirad et al. used a Diels–Alder reaction to produce diarylethene by dithienylfuran and maleimide monomers. This polymer showed a reversible adhesion after UV irradiation and visible light exposure. [51]

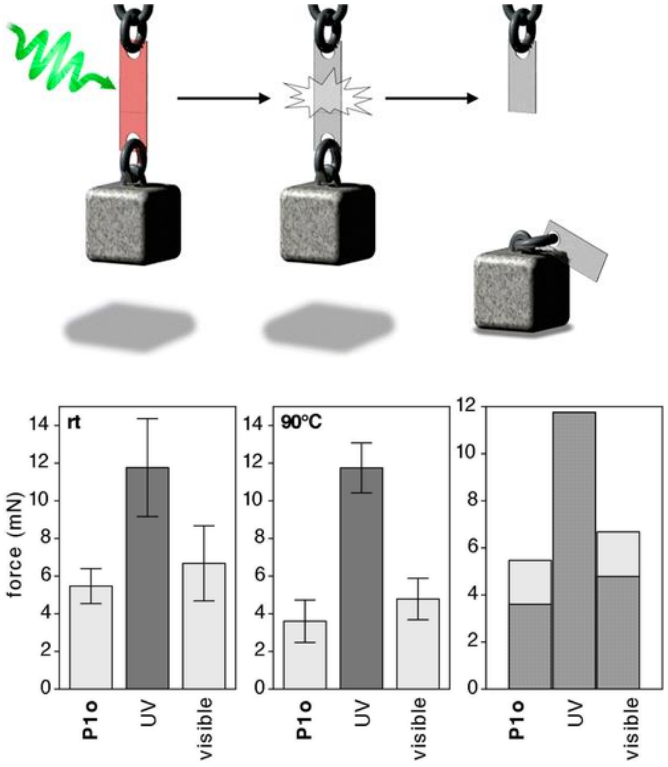

Figure 1- 6: a) Photo-induced de-adhesion; b) Shear test when two strips of synthesized polymer are glued together. UV irradiation was 312 nm for 5 minutes and visible light was 435 nm for 2 hours. The first figure (left) is at room temperature and the second figure (middle) is at 90 °C and the third figure (right) is the difference between 23 and 90 °C. [51]

Saito et al. designed a light-induced reversible adhesive by using liquid crystal compounds in the structure of their adhesives. These developed materials melt-down upon UV irradiation.[52]

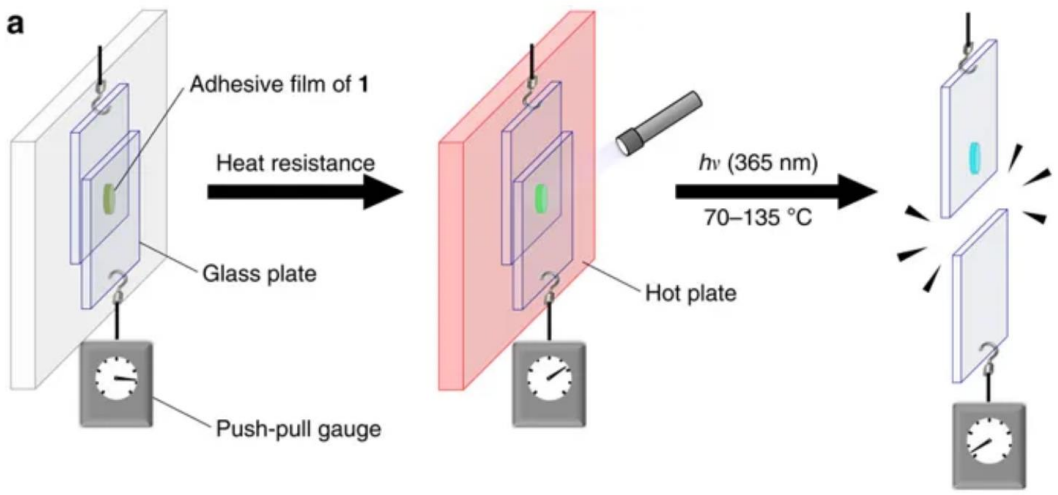

Figure 1- 7: Photo-induced deadhesion of 2 glass substrate[52]

Sasaki et al. developed a light-detachable adhesive by utilizing a photo-depolymerizable cross-linked polyolefin sulfone. Thermal curing the polymer will increase the adhesion of two quartz plate upto 7 M Pa. Depolymerization induced by UV irradiation ($\lambda = 254$ nm).[54]

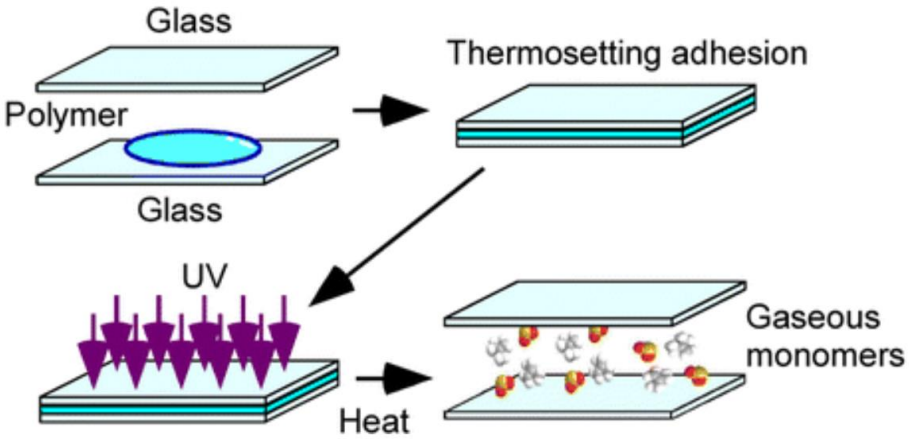

Figure 1- 8: Photoinduced depolymerization of poly(olefin sulfone)s.[54]

Different sources of irradiation have been used to induce adhesion; among them, UV-induced adhesions have attracted the most attention, and their sales in the market are expected to increase up to $1.2 billion by 2021 (report published by MarketsandMarkets). Light-induced adhesion has advantages when compared to temperature-induced adhesion, including rapid curing, room temperature experimentation, being environmentally friendly, and being a solvent-free, which all make it a perfect candidate for adhesions. However, there are some problems that come with light-induced adhesion. The substrate have to be transparent, otherwise light will not penetrate the polymer and adhesion may not form efficiently. When the sample is thick, the same problem may occur as well. To avoid this problem, most light-induced adhesion occurs at the surface of the polymer. For instance, extensive studies were conducted, and different methods were developed to increase light-

induced cell adhesion on chemically modified surfaces. Higuchi et al. designed poly (spiropyran-co-methyl methacrylate) membranes to be able to control cell adhesion and de-adhesion to the substrate. After irradiating UV light to A copolymer of nitrobenzospiropyran and methyl methacrylate (poly(NSP-co-MMA)) was used as a material with a photosensitive surface poly (NSP-co-MMA)-coated glass plates, the contact angle dropped and showed light-induced detachment of platelets and mesenchymal stem (KUSA-A1) cells. [53]

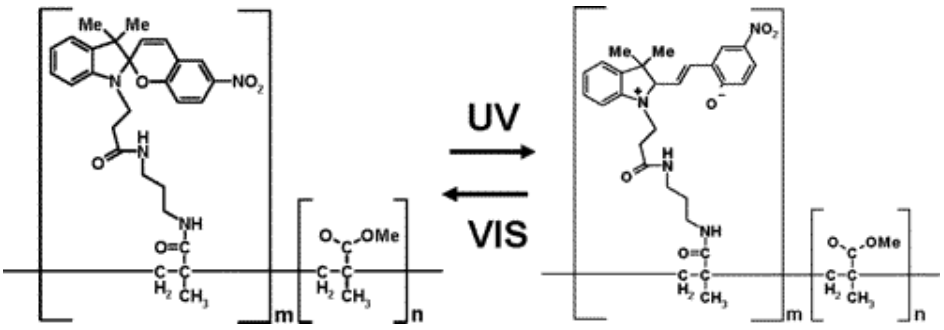

Figure 1- 9: Photo-switch of poly (NSP-co-MMA) UV irradiation. [53]

Tada et al. grafted nitrospirobenzopyran residues into poly(ethylene glycol), and they used it as a photo-responsive cell culture substrate. UV light (350-400 nm) was used , and cell adhesion increased significantly after a 5 minutes irradiation. Cell adhesion was measured by cell growth indicators.[55] In another study, Matsuyama et al. controlled cell adhesion on a surface by irradiating the surface, which was functionalized with a caged arginine-glycine-aspartate (RGD) peptide. [56] A commercially available culture dish was

modified with poly-L-lysine (PLL) to make it photo-responsive by using a bifunctional cross-linked polyethylene glycol (PEG) and the caged RGD peptide. HeLa cells cannot attach to the surface until photolysis occurs through exposure to UV light, which cleaves the nitrobenzyl group and prepares an active location for cells to adhere.

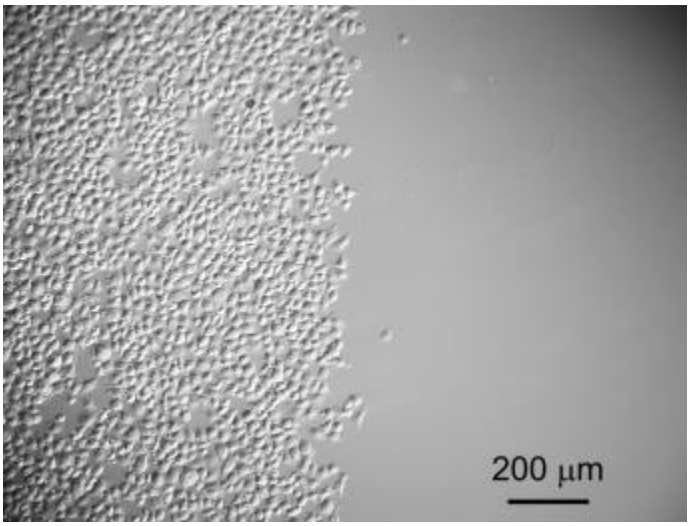

Figure 1- 10: A half-irradiated dish culture functionalized with a nitrobenzyl-substituted tri-peptide (arginine-glycine-aspartate) clearly shows a controlled cell adhesion. [56]

Azobenzene derivatives are widely used photochromic molecules. Linked to these azobenzene derivatives, α-D-mannoside ligands stabilized at the surface can be recognized by proteins on E. coli, and the proteins can be attached to these ligands. Researchers at the University of Frankfurt showed the effect of photoswitching and carbohydrate orientation for cell adhesion on a glycosylated surface. They immobilized azobenzene glycosides on a

gold substrate and formed a photo-switchable, self-assembled monolayer. Photoswitching of azobenzene made the cell attachment unfavorable.[57]

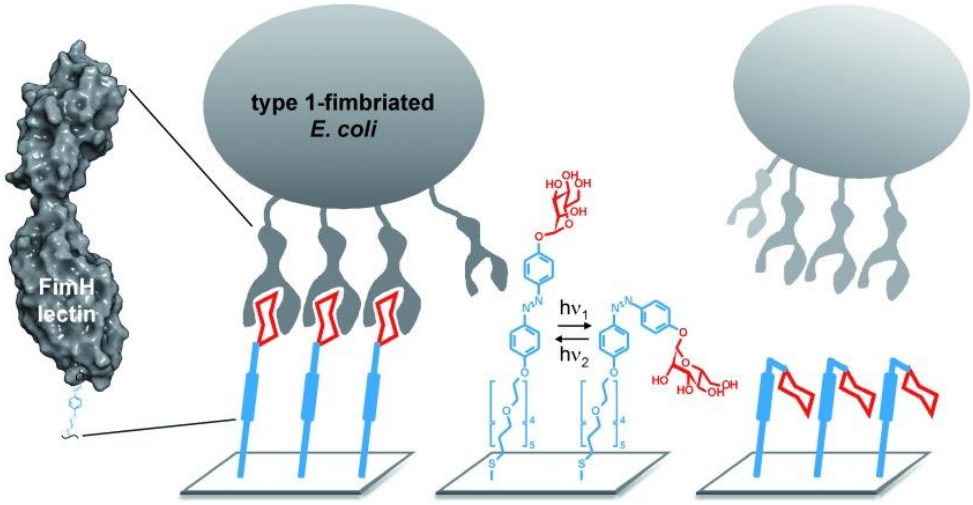

Figure 1- 11: Light exposure will lead to photoswitching of the azobenzene molecules, and E. coli will not be able to attach to the surface. Attachment of Fimbrial tip on E. coli to α-D-mannoside ligands is an indication of adhesion.[57]

1-7 Covalent adhesion

Another strategy to achieve robust reversible adhesion is to form covalent bonds between the adhesive and the substrate. The [4+4] photocycloaddition is a photochemical reaction in which two unsaturated molecules are covalently connected to each other by four atoms from each molecule. Anthracene photo dimerization is one of the earliest [4+4] photocycloaddition reactions, and its kinetics are very well studied. Anthracene can be

dimerized by UV irradiation (figure 1-10). Dimerized anthracene is called dianthracene. The dimerization can be reversed by heat.[58]

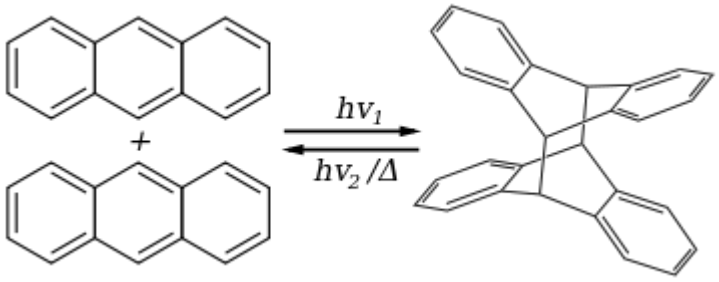

Figure 1- 12: Photo dimerization of Anthracene, The [4+4] Photocycloaddition is a photochemical reaction in which two unsaturated molecules are covalently connected to each other by four atoms from each molecule.

The innovative part of this research is engineering multi-functional nanoparticles and substrates with switchable adhesion. Our plan was to use [4+4] photocycloaddition of anthracenes to selectively assemble nanoparticles via a bimolecular reaction. This technology is not only beneficial for making microstructures, but also it will provide a platform where these particles can deliver and release molecules to the target. In drug delivery, these nanoparticles can attach to a drug upon activation of the first stimuli and then release drug molecules to the target with the second stimuli. In microfluidic devices, these nanoparticles can stop the flow of liquid with light in one direction, force the current to follow in another path for short periods of time, and re-open the blockage in response to heat or visible light. These reconfigurable nano particles (NPs) can move in a certain

direction and stabilize to a functionalized surface when they reach the target and make 3D microstructures.[59–61]

1-8 Project Summary:

The field of photo-induced adhesion is very promising, and adhesion methods still need to improve. In this thesis, we tried to investigate two types of photo-induced adhesion.

The first is non-covalent photo-induced reversible adhesion. We developed an original method to induce adhesion and de-adhesion by light exposure. In this method, we explored whether the photochromic reaction of a molecule embedded in a polymer film can affect its surface adhesion properties by measuring shear strength and delamination in water. The adherence of polystyrene (**PS**) to glass was chosen as a model system. Two commercially available photochromes, a spiropyran (**SP**) derivative 1′, 3′-dihydro-1′, 3′, 3′-trimethyl-6-nitrospiro [2*H*-1-benzopyran-2, 2′-(2*H*)-indole]) (**SP**) and a diarylethene derivative 1,2-bis(2,4-dimethyl-5-phenyl-3-thienyl)-3,3,4,4,5,5-hexafluoro-1-cyclopentene (**DAE**) are studied in detail. Both photochromic reactions can significantly enhance the adhesion of **PS** to a glass surface. The most dramatic results were obtained for **PS/SP** films, whose shear strength increased by a factor of 7 while the delamination rate was suppressed by at least 2 orders of magnitude after exposure to UV light. The enhanced polymer adhesion could only be partially reversed, even after extended exposure to visible light completely regenerated the UV-absorbing isomer. Nanoindentation and heating experiments suggest

that the limited reversibility results from changes in polymer internal structure. We hypothesize that the adhesion changes arise from localized polymer and molecular motions that eliminate void spaces and surface gaps at the polymer-glass interface. The results show that adhesive forces between a prototypical polymer and an inorganic substrate can be modulated by photochromic reactions of embedded molecules.

In the next project a different photochromic reaction, the visible-light induced cyclization of a donor-acceptor Stenhouse adduct (**DASA**) leads to the opposite effect: the de-adhesion of a polystyrene film from a clean glass surface. Measurements of the shear and pull-off adhesion strengths before and after visible irradiation show a light-induced decrease of 20-30%. The time required for delamination in water shows an even more dramatic decrease of 90%. Changes in the water contact angle and other measurements suggest that molecular-level noncovalent interactions between the polymer and glass are weakened after photoisomerization, possibly due to the molecular contraction of the DASA that disrupts the interaction between its amine groups and the surface silanols. The ability to reduce polymer adhesion using visible light enables the controlled release of dye molecules from a glass container, where they have been stored as a dry powder, into an aqueous solution. Embedding photochromic molecules in a polymer can lead to new effects that may have practical applications in stimuli-responsive materials.

In my third project, we have used photoinduced cross-linking based on the [4+4] photocycloaddition reaction to induce covalent adhesion. The goal of this work is to extend this capability to silica nanoparticles using surface-tethered anthracenes (**AN**s) and assess

the cross-linking kinetics. We find that the **AN** attachment leads to multiple fluorescence lifetimes, suggesting that the **AN** molecules experience different environments on the silica surface. Under ultraviolet (365 nm) illumination, the photochemical kinetics can be followed using absorption spectroscopy. Both unimolecular and bimolecular photochemical reactions lead to the loss of surface-bound **AN** absorbance, with the unimolecular decomposition reactions possibly mediated by the triplet excited state. These competing reaction pathways limit the efficiency of the bimolecular cross-linking and in some cases may prevent it altogether. Our results confirm that surface conjugated **AN**s can cross-link silica NPs but also suggest that SiO_2's chemical heterogeneity provides environments that enhance the photodecomposition of surface-bound **AN**. In order to utilize the SiO_2 surface as a robust platform for organic photochemistry to enable photoresponsive nanomaterials, a clearer understanding of its heterogeneous nature and effect on photochemical reactions is required.

1-9 References:

1. Brieke, C., Rohrbach, F., Gottschalk, A., Mayer, G. & Heckel, A. Light-controlled tools. *Angewandte Chemie - International Edition* vol. 51 8446–8476 (2012).

2. Kendrick, Richard E., and G. H. K., Kendrick, R. & Kronenberg, G. *Photomorphogenesis in plants*. (Springer Science & Business Media., 2012).

3. Jewett, M. E. *et al.* Human circadian pacemaker is sensitive to light throughout subjective day without evidence of transients. *Am. J. Physiol. - Regul. Integr. Comp. Physiol.* **273**, (1997).

4. Kinloch, A. *Adhesion and adhesives: science and technology*. (Springer Science & Business Media., 2012).

5. Rawat, M. S. M., Mal, S. & Singh, P. Photochromism in Anils - A Review. *Open Chem. J.* **2**, 7–19 (2015).

6. Yoon, J. & De Silva, A. P. Sterically Hindered Diaryl Benzobis(thiadiazole)s as Effective Photochromic Switches. *Angew. Chemie - Int. Ed.* **54**, 9754–9756 (2015).

7. Periyasamy, A. P., Vikova, M. & Vik, M. A review of photochromism in textiles and its measurement. *Text. Prog.* **49**, 53–136 (2017).

8. Helmy, S. *et al.* Photoswitching using visible light: A new class of organic photochromic molecules. *J. Am. Chem. Soc.* **136**, 8169–8172 (2014).

9. Zhang, J., Zou, Q. & Tian, H. Photochromic materials: More than meets the eye. *Advanced Materials* vol. 25 378–399 (2013).

10. Van Gemert, B. Benzo and Naphthopyrans (Chromenes). *Org. Photochromic Thermochromic Compd.* **1**, 111–140 (2002).

11. Helmy, S. Design and Development of Donor-Acceptor Stenhouse Adducts: A New Visible Light Activated Photochromic Compound. (UC Santa Barbara, 2015).

12. Helmy, S. & Read de Alaniz, J. Photochromic and Thermochromic Heterocycles. *Adv. Heterocycl. Chem.* **117**, 131–177 (2015).

13. Kobatake, S. and Terakawa, Y. Acid-induced photochromic system switching of diarylethene derivatives between P-and T-types. *Chem. Commun.* **17**, 1698–1700 (2007).

14. Khan, N. *et al.* Towards thermally stable cyclophanediene-dihydropyrene photoswitches. *J. Mol. Model.* **21**, 148 (2015).

15. Aiken, S., Edgar, R.J., Gabbutt, C.D., Heron, B.M. and Hobson, P. A. Negatively photochromic organic compounds: Exploring the dark side. *Dye. Pigment.* **149**, 92–121 (2018).

16. Klajn, R. Spiropyran-based dynamic materials. *Chemical Society Reviews* vol. 43 148–184 (2014).

17. Komber, H., Müllers, S., Lombeck, F., Held, A., Walter, M. and Sommer, M. Soluble and stable alternating main-chain merocyanine copolymers through quantitative spiropyran–merocyanine conversion. *Polym. Chem.* **5**, 443–453 (2014).

18. Wohl, C. J. & Kuciauskas, D. Excited-state dynamics of spiropyran-derived merocyanine isomers. *J. Phys. Chem. B* **109**, 22186–22191 (2005).

19. Petriashvili, G., Devadze, L., Zurabishvili, T., Sepashvili, N. and Chubinidze, K. Light controlled drug delivery containers based on spiropyran doped liquid crystal micro spheres. *Biomed. Opt. Express* **7**, 442–447 (2016).

20. García-Iriepa, C. & Marazzi, M. Level of theory and solvent effects on DASA absorption properties prediction: Comparing TD-DFT, CASPT2 and NEVPT2. *Materials (Basel).* **10**, 1025 (2017).

21. Mittal, K. L. Adhesion Measurement of Thin Films. *Electrocompon. Sci. Technol.* **3**, 21–42 (1976).

22. Frey, H. & Khan, H. R. *Handbook of Thin-Film Technology*. *Handbook of Thin-Film Technology* (Springer Berlin Heidelberg, 2015). doi:10.1007/978-3-642-05430-3.

23. Thomas, R., Kaufman, F., … J. K.-J. of T. & 1996, U. Wettability of polished silicon oxide surfaces. *J. Electrochem. Soc.* **143**, 643–648 (1996).

24. Hasanuzzaman, M., Rafferty, A., Sajjia, M. & Olabi, A.-G. Properties of Glass Materials. *Materials Science and Materials Engineering* 1–12 (2016) doi:10.1016/b978-0-12-803581-8.03998-9.

25. Zeng, H. *Polymer adhesion, friction, and lubrication*. (John Wiley & Sons, 2013).

26. Von Fraunhofer, J. A. Adhesion and cohesion. *International Journal of Dentistry* (2012) doi:10.1155/2012/951324.

27. Landrock, A. & Ebnesajjad, S. *Adhesives technology handbook*. (William Andrew, 2008).

28. Williamson, J.B.P., Greenwood, J.A. and Harris, J. The influence of dust particles

on the contact of solids. *Proc. R. Soc. London. Ser. A. Math. Phys. Sci.* **237**, 560–573 (1956).

29. Bowden, Frank Philip, Frank Philip Bowden, and D. T. *The friction and lubrication of solids*. (Oxford university press, 2001).

30. McFarlane, J. S., and D. T. Adhesion of solids and the effect of surface films. *Proc. R. Soc. London. Ser. A. Math. Phys. Sci.* **202**, 224–243 (1950).

31. DelRio, F. W., Dunn, M. L., Phinney, L. M., Bourdon, C. J. & De Boer, M. P. Rough surface adhesion in the presence of capillary condensation. *Appl. Phys. Lett.* **90**, 163104 (2007).

32. Wang, J., Qian, J. & Gao, H. Effects of capillary condensation in adhesion between rough surfaces. *Langmuir* **25**, 11727–11731 (2009).

33. Stange, T. G., Evans, D. F. & Hendrickson, W. A. Nucleation and growth of defects leading to dewetting of thin polymer films. *Langmuir* **13**, 4459–4465 (1997).

34. Seu, K. *et al.* Effect of surface treatment on diffusion and domain formation in supported lipid bilayers. *Biophys. J.* **92**, 2445–2450 (2007).

35. Davis, G. D. Contamination of surfaces: Origin, detection and effect on adhesion. *Surf. Interface Anal.* **20**, 368–372 (1993).

36. Fuller, K. N. G. & Tabor, D. The Effect of Surface Roughness on the Adhesion of Elastic Solids. *Proc. R. Soc. A Math. Phys. Eng. Sci.* **345**, 327–342 (1975).

37. Persson, B. N. On the theory of rubber friction. *Surf. Sci.* **401**, 445–454 (1998).

38. Gay, C. Stickiness—some fundamentals of adhesion. *Integr. Comp.* **42**, 1123–1126 (2002).

39. Krupp, H. Particle Adhesion: Theory and Experiment, Advances in Colloid and Interface Science. *Adv. Colloid Interface Sci.* (1967).

40. Contact of nominally flat surfaces. *Proc. R. Soc. London. Ser. A. Math. Phys. Sci.* **295**, 300–319 (1966).

41. Haisma, J. & Reports, G. S.-M. S. and E. R. Contact bonding, including direct-bonding in a historical and recent context of materials science and technology, physics and chemistry: historical review in a broader. *Mater. Sci. Eng. R Reports* **37**, 1–60 (2002).

42. Bascom, W. D. & Cottington, R. L. Air Entrapment in the Use of Structural

Adhesive Films. *J. Adhes.* **4**, 193–209 (1972).

43. Marshall, S., Bayne, S., Baier, R., Materials, A. T.-D. & 2010, U. A review of adhesion science. *Dent. Mater.* **26**, e11–e16 (2010).

44. Mostafavi, S. H., Tong, F., Dugger, T. W., Kisailus, D. & Bardeen, C. J. Noncovalent Photochromic Polymer Adhesion. *Macromolecules* **51**, 2388–2394 (2018).

45. Hohl, D. K. & Weder, C. (De)bonding on Demand with Optically Switchable Adhesives. *Adv. Opt. Mater.* **7**, 1900230 (2019).

46. Swenson, D. A. Apparatus and method for applying heat-sensitive adhesive tape to a web moving at high speed. *Google Patents* (1991).

47. Shitara, Koji, Hiroko Ikenaga, and H. K. Pressure-sensitive adhesive sheet,U.S. Patent 9,045,670. (2015).

48. Gelmi, A., Zanoni, M., Higgins, M.J., Gambhir, S., Officer, D.L., Diamond, D. and Wallace, G. G. Optical switching of protein interactions on photosensitive–electroactive polymers measured by atomic force microscopy. *J. Mater. Chem. B* **1**, 2162–2168 (2013).

49. Blass, J., Bozna, B.L., Albrecht, M., Krings, J.A., Ravoo, B.J., Wenz, G. and Bennewitz, R. Switching adhesion and friction by light using photosensitive guest–host interactions. *Chem. Commun.* **51**, 1830–1833 (2015).

50. Kaiser, S., Radl, S., Manhart, J., Matter, S. A.-K.-S. & 2018, U. Switching "on" and "off" the adhesion in stimuli-responsive elastomers. *Soft Matter* **14**, 2547–2559 (2018).

51. Asadirad, A. M., Boutault, S., Erno, Z. & Branda, N. R. Controlling a polymer adhesive using light and a molecular switch. *J. Am. Chem. Soc.* **136**, 3024–3027 (2014).

52. Saito, S. *et al.* Light-melt adhesive based on dynamic carbon frameworks in a columnar liquid-crystal phase. *Nat. Commun.* **7**, 12094 (2016).

53. Higuchi, A. *et al.* Photon-modulated changes of cell attachments on poly(spiropyran-co-methyl methacrylate) membranes. *Biomacromolecules* **5**, 1770–1774 (2004).

54. Sasaki, T. *et al.* Dismantlable Thermosetting Adhesives Composed of a Cross-Linkable Poly(olefin sulfone) with a Photobase Generator. *ACS Appl. Mater. Interfaces* **8**, 5580–5585 (2016).

55. Tada, Y. *et al.* Development of a photoresponsive cell culture surface: Regional enhancement of living-cell adhesion induced by local light irradiation. *J. Appl. Polym. Sci.* **100**, 495–499 (2006).

56. Ohmuro-Matsuyama, Y. & Tatsu, Y. Photocontrolled cell adhesion on a surface functionalized with a caged arginine-glycine-aspartate peptide. *Angew. Chemie - Int. Ed.* **47**, 7527–7529 (2008).

57. Weber, T. *et al.* Switching of bacterial adhesion to a glycosylated surface by reversible reorientation of the carbohydrate ligand. *Angew. Chemie - Int. Ed.* **53**, 14583–14586 (2014).

58. Breton, G. W. & Vang, X. Photodimerization of anthracene: A [4πs + 4πs] photochemical cycloaddition. *J. Chem. Educ.* **75**, 81–82 (1998).

59. Vitale, Alessandra, Giuseppe Trusiano, and R. B. UV-curing of adhesives: a critical review. *Rev. Adhes. Adhes.* **5**, 105–161 (2017).

60. Goulet-Hanssens, A., Magdesian, M.H., Lopez-Ayon, G.M., Grutter, P. and Barrett, C. J. Reversing adhesion with light: a general method for functionalized bead release from cells. *Biomater. Sci.* **4**, 1193–1196 (2016).

61. Wang, N., Li, Y., Zhang, Y., Liao, Y. & Liu, W. High-strength photoresponsive hydrogels enable surface-mediated gene delivery and light-induced reversible cell adhesion/detachment. *Langmuir* **30**, 11823–11832 (2014).

Chapter 2- Experimental Methods:

2-1 Non-Covalent Photochromic Polymer Adhesion

2-1-1 Materials:

The photochromic molecules 1′, 3′-dihydro-1′, 3′, 3′-trimethyl-6-nitrospiro [2*H*-1-benzopyran-2, 2′-(2*H*)-indole]) (**SP**), 1,3,3-trimethylindolinonaphthospirooxazine, and 1,2-bis(2,4-dimethyl-5-phenyl-3-thienyl)-3,3,4,4,5,5-hexafluoro-1-cyclopentene (**DAE**) were all purchased from TCI Chemicals. Polystyrene ((**PS**, MW=280,000) and another spiropyran derivative, nitro 1′, 3′-dihydro-8-methoxy-1′, 3′, 3′-trimethyl-6-nitrospiro[2*H*-1-benzopyran-2,2′-(2*H*)-indole], were purchased from Sigma Aldrich. Hydrogen peroxide (30%), ammonium hydroxide, concentrated H_2SO_4 (95.0-98.0%), and methylene chloride were obtained from Fisher Scientific. All chemicals were used as received.

2-1-2 Sample Preparation:

Glass microscope slides (Fisherbrand, 25×27×1mm) were cleaned using freshly prepared piranha solutions. Two types of piranha solutions were used. An acidic piranha solution was prepared by adding a 30% hydrogen peroxide solution to the concentrated H_2SO_4 in a volume ratio of 1:3. A basic piranha solution was prepared by mixing the 30% hydrogen peroxide solution with ammonium hydroxide solution (30% w/w) in a volume ratio of 1:3. In both cases, the mixtures were brought to boiling and the glass slides were submerged

for 20 minutes. After immersion in the piranha solution, the glass slides were rinsed thoroughly by Milli-Q purified water, spin dried and used immediately.

Photochrome stock solutions with concentrations of 10^{-3} M were prepared in methylene chloride. Varying amounts of the stock solutions were added to a 1.1% (w/v) solution of polystyrene in methylene chloride. A microsyringe was used to inject 10 microliters of the solution onto a cleaned glass surface to form films with diameters of ~1 cm. Care was taken to ensure that the edges of the films were not close to the edge of the slide. The films typically had a thickness of 300-400 nm, as measured using a Veeco Dektak 8 Surface Profiler.

2-1-3 Sample Characterization:

The single lap joint shear test was used to measure adhesive strengths of UV treated **PS**-photochrome to glass slides quantitatively (figure 2-1).[1] Polymer films containing 0%, 5%, 10%, 15% and 29% mass fraction (Equation (2)) were used to glue two microscopic glass slides together.

$$Mass\ Fraction = \frac{Mass\ of\ SP}{Total\ mass\ of\ SP\ and\ PS} \quad (2)$$

10 microliters of **PS**-photochrome solution was dropped on one slide and the second one was pressed on top. The contact area was 10 mm×10 mm. The sandwich structure was allowed to dry overnight. UV-exposed slides were irradiated with a 365 nm bench lamp

(UVP 15 Watt) with an intensity at the sample of 0.6 mW/cm^2 for 10 minutes. The slides were pulled with the speed of 3 mm/min in opposite directions using an Instron Model 5942 Testing System (Figure 2-1 and Table 2-1). Each experiment repeated 5 times and the results were averaged. The shear strengths is reported as force needed to break the slides apart divided by the contact area.

a) b)

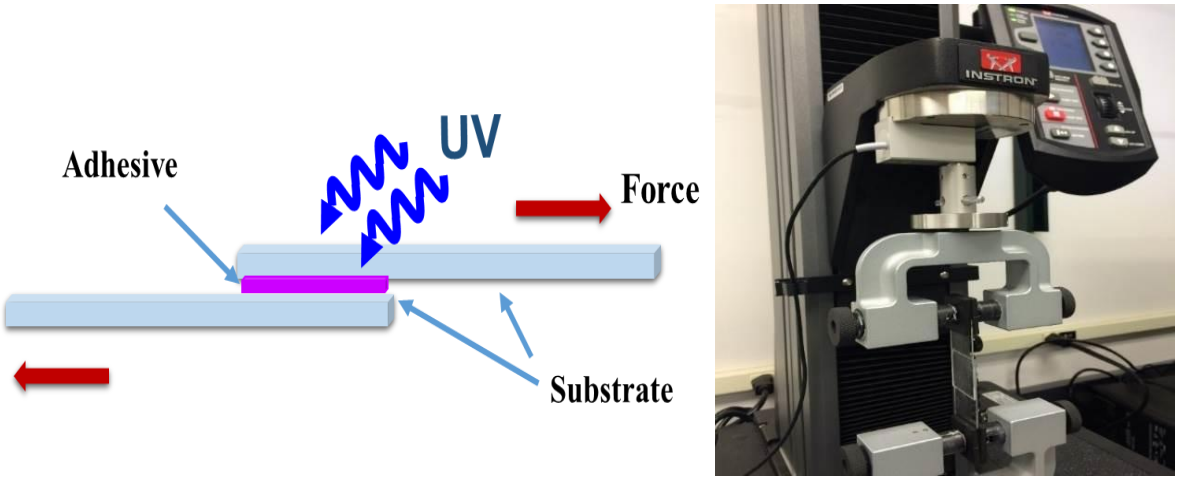

Figure 2- 1: a) Schematic of lap shear test measurement. In this experiment the polymer loaded with the photochromic molecule was sandwiched between two glass slides. These slides were then pulled in opposite directions and the force needed to break the adhesion was measured using the Instron 5942 Test Instrument, shown in (**b**).

To measure the detachment rate of the **PS** films from a glass surface in the presence of water, 18 film spots were deposited onto a single slide, 9 with **PS**-only films as control samples, and 9 with **PS**-photochrome films. The slides were irradiated with a 365 nm

bench lamp (UVP 15 Watt) with an intensity at the sample of 0.6 mW/cm^2 for one minute, while the other half of **PS-SP** coated slides were left un-irradiated. Then the microscopic glass slides were submerged into a vigorously stirred water bath and the number of detached films was monitored over time (Figures 2-2 and 2-3, Table 2-2). Care was taken that the stir bar did not touch the samples. To study the reversibility of adhesion, UV-irradiated films were prepared as previously described and then either exposed to room light or irradiated with a laser (532 nm, 575 mW/cm^2) for 10 hours.

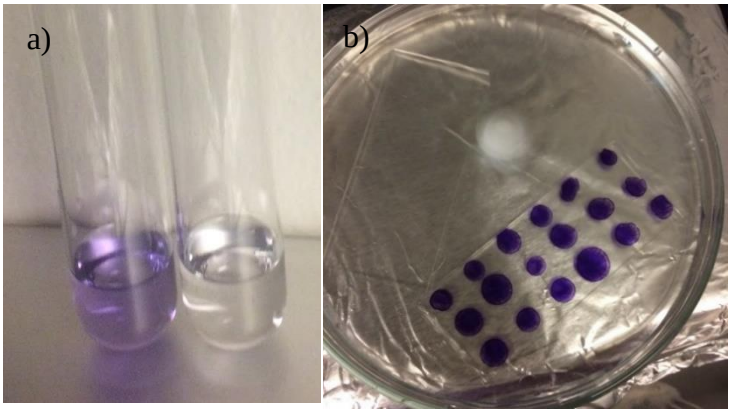

Figure 2- 2: a) Solution of nitro-spiropyran (**SP**) and **PS** in CH_2Cl_2 before (right) and after (left) UV irradiation. b) 2 microscope slides, each with 18 polymer film spots. Each polymer is loaded with 0.29 mass fraction **SP**. The top slide has not been irradiated and the spots are colorless, while the bottom slide has been irradiated at 365 nm, leading to the purple color indicative of the merocyanine isomer. The slides are submerged in water in a Petri dish with stirring (white stir bar is spinning in the middle between the two slides). The sample is observed at regular time intervals and the number of detached spots is recorded.

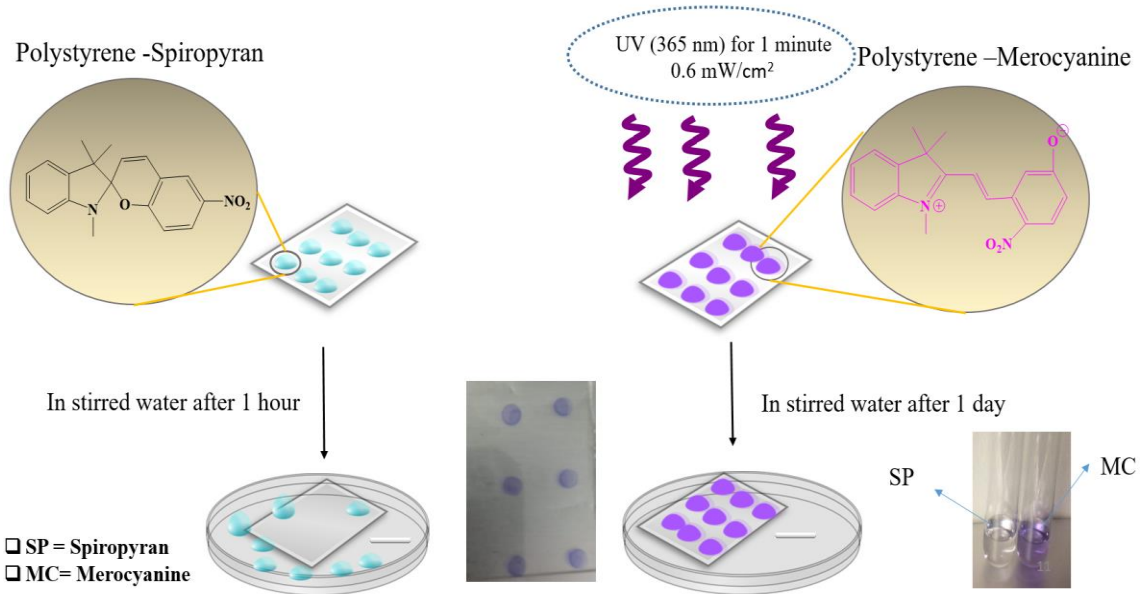

Figure 2- 3: Schematic of method used to measure detachment rates.

Contact angles were measured using a Kruss DO4010 Easy drop instrument. UV-Vis absorption spectra of irradiated and non-irradiated **SP-PS** films were obtained using a Varian CARY 500 UV/Vis spectrometer.

In order to measure polymer elastic modulus and hardness, films drop-cast on glass slides were indented before and after UV irradiation using a TI 950 TriboIndenter (Hysitron, USA) with a 5 μm radius conospherical diamond tip. Sections of the films with a thickness range of 10-15 μm were used to minimize substrate effects on the resulting modulus and hardness measurements. Indents were placed in similar regions of the pre- and post-irradiated film, spaced 100-200 μm apart to minimize variance due to

film thickness and roughness. An 8 x 8 square array of indents, each 1 μm deep and each spaced 6 μm apart, was collected using a quasi-static load function with load, hold, and unload segment durations of 5 seconds. Unload curves were fitted to determine the hardness and reduced modulus using the Oliver-Pharr method.[2]

2-2 Photoinduced De-Adhesion of a Polymer Film Using a Photochromic Donor-Acceptor Stenhouse Adduct

2-2-1 Sample Preparation:

The third-generation donor–acceptor Stenhouse adduct (**DASA**) was synthesized as reported previously.[3] Polystyrene was purchased from Sigma Aldrich. The glass microscope slides, hydrogen peroxide (30%), ammonium hydroxide, concentrated sulfuric acid (95.0–98.0%), and methylene chloride (CH_2Cl_2) were obtained from Fisher Scientific. The water-soluble dye Allura Red was obtained from TCI.

Glass microscope slides (Fisherbrand, 25×27×1mm) were cleaned using freshly prepared piranha solutions. In this study both acidic and basic piranha solutions were used. The acidic piranha solution was prepared by adding a 30% hydrogen peroxide solution to concentrated H_2SO_4 in a volume ratio of 1:3. The basic piranha solution was prepared by mixing the 30% hydrogen peroxide solution with ammonium hydroxide solution (30% w/w) in a volume ratio of 1:3. In both cases, the mixtures were brought to boiling and the glass

slides were submerged for 20 minutes. After immersion in the piranha solution, the glass slides were rinsed thoroughly by Milli-Q purified water, spin dried and used immediately.

DASA 3.0 stock solutions were made (1 mM in CH_2Cl_2) and various amounts were added to a 1.1% (w/v) solution of polystyrene in CH_2Cl_2. A 200 μL Hamilton microsyringe was used to inject a controlled amount of the **DASA**/PS/CH_2Cl_2 mixture onto a piranha washed glass surface to form polymer films, which were typically left to dry for at least 12 hr to ensure solvent evaporation. A solid-state 532 nm laser was used for sample irradiation. A beam diffuser (Thorlabs) was used to ensure uniform irradiation of the entire sample.

2-2-2 Sample Characterization:

A Cary 500 spectrophotometer was utilized to measure the UV –Visible absorption spectra. A Kruss DO4010 Easy Drop instrument was used for contact angle measurements. Atomic force microscopy (AFM) images were collected in tapping mode using a Digital Instruments Nanoscope IIIA scanned probe microscope system (AFM Probe: NSG01, NT-MDT Spectrum Instruments). The AFM cross-section analysis (or roughness) was performed on the AFM image using Nanoscope Control software.

Three methods of measurement were utilized to evaluate the adhesion of the **DASA**/**PS** films to the glass substrates. In all cases, the results report the mean and standard deviation for at least 5 different samples. The first method was the single lap-

joint shear adhesion test that measures the shear force (parallel to the film) required to break the glass-polymer bond (Figure 2-4). 10 μL of the **DASA**/PS/CH_2Cl_2 solution was used to glue two cleaned microscopic glass slides together, which were then allowed to dry overnight. The samples were then irradiated by 532 nm light with an intensity of 6 mW/cm^2 at the sample until the blue color completely disappeared (10-15 hr). An Instron Model 5942 testing system was used to pull slides in opposite directions at a speed of 3 mm/min until they separated. The force applied at the breaking point was recorded and divided by the glued area to give a shear adhesion value in units of N/cm^2. The reported values represent averages over at least 5 trials.

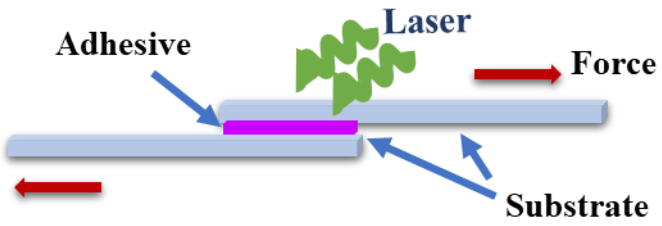

Figure 2- 4: Schematic of single lap-joint shear adhesion test. The **DASA**/PS film (purple) is used as an adhesive between two precleaned glass slides. The slides are pulled in different directions until the adhesive bond fails and the slides separate.

The second method was the pull-off adhesion test that measures the force applied perpendicular to the film required to break the adhesion (Figure 2-5). This test was done by gluing one microscopic slide as a bridge between two other slides using the

DASA/PS/CH_2Cl_2 solution. After letting the sample dry, it was irradiated until no blue color could be observed. The adhesion was measured by putting weights incrementally on the bridging slide until it broke free. The mass that caused the adhesion failure was then converted to N/cm^2 by multiplying by 9.8 m/s^2 and dividing by the contact area.

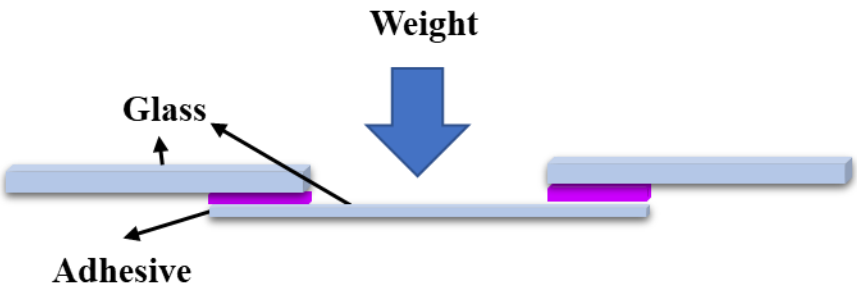

Figure 2- 5: Schematic of pull-off adhesion test. For this test one precleaned microscopic slide is glued to two other clean glass slides using the **DASA**/PS film (purple) as an adhesive. Slides dried for 24 hours in room temperature and then adhesion measured by putting weights on top of middle glass until the adhesion between the slides fails.

The third measurement method was a water detachment test (Figure 2-6). A microsyringe was used to deposit 5 μL of the **DASA**/PS/CH_2Cl_2 solution on a cleaned glass slide. Typically, 18 film spots with a diameter of a few mm were deposited on a single slide. A solution of 1.1 % (w/v %) polystyrene in methylene chloride were used as a control sample. After drying, the **DASA**/PS films were subjected to the same irradiation conditions described above, then submerged in stirred water (deionized) and the number of detached films was monitored.

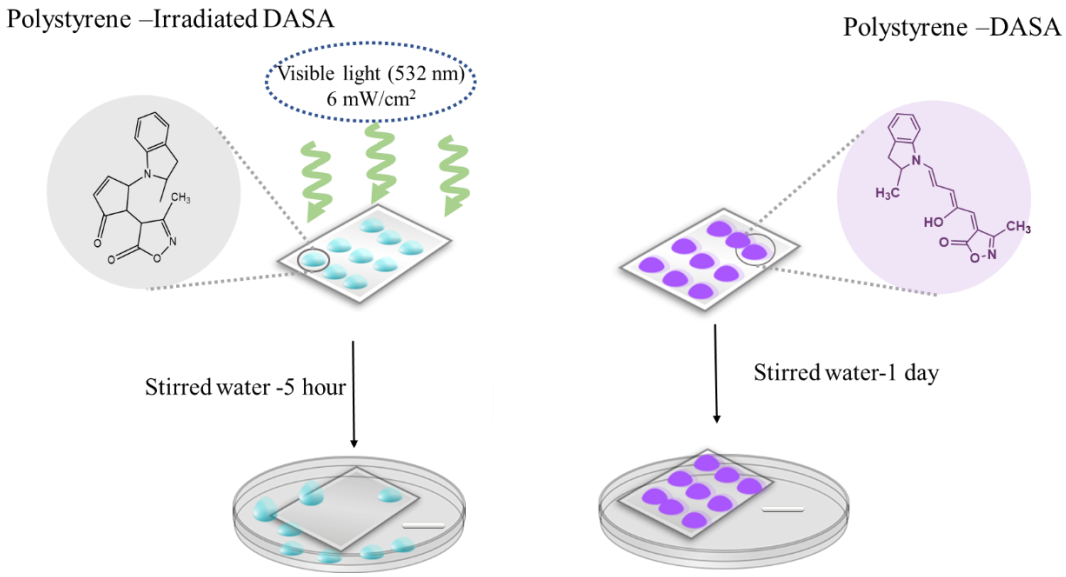

Figure 2- 6: Schematic for water detachment test. For this test, **DASA**/PS films are drop cast on precleaned slides and number of detached films is recorded at specific time intervals. Typically, the irradiated samples (which lost their purple color) detached more rapidly than the non-irradiated samples.

2-3 Heterogeneous Kinetics of Photoinduced Cross-Linking of Silica Nanoparticles with Surface-Tethered Anthracenes

2-3-1 Synthesis of 9-anthracene- N-hydroxysuccinimide:

In a 250 mL round bottle flask equipped with magnetic stir bar was added 9-Anthracenecarboxylic acid (2.0 g, 8.9 mmol) and N-hydroxysuccinimide (1.2 g, 10.8 mmol) in 4 mL of dry dichloromethane. The reaction was stirred for 15 min at 0 ^{o}C under N_2 atmosphere followed by slow addition of N, N'-dicyclohexylacarbodiimide (DCC) (1.9

g, 8.9 mmol) to the mixture. After complete addition, the reaction was stirred for 4 hr at 0 ^{o}C. Excess DCC was removed by vacuum filtration through a short silica plug and the dichloromethane layer was concentrated by rotary evaporation. The crude product was recrystallized in toluene. Finally, the product was purified *via* silica column eluted by dichloromethane to yield pure white product (2.5 g, 88%). ^{1}H NMR (400 MHz, $CDCl_3$) δ 8.63 (s, 1H), 8.41 (dt, J = 8.8, 1.0 Hz, 2H), 8.04 (d, J = 8.5 Hz, 2H), 7.64 (ddd, J = 9.0, 6.6, 1.3 Hz, 2H), 7.53 (ddd, J = 7.9, 6.6, 1.1 Hz, 2H), 3.37 – 2.70 (m, 4H). ^{13}C NMR (126 MHz, $CDCl_3$) δ 169.38, 165.00, 131.46, 130.68, 129.55, 128.56, 128.15, 125.88, 124.88, 121.34, 25.91. ESI-MS: *m/z* $C_{19}H_{14}NO_4$ (MH^+) calculated = 320.0918, found: $[MH]^+$ = 320.9090.

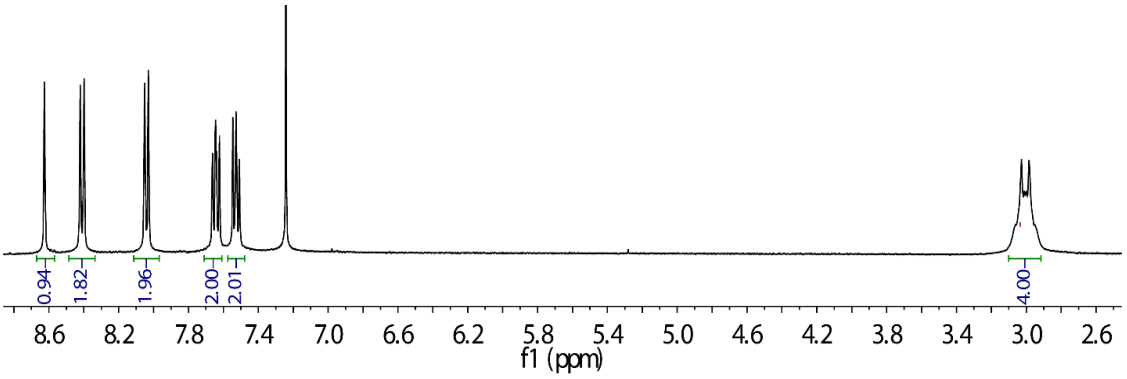

Figure 2- 7: ^{1}H NMR spectrum of anthracene-NHS linker (400 MHz, $CDCl_3$)

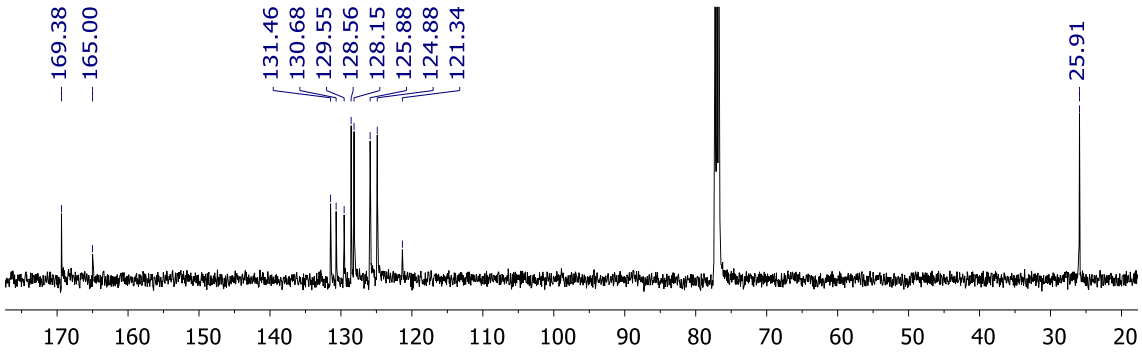

Figure 2- 8: ^{13}C NMR spectrum of anthracene-NHS linker (100 MHz, $CDCl_3$)

2-3-2 Anthracene attachment to silica nanoparticles.

3-aminopropyl functionalized silica NPs, suspended in ethanol, were purchased from Sigma-Aldrich (catalog number 660442). 1 mL of this suspension was mixed with 2 ml of anhydrous ethyl alcohol and 2 ml of dry dichloromethane, and then 10.8 mg of the 9-anthracene- N-hydroxysuccinimide linker was added to the solution. The mixture was sonicated for 1 minute and then gently stirred for 24 hours at 35 ºC. After completion, the reaction mixture was centrifuged at the speed of 13,000 rpm for 30 minutes. The supernatant was discarded and the pellet resuspended in anhydrous ethanol and centrifuged again. The procedure was repeated 4-5 times, until no trace of the **AN** linker absorption could be detected in the supernatant. The anthracene coverage was calculated using absorption spectroscopy.

2-3-3 Photoinduced NP aggregation.

Various concentrations of the **AN**-SiO_2 NPs were irradiated in a 1 cm pathlength quartz cuvette using a 365 nm lamp source with an intensity of 2.5 mW/cm^2. The absorbance was measured at various time intervals using a Cary 500 spectrophotometer.

2-3-4 Characterization

The **AN**-SiO_2 NPs were characterized using scanning electron microscopy (SEM) with a NovaNanoSEM 450 scanning electron microscope. The dried samples were coated with a thin layer of palladium using a Cressington 108 sputter coater. Dynamic Light Scattering (DLS) and zeta potential measurements were performed using a Malvern ZetaSizer instrument. The **AN**-SiO_2 NPs were sonicated for 10 minutes to disperse them before injection into the ZetaSizer instrument. Time-resolved photoluminescence measurements were done using 400 nm femtosecond pulses at a 1 kHz repetition rate. The 400 nm excitation wavelength was generated by using a Beta Barium Borate crystal to frequency double the 800 nm fundamental of a Coherent Libra regeneratively amplified Ti:sapphire laser system. The sample was degassed using by bubbling argon gas through it and the fluorescence was collected using front-face detection and a Hanamatsu C4334 streak camera with a time resolution of 25 ps and a wavelength resolution of 2 nm.

2-4 Instructions and techniques

2-4-1Cleaning and hydrophilization of substrates

Surfaces must be clean and completely free of organic solvents from previous wash steps before coming into contact with piranha solution. Great care is necessary to prepare the piranha solution because it is highly explosive, extremely corrosive, and one of the most powerful oxidizers. Piranha solution dissolves organic contaminants and a large amount of violent bubbles are produced in order to release gas, which can potentially cause an explosion. This solution should be prepared by adding hydrogen peroxide slowly to sulfuric acid; the reverse may cause splashing since this reaction is extremely exothermic. For this experiment, glass slides were submerged in freshly prepared and boiling piranha solution (30% hydrogen peroxide solution to the concentrated H_2SO_4 in a volume ratio of 1:3) for 20 minutes. Then, the glass slides were rinsed thoroughly by Milli-Q purified water, were spin dried, and used immediately.[4,5] By increasing the number of silanol groups on the surface (hydroxylating the surface), piranha solution makes glass more hydrophilic.[6]

2-4-2 Increase the hydrophobicity of the glass substrate:

Heating the cleaned glass substrates in an oven to over 280 ºC for 3-5 hours will significantly reduce the silanols on glass and produce siloxane to make the surface more hydrophobic. Upon heating, there is a steady decrease in silanol concentration on the surface since heating causes evaporation and condensation of silanol functional groups.[7]

During our study of testing the effects of silanols on adhesion, cleaned glass slides were heated to 280 ºC for 4 hours and then cooled down to room temperature. The polymer-photochrome mixture was drop cast on the surface and the water detachment was monitored as an indication for changing adhesion.

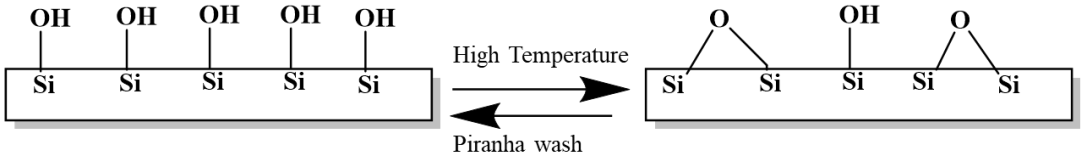

Figure 2- 9: Extreme heating reduces silanol concentration by producing solixane groups and making the surface more hydrophobic. Piranha solution can reverse this reaction by hydroxylating the surface. [7]

2-4-3 Contact angle measurement

In this study, contact angles were measured using a Kruss DO4010 Easy drop instrument. A freshly prepared polymer-photochrome solution was spin coated onto cleaned glass slides with the speed of 2000 rpm for 20 s and dried. The spin coated film looked uniform at this point. These samples were carried in a sealed and dark container to Dr. Vullev's lab for measurements. The contact angle of water droplets on the surface were collected before and after irradiation. For more accurate results, the syringe needed to be emptied and filled with fresh DI water at the beginning of experiments. It is possible to

change the pH of water if required, however, after getting permission, the syringe needed to be cleaned 3 times and filled with fresh DI water at the end of experiments.

2-4-4 Water Detachment adhesion measurement

The water detachment adhesion method was developed and used for the first time in our group.[8] This method is cheap and easy to perform, and it can easily provide us with a reliable and comparative method for measuring adhesion.

In this method, we are trying to explore delamination of attached polymers to a substrate in the presence of water. Typically, 18 film spots with a diameter of a few mm were deposited on a pre-cleaned single slide. A microsyringe was used to deposit 5 µL of the polymer-photochrome solution on a piranha washed glass slide. A solution of 1.1 % (w/v %) polystyrene in methylene chloride was used as a control sample on one slide. After drying, the polymer-photochrome films were irradiated, then submerged in stirred water and the number of detached films was monitored over time. The number of detached films versus time (N_{detach}) was fit using an exponential function:

$$(1).\ N_{detach} = N_0\left(1 - e^{-k_{detach}t}\right)$$

where N_0 is the number of film spots originally on the slide and k_{detach} is the characteristic detachment rate and *t* is the time spent in the agitated water solution.[8]

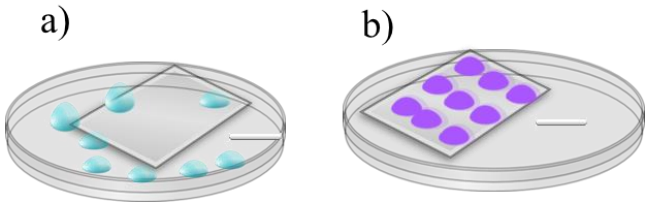

Figure 2- 10: Multiple spots were drop casted on cleaned glass slides and put in stirred water a) Before irradiation, dried PS-SP has a weak interaction with the glass b) UV irradiation significantly increased the adhesion. [8]

2-4-5 Single Lap Shear Test:

Procedure for working with Instron:

1. Clean glass substrate with piranha solution for 20 minutes
2. Rinse with water and dry
3. Use a certain amount of dissolved polymer-photochrom to glue two different substrates together
4. Irradiate the samples with the appropriate wavelength
5. Do not touch the samples until they are dry
6. Measure the attached area in square centimeters
7. Stabilize each end of the slides in the grips of the Instron instrument
8. Apply a force at a controlled rate in different directions until the adhesion fails and record the maximum force
9. Measure the maximum force at breaking point of adhesion

10. Measure the maximum shear stress by dividing the maximum force by the shear area. In most cases, units are newtons/square centimeters.

Extra care is needed to stabilize the slides on sample holders and tighten the clamps until we feel that the sample cannot move under high pressure. For the shear measurement, we need to: a) open the “Bluehill 3” software on the desktop, b) choose the test, c) select the most relevant method among the options, d) click on next and pick the preferred name and location for each sample, e) make the value of load and extension 0 before starting the measurement, and f) run the experiment. The Instron pulls both sides of the glass slides in different directions until the adhesion fails and the device calculates the maximum force required to break it.

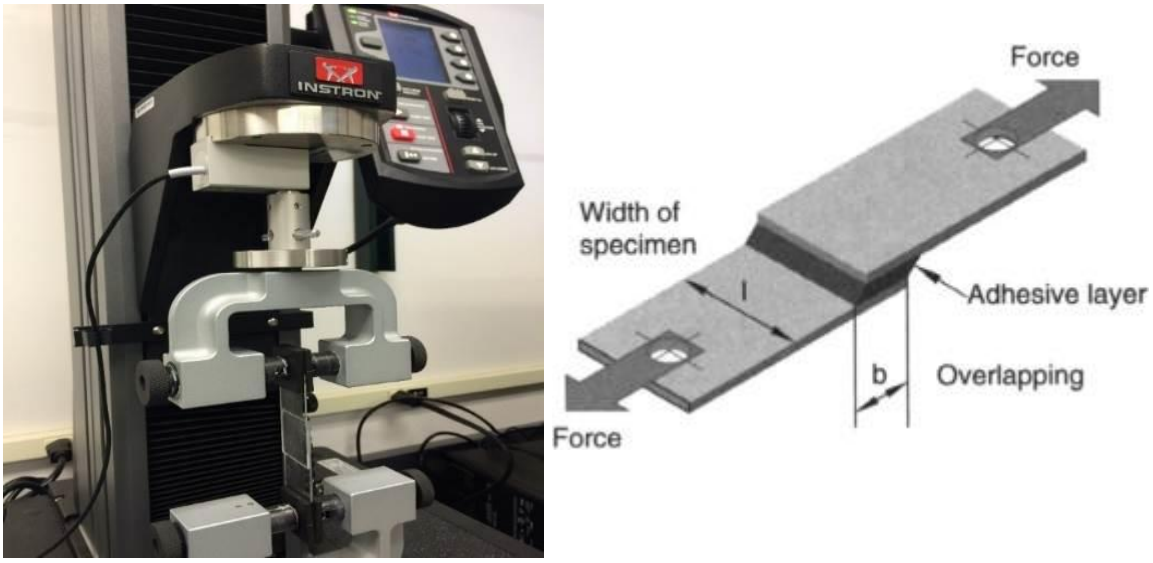

Figure 2- 11: a) Shows the Instron instrument b) Schematic of single lab shear test. In this test the glass slides are glued together by adhesives and pulled in different directions until adhesion fails to keep the two slides together. Shear stress is the maximum force needed to break the adhesion divided by the overlapping area (b cm×I cm).[9]

2-4-6 Pull-off adhesion test:

The pull-off adhesion method is based on gluing two surfaces together using the polymer-photochrome solution. In this method, the amount of force required to break the adhesion was applied perpendicular to the film. This test was performed by gluing one microscopic slide as a bridge to two other slides by polymer-photochrome mixture. For this test, glass slides need to be cut to about 6-8 mm in width and their contact area needs to be minimized as much as possible. All slides need to be washed with piranha solution to

be in their most hydrophilic state and contamination free before gluing them together. After letting the sample dry and exposing it to the appropriate wavelength of light, adhesion was measured by adding weights incrementally on the bridging slide until the adhesion failed. Then, the maximum mass was converted to Newtons (by multiplying by 9.8 m/s^2) and divided by the area of slide contact to measure adhesion in N/cm^2.

2-4-7 Time-resolved photoluminescence measurements

Anthracene covered nanoparticles were analyzed by time-resolved photoluminescence. These measurements were done using 400 nm femtosecond pulses at a 1 kHz repetition rate. The sample fluorescence was collected using front-face detection and a Hanamatsu C4334 streak camera with a time resolution of 15 ps. The fluorescence decays of AN by itself and the crosslinked nanoparticle-linker were taken on time scale increments of fifty nanoseconds.

2-4-8 Surface profilometer

In this study, the Veeco Dektak 8 profilometer was used to measure the thickness of the spin-coated films. The system is a Bench-Top Surface Profiler that measures the step heights of any surface. The spin-coated polymer was cut into two parts using a razor blade and then the sample was loaded on the stage. To begin the procedure, the system needs to log in to the Dektak software, and the system will initialize automatically. After completing

this procedure, an interesting position was located on the polymer by rolling the track ball in the X or Y direction, the area that was previously cut by the razor was found. After finding this position, the starting point and the scanning parameters were defined. The most important input was stylus force, which had a range between 3-15 mg. In this study, 5 mg was used. Once scanning was completed, plot appeared on the screen. Then, the scanning curve was leveled by moving the red marker to the left on the flat surface of the polymer and by moving the green marker to the right and positioning it on the exact area of the initial cut, which is always the deepest location in the scanned area. The Dektak instrument showed the thickness of the polymer in nanometers on screen.

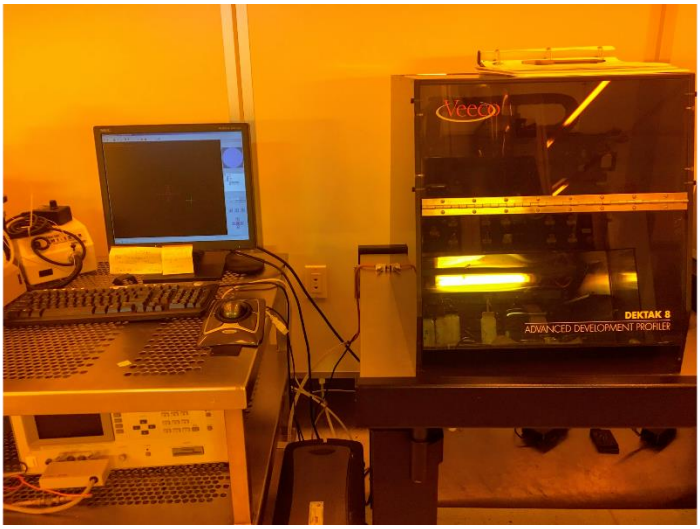

Figure 2- 12: Surface profilometer in the The NanoFab lab provides the thickness of the polymer in our experiment

2-4-9 Atomic force microscopy

Atomic force microscopy (AFM) was used to evaluate variation in topography of thin films containing photochrome after laser irradiation and analyze the samples in-situ. To make sure that data was collected from the exact same point during each analysis, the samples were not moved before or after irradiation. The polymer-photochrome solution was spin-coated on cleaned glass slides and stabilized on an AFM sample holder. The green laser was also safely set up and aligned in the room to hit the sample in-situ. AFM images were collected in tapping mode using a Digital Instruments Nanoscope IIIA scanned probe microscope system (AFM Probe: NSG01, NT-MDT Spectrum Instruments). The AFM cross-section (or roughness) analysis was performed on the AFM image using Nanoscope Control software.

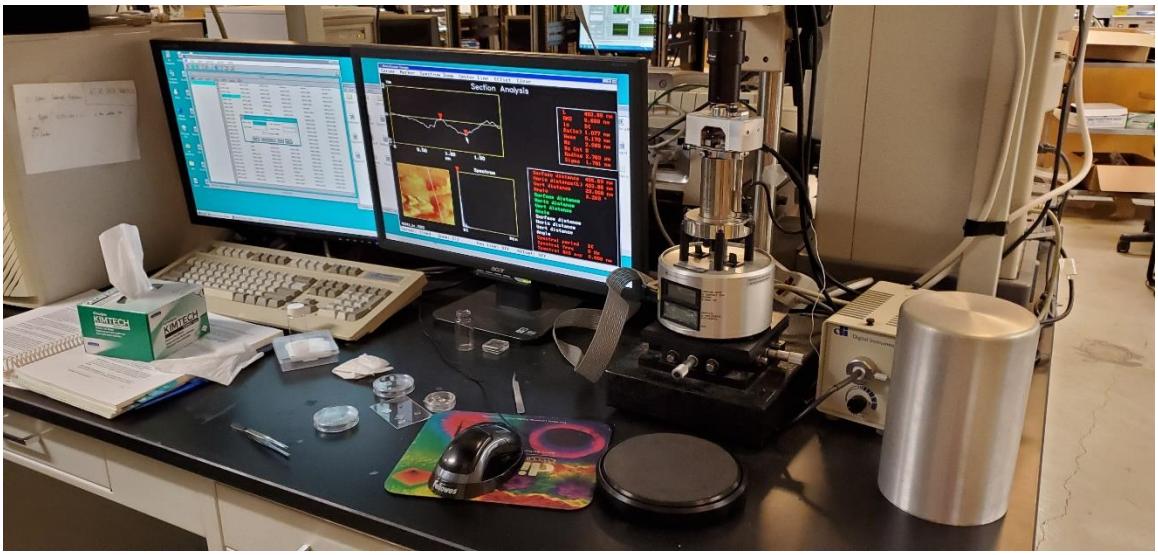

Figure 2- 13: AFM images were collected in tapping mode using a Digital Instruments Nanoscope IIIA scanned probe microscope system. As it is shown, the sample is not in a closed chamber, and this provided the opportunity to irradiate the sample in-situ without moving the sample.

2-4-10 Drug design software

VEGA ZZ is a very interesting and useful drug design software for molecular modeling applications, which was designed by the University of Milan. This software is free for non-profit academic use and can be easily downloaded and installed. This software was used to analyze the photochromic molecular structure before and after photo-switching and was specifically utilized to calculate the molecular volume. This software uses the van der Waals radius to create a set of spheres and calculates the final volume of the molecule. Initially, the molecule was drawn with ChemDraw software, and it was saved in a VEGA ZZ recognizable format. After selecting the View tab from the toolbar, “information” was

selected, and we chose to order the calculation of the molecular properties. The properties the software calculated included: molecular weight, approximate dimension, surface area, polar area, and, most importantly, the molecular volume. The calculated results were used to compare the molecular volume of the photochromes before and after photo-switching.

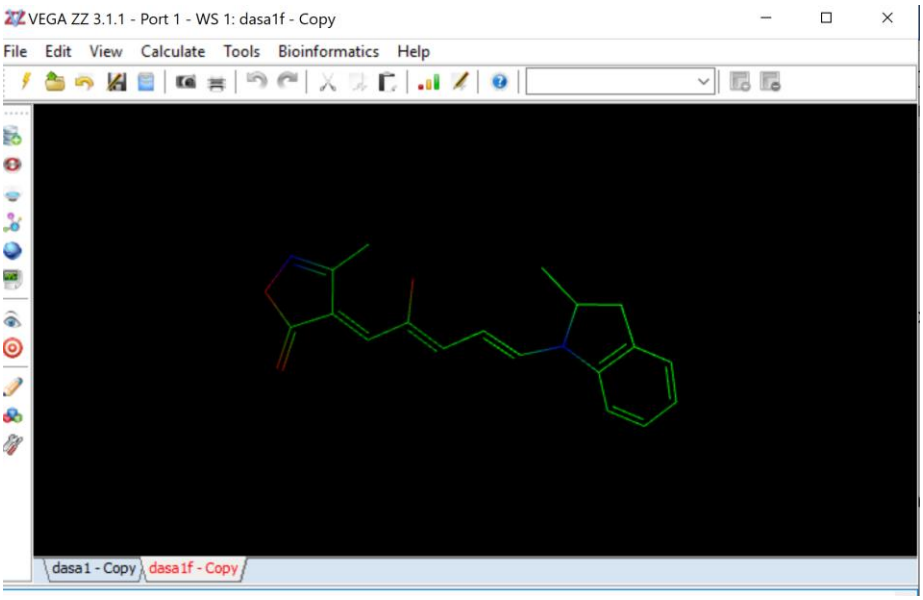

Figure 2- 14: VEGA ZZ software shows a **DASA** molecule

2-4-11 Nanoindentation

Film drop-casts on glass slides were indented before and after UV irradiation using a TI 950 TriboIndenter (Hysitron, USA) with a 5 μm radius conospherical diamond tip (Thickness range: 15-20 μm). Sections of the films were used to minimize substrate effects on the resulting modulus and hardness measurements. Indents were placed in

similar regions of the pre- and post-irradiated film, spaced 100-200 μm apart to minimize variance due to film thickness and roughness. An 8 x 8 square array of indents, each 1 μm deep and each spaced 6 μm apart, was collected using a quasi-static load function with load, hold, and unload segment durations of 5 seconds. Unload curves were fitted to determine the hardness and reduced modulus using the Oliver-Pharr method.[2,8]

2-4-11 Dye release experiment:

In the lab, a technique was developed to release chemicals upon light irradiation in order to demonstrate the potential application of the photo-induced de-adhesion. A soluble dye (Allura Red) was used as a model molecule to illustrate a control release system. For the experiment, Allura Red (.5mg) was placed in a piranha-washed microscope well plate. A second precleaned glass slide (preferably a cover slip) was then glued to the well slide using the polymer-photochrome and allowed solution to dry. For more rapid release, the cover glass needed to be the exact size of the well to completely cover up the boundaries of each well. 20 μl of polymer-photochrome was used to glue both glasses together and then they were irradiated and left to dry. As shown in Figure 2-13, samples were irradiated until no color was observed. Then, the time needed for adhesion failure in vigorously stirred water was monitored and the data was compared to a sample of identical assembly that was in stirred water but left in the dark. Observation and UV absorption proved that dye release was induced by visible light exposure.

2-4-12 Spin Coater:

Spin coating (Laurell Spin coater Model WS-400B-6NPP/Lite) is a procedure to deposit a uniform thin film on a flat substrate. A small amount of the coating solution was drop-cast to the center of the substrate and then the instrument was run. The speed of spin coating may vary based on the coating material, concentration of the polymer, and needed thickness of the thin film. The other usage of this instrument is to dry samples, and it is a preferred method over air drying since it minimizes the amount of handling.

2-4-12-1 Spin-coater instructions:

1. Place the substrate (e.g. a glass slide) upon the O-Ring
2. Turn on the spin coater
3. Open the vacuum line
4. Open the N_2 line
5. Press the blue vacuum button on the keypad to attach the substrate
6. Set the parameters
    a- Program select: select one of the predesigned programs
    b- F1: allows changes to parameters to preferred parameters
7. Press run/stop to start/stop spinning
8. Clean off surface of spin coater lid with wipe
9. Turn off vacuum and N_2 lines
10. Turn off the instrument

Figure 2- 15: The spin coater was used in this experiment to deposit a uniform thin film on a flat substrate with a specific thickness. This device also was used for drying substrates.

2-5 References:

1. Khoee, Sepideh, and Z. K. Design and development of novel reactive amine nanocontainers for a self-healing epoxy adhesive: self-repairing investigation using the lap shear test. *RSC Adv.* **5**, 21023–21032 (2015).

2. Oliver, W. C. & Pharr, G. M. Measurement of hardness and elastic modulus by instrumented indentation: Advances in understanding and refinements to methodology. *J. Mater. Res.* **19**, 3–20 (2004).

3. Hemmer, J. R. *et al.* Controlling Dark Equilibria and Enhancing Donor-Acceptor Stenhouse Adduct Photoswitching Properties through Carbon Acid Design. *J. Am. Chem. Soc.* **140**, 10425–10429 (2018).

4. Davis, G. D. Contamination of surfaces: Origin, detection and effect on adhesion. *Surf. Interface Anal.* **20**, 368–372 (1993).

5. Stange, T. G., Evans, D. F. & Hendrickson, W. A. Nucleation and growth of defects leading to dewetting of thin polymer films. *Langmuir* **13**, 4459–4465 (1997).

6. Seu, K., Pandey, A., Haque, F. & Proctor, E. Effect of surface treatment on diffusion and domain formation in supported lipid bilayers. *Biophys. J.* **92**, 2445–2450 (2007).

7. Thomas, R.R., Kaufman, F.B., Kirleis, J.T. and Belsky, R. A. Wettability of polished silicon oxide surfaces. *J. Electrochem. Soc.* **143**, 643–648 (1996).

8. Mostafavi, S. H., Tong, F., Dugger, T. W., Kisailus, D. & Bardeen, C. J. Noncovalent Photochromic Polymer Adhesion. *Macromolecules* **51**, 2388–2394 (2018).

9. Comyn, J., Cognard, P., Moulds, R. J., Rabilloud, G., Decker, C., Burchardt, B. R., & Merz, P. W. *Handbook of adhesives and sealants*. *Elsevier* vol. 2 (2006).

Chapter 3 Non-Covalent Photochromic Polymer Adhesion

3-1 Introduction

The adhesion of a polymer to a substrate is an important technological problem that encompasses phenomena on multiple length scales, from molecular-level bonding to macroscopic film morphology.[1] While developing a fundamental understanding of this adhesion remains an important goal, it is also desirable to control it using an external stimulus. In many respects, light is an ideal control field since it can be delivered to closed systems with high spatial and temporal resolution. Photoswitching of adhesion can be accomplished by modifying the polymer morphology through light-induced sintering or melting[2-3] or by using photochemistry to modify molecular binding interactions.[4-7] Both methods tend to require the synthesis of specially designed molecules or polymers. It would be useful to develop a simple and reasonably general method to manipulate polymer adhesion using light.

An example of poor adhesion occurs when the hydrophobic polymer polystyrene (**PS**) is deposited onto a hydrophilic surface like SiO_2.[8-9] When **PS**-coated glass surfaces are placed into room temperature water, the polymer film typically delaminates from the glass within 30 minutes [10], presumably because the polar H_2O molecules diffuse into the interface and displace the weak Van der Waals interactions between the hydrophilic surface siloxy groups and the hydrophobic polymer. The adhesive strength of this interface is also quite weak – the polymer will detach from the glass under relatively small loads. Photoinduced cross-linking has been demonstrated to be an effective strategy for

permanently bonding polystyrene (**PS**) to surfaces like Si and SiO_2, but this process introduces irreversible chemical changes in the polymer.[11]

In this chapter, we explore how a photochromic molecule that can be switched between two isomers can be used to modify adhesion between a polymer film and a glass surface. The adherence of **PS** to glass was chosen as a model system. The idea is to use the photochromic reaction to alter the molecular interactions at the glass-polymer interface. There exist a large variety of photochromic molecules that can be used.[12] For this research, we examined two commercially available photochromes, a spiropyran derivative 1′, 3′-dihydro-1′, 3′, 3′-trimethyl-6-nitrospiro [2*H*-1-benzopyran-2, 2′-(2*H*)-indole]) (**SP**) and a diarylethene derivative 1,2-bis(2,4-dimethyl-5-phenyl-3-thienyl)-3,3,4,4,5,5-hexafluoro-1-cyclopentene (**DAE**). These two molecules belong to classes of photochromes that absorb in the ultraviolet (UV) region and undergo reversible unimolecular isomerizations to generate photoisomers (Scheme 3-1).[13-15] The photoisomers absorb at visible wavelengths, making it straightforward to completely reverse the reaction using a different light source. We test adhesion by looking at shear strength and delamination rates in water. Both photochromic reactions can significantly enhance the adhesion of **PS** to a glass surface, although the effect of the **DAE** is limited by its lower reactivity in the **PS** matrix. The enhanced polymer adhesion could only be partially reversed, even after extended exposure to visible light completely regenerated the UV-absorbing isomer. Nanoindentation and heating experiments suggest that the limited reversibility results from an effective polymer annealing process that accompanies the photoisomerization reaction.

While these noncovalent changes enhance adhesion, they do not affect the chemical properties of the polymer, like solubility or optical clarity. The results of this chapter show that adhesive forces between dissimilar materials can be modulated by photochromic reactions of embedded molecules. This work provides a simple path to materials that possess photo-switchable adhesive properties without covalent crosslinking.

SP:

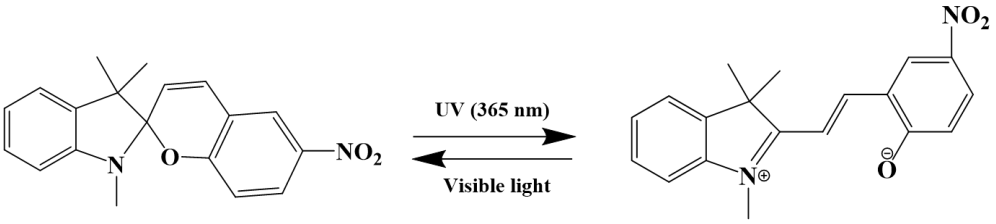

DAE:

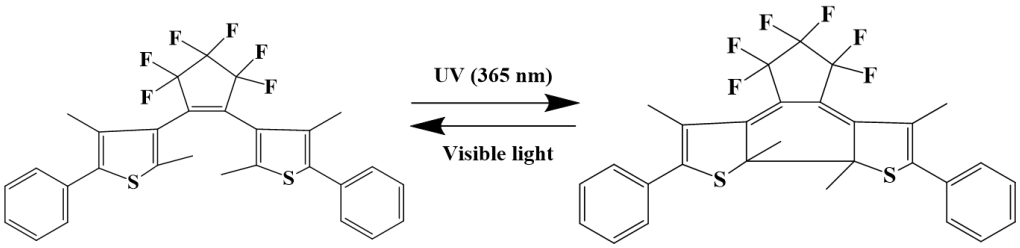

Scheme 3-1. The two photochromic molecules, **SP** and **DAE**, studied in this chapter.

3-2 Results and Discussion

Both **SP** and **DAE** photochromes react in **PS**, but not to the same extent. Figure 3-2 shows the absorption change due to the photochromic reactions of **SP** and **DAE** in **PS**. Under 365 nm illumination, the UV absorption due to the **SP** form completely disappears, replaced by the merocyanine absorption (peaked around 600 nm). This photochromic change can be reversed by exposure to visible light (Figure 3-1). Using 365 nm light, we can essentially convert 100% of the **SP** to its merocyanine isomer. The **DAE** photochrome, however, loses only about 5% of its absorbance under the same conditions, as shown in Figure 3-2 b. This low conversion may be due to the fact that the ring-open isomer absorbs weakly at this wavelength, while the ring-closed isomer absorbs more strongly. This situation can lead to a photostationary state that favors the reactant. Using a shorter wavelength excitation source would be expected to increase the conversion. A second possibility is that there is heterogeneity in the local environment around the **DAE** molecules, allowing only a small fraction to react while the others are prevented by steric constraints. The important point is that this photochrome is less reactive in the **PS** and thus its effect on adhesion is expected to be diminished.

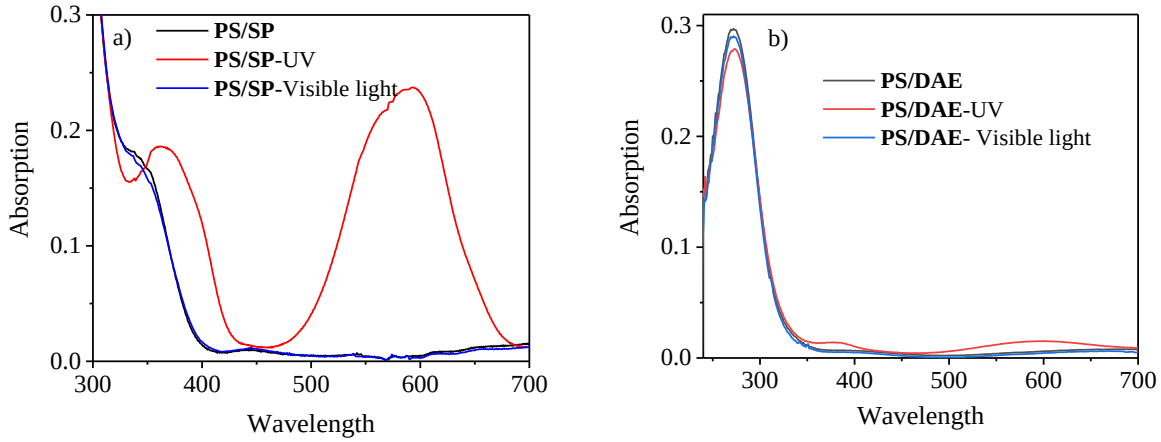

Figure 3-1: **a)** Absorption of 1′, 3′-dihydro-1′, 3′, 3′-trimethyl-6-nitrospiro [2*H*-1-benzopyran-2, 2′-(2*H*)-indole]) (**SP**) in polystyrene before and after UV irradiation (365 nm), and after visible light exposure. **b)** Absorption of 1,2-bis(2,4-dimethyl-5-phenyl-3-thienyl)-3,3,4,4,5,5-hexafluoro-1-cyclopentene (**DAE**) in polystyrene before and after UV (365 nm) irradiation, and after visible light exposure. Both photochromes completely recover the reactant absorption after 30 hr of visible light exposure.

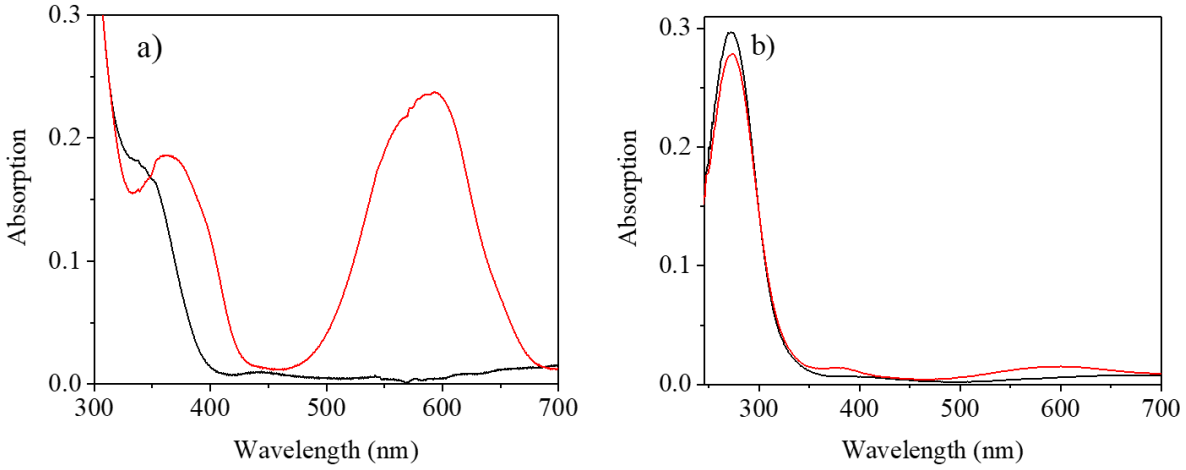

Figure 3-2: **a)** Absorption spectra for 0.29 mass fraction **PS/SP** sample (equivalent to a mass ratio **SP:PS** = 29:71) film before (black) and after (red) 1 minute of 365 nm irradiation. **b)** Absorption spectra for **PS/DAE** 0.29 mass fraction of **DAE** (equivalent to a mass ratio **DAE:PS** = 29:71)film before (black) and after (red) 1 minute of 365 nm irradiation.

The next question concerns how the photochromic reactions affect **PS** adhesion to the glass. A standard lap-shear test was used to evaluate the adhesive strength between two glass plates that sandwich a polymer film. The force per unit area (shear) required to separate the plates was determined (Figure 3-3 a, Table 3-1). With neat **PS** or unirradiated **PS**/**SP** films, the average shear required was relatively low, 9.3±1.3 N/cm^2. After UV irradiation, this value for a 0.29 mass fraction **PS**/**SP** film jumped to 69±4 N/cm^2. Here, mass fraction refers to the weight of the photochrome as a fraction of the total weight, for example a 0.29 mass fraction **PS**/**SP** sample has the mass ratio **SP**:**PS** is 29:71. These

highly colored films could be returned to their original, uncolored state after 30 hours of visible light exposure, but resulted in only a slight decrease in shear strength to 51±4 N/cm^2. Even though the chemical change could be reversed, the adhesion change was mostly permanent. A similar but smaller photoinduced change was observed in the **PS**/**DAE** films, where the shear strength approximately doubled to 21±1.2 N/cm^2 for the UV irradiated samples, then relaxed slightly to 16±2 N/cm^2 after the ring-closed isomer was converted back to the uncolored, ring-open form. The smaller effect for the **PS**/**DAE** films was expected based on **DAE**'s lower photoconversion efficiency.

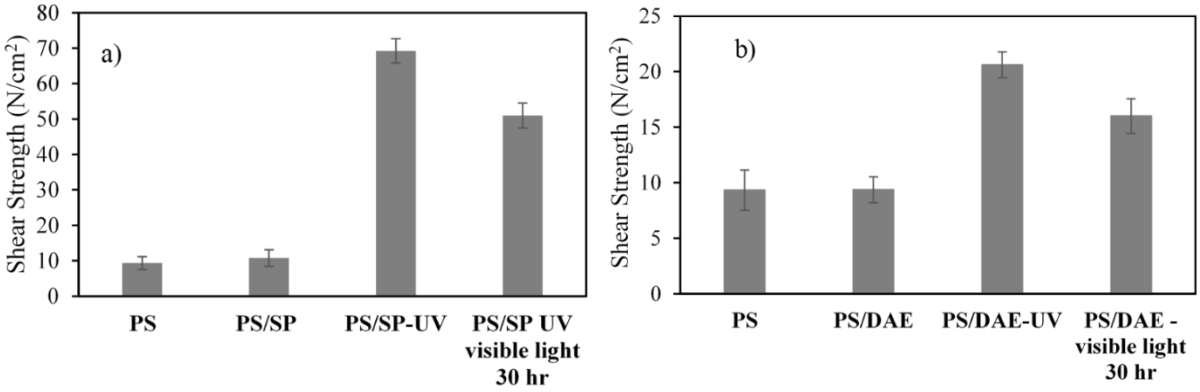

Figure 3-3: **a)** Lap-shear test results for **PS/SP** 0.29 mass fraction films sandwiched between two glass plates. The measured force per unit area (shear) required to pull the plates apart for neat **PS**, the **PS/SP** film before irradiation, the **PS/SP** UV irradiated film, and the **PS/SP** UV irradiated film after exposure to visible light for 30 hr has regenerated the **SP** reactant. **b)** The same experiment as in a) but for a **PS/DAE** mass fraction film.

Table 3- 1: **Results of the standard lap-shear test on different polymer samples.**

	Lab shear test (N/cm^2)
PS	9.3 ± 1.8
PS/SP	10.7 ± 2.33
PS/DAE	9.38 ± 1.16
PS-Heat	16.5 ± 3.62
PS/SP-UV	69.25 ± 3.41
PS/DAE-UV	20.6 ± 1.16
PS/SP-UV visible light 30 hr	51 ± 3.51
PS/DAE - visible light 30 hr	16 ± 1.56

In all the shear experiments, the samples broke apart at the polymer glass interface, which appears to be the "weak link" in the glass-polymer sandwich. The vulnerability of this interface could be further probed by measurements of the water-induced delamination of the polymer films. If a neat **PS** film was deposited onto a piranha cleaned microscope slide and then immersed in stirred water, it typically detached within about 30 minutes. To quantify the detachment rate, we monitored multiple films and measured how many were still attached to the glass at regular time intervals. Delamination often results from internal stress between the two layers[16], but can also result from interface debonding, in this case due to penetration of water into the interface. Interface debonding relies on diffusive transport and can be modeled as a chemical rate process.[17-18] In our case, we assume it can

be described by first-order kinetics, with the number of detached films (N_{detach}) predicted by an exponential function:

$$N_{detach} = N_0\left(1 - e^{-k_{detach}t}\right) \quad (1)$$

N_0 is the number of film spots originally on the slide, k_{detach} is the characteristic detachment rate, and t is the time spent in the agitated water solution. Examples of the data and fitting using Equation (1) are shown in Figure 3-4. k_{detach} for a **PS**-only film was measured to be $(2.9\pm0.2)\times 10^{-2}$ min^{-1}. When **SP** is added to the **PS** with a 0.29 mass fraction, the film delaminates slightly more slowly with $k_{detach} = (1.2\pm0.1)\times 10^{-2}$ min^{-1}. When the film was exposed to 365 nm light at an intensity of 0.6 mW/cm^2 for 1 minute, the film changed from colorless to purple and stayed attached even after several days in an agitated H_2O solution (Figure 3-4 a). Given the low number of detached films in this sample, it is difficult to extract a reliable estimate for k_{detach}, but we estimate that it is less than 10^{-5} min^{-1}, or 2-3 orders of magnitude smaller than that of an unirradiated doped film.

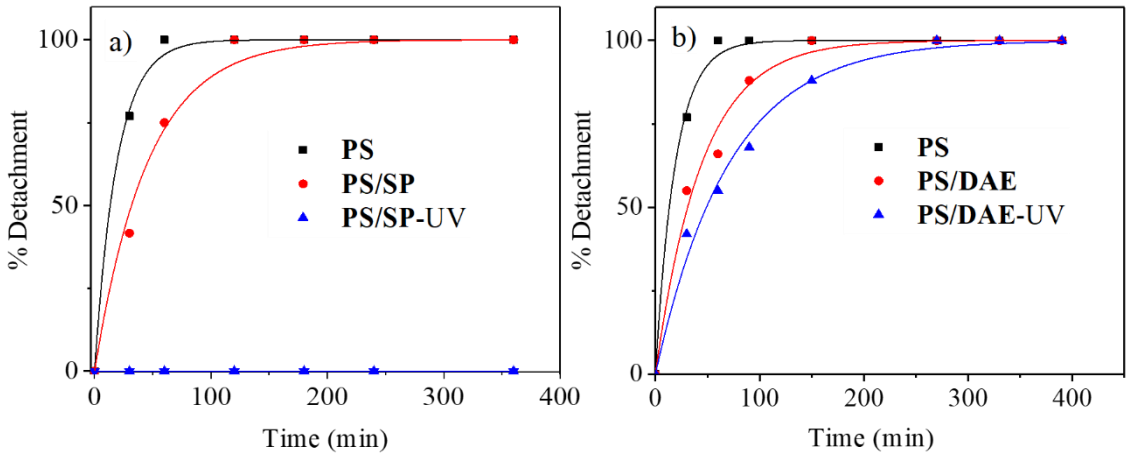

Figure 3-4: **a)** Time dependent detachment percentage of neat polystyrene films (**PS**), 0.29 mass fraction polystyrene-spiropyran (**PS/SP)** films, and polystyrene-spiropyran films after UV exposure (**PS/SP**-UV). **b)** Time dependent detachment percentage of **PS**, **PS/DAE** and **PS/DAE**-UV films under the same conditions.

Table 3- 2: k_{detach} values for different mass fraction of PS/SP films before and after UV irradiation.

Mass fraction	k_{detach} before UV (min^{-1})	k_{detach} after UV (min^{-1})
0	0.05±.003	0.05±.003
0.05	0.0359±.006	0.012±.001
0.15	0.026±.002	0.006±.0001
0.2	0.021±.001	0.0016±.00003
0.29	0.018±.001	No detachment
0.4	0.008±.0005	No detachment

The photoinduced slowing of the delamination was observed for other photochromic molecules. The magnitude of k_{detach} suppression for another spiropyran derivative, nitro 1′, 3′-dihydro-8-methoxy-1′, 3′, 3′-trimethyl-6-nitrospiro[2*H*-1-benzopyran-2,2′-(2*H*)-indole] was similar to that for **SP**. When the spirooxazine photochrome 1,3,3-trimethylindolinonaphthospirooxazine was used, UV light similarly changed the film from colorless to a deep blue. But the photoinduced change in k_{detach} was smaller, decreasing from 8×10^{-3} min^{-1} to 1.5×10^{-3} min^{-1}. The **PS/DAE** films also exhibited a smaller change in the delamination rate, with k_{detach} $=2.2\times10^{-2}$ min^{-1} before irradiation and k_{detach} $=1.5\times10^{-2}$ min^{-1} afterward (Figure 3-4 b). We did not undertake an exhaustive survey of all possible photochromic reactions, but the k_{detach} values for the doped and undoped **PS** films studied in this work are given in this study. Finally, cleaning the glass slide using either acidic and basic piranha solutions resulted in the same decrease in k_{detach}. If the glass was not cleaned, the inhibition effect was much less reproducible, presumably due to the presence of hydrophobic surface contaminants that affected **PS** adhesion to the surface.

The magnitude of the photoinduced adhesion change was sensitive to the photochrome concentration, with a greater fraction of **SP** leading to stronger adhesion. The shear strength of the unexposed films was independent of the **SP** concentrations to within the experimental error. Figure 3-5 a shows how the shear strength of the UV-exposed films steadily increases as the **SP** loading increases. The dependence of k_{detach} on **SP** loading is harder to visualize because k_{detach} for unexposed samples increases with higher **SP** loading.

Moreover, k_{detach}(after UV) became effectively zero for the more concentrated samples. In Figure 3-5 b, we plot the ratio k_{detach}(after UV)/k_{detach}(before UV) to illustrate the suppression of the delamination rate for different **SP** concentrations. For a pure **PS** film, exposure to 365 nm light has no effect and this ratio is 1.0. But for films with high amounts of **SP**, this ratio rapidly drops to 0.0 as the films become permanently resistant to delamination.

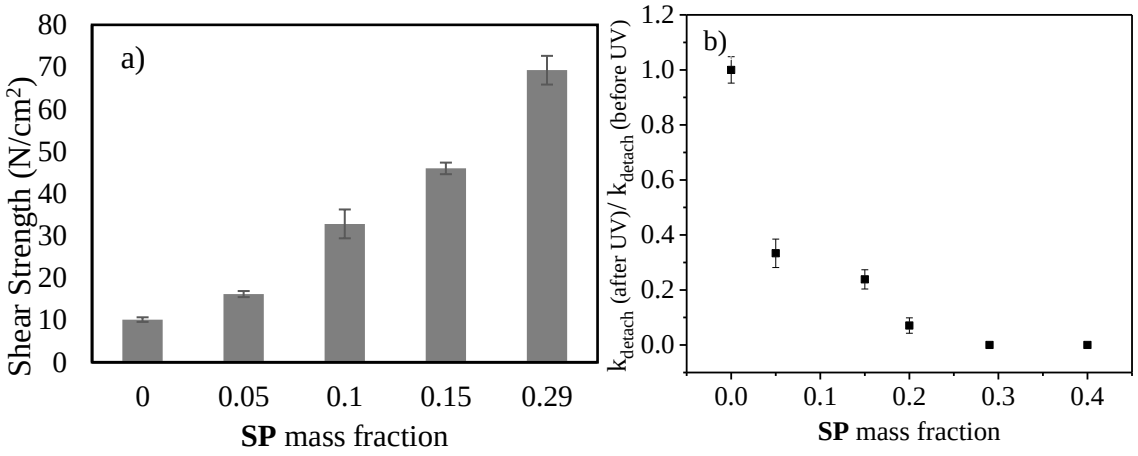

Figure 3-5 : **a)** Lap-shear test results for **PS/SP** films with varying **SP** mass fractions after UV exposure, showing enhanced photoinduced adhesion with increasing **SP** concentration. **b)** The dependence of the ratio k_{detach}(before UV)/k_{detach}(after UV) for varying **SP** mass fractions, showing that the photoinduced resistance to delamination increases with increasing **SP** concentration).

Having established that photochromic reactions in a polymer film can affect its adhesion to a clean glass surface, we now consider possible mechanisms for this effect.

We found that even when strongly attached to the glass, all of the UV-exposed films could still be easily dissolved in organic solvents and the photochrome absorption recovered. There was no evidence of a permanent chemical change in the polymer. The merocyanine isomer is more polar than the spiropyran form, and we considered the possibility that this polarity change strengthens the interaction of the polymer film with the hydrophilic surface. To assess the change in surface polarity, we measured the water contact angle. A neat **PS** film had a measured contact angle of 85.6º, in good agreement with previously measured values.[19-20] When the **PS** is doped with a 0.29 mass fraction of **SP**, the contact angle slightly decreased to 83.2±0.6°. After irradiation, the film color changed from colorless to purple, and the contact angle decreased to 78.6±0.4° (Figure 3-6). The contact angle change of ~5° is comparable to that observed for nitro-spiropyran doped poly(ethyl methacrylate) polymers[21] but less than that typically observed for polymer films with a high surface density of spiropyrans.[22-23] It is certainly possible that this polarity change contributes to the improved adhesion. But for the adhesion to persist after prolonged visible illumination, it must be assumed the merocyanines close to the glass surface resist conversion back to the **SP** form. Studies of **SP** isomerization on functionalized glass[22, 24-25] and alumina[26] provide no evidence that the reversibility can be prevented by a hydrophilic surface. The relatively small change in contact angle, the continued adhesion even after the less polar **SP** is regenerated, and the ability of **DAE** to promote adhesion, all suggest that a photoinduced surface polarity change is not primarily responsible for the increased adhesion.

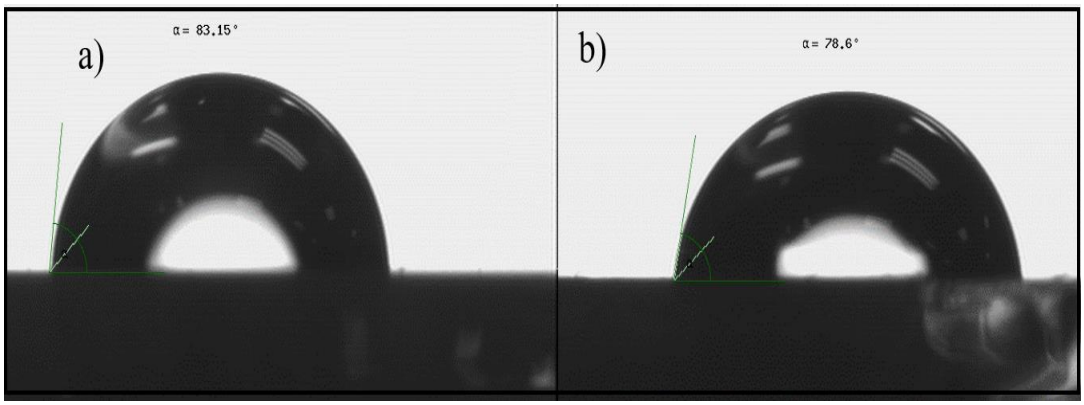

Figure 3-6: Contact angle measurement to measure change in surface polarity. **a)** contact angle for 0.29 mass fraction **PS/SP** before UV, **b)** contact angle after UV.

The fact that the adhesion changes are largely irreversible, even after the photochrome returns to its original state, suggests that the photochromic reaction induces a permanent change in the nanoscale polymer morphology. For example, local heating or softening could allow the **PS** to flow and conform to the glass surface. This would increase the surface contact of the polymer to the glass while removing small void spaces and channels that allow H_2O molecules to penetrate and decrease adhesive strength.[27] These morphology changes would not be photoreversible but would still allow the polymer film to be readily dissolved, as observed experimentally. To test this hypothesis, we measured the polymer mechanical properties.

Any annealing process that eliminates voids would be expected to make the material more dense and resistant to indentation, leading to higher elastic modulus and hardness values. Changes in the elastic modulus and hardness before and after UV exposure can be measured using nanoindentation. Unlike the delamination rate, there was no consistent trend in hardness and modulus values with increased **SP** loading before UV treatment. For pure **PS** films, there was no change in the hardness after UV exposure to within the error, and a very small decrease in elastic modulus that was close to the error. For the **PS/SP** films, UV exposure caused both the elastic modulus and hardness to increase by 5-10%, which is greater than the error range. The fractional changes in hardness and elastic modulus are plotted in Figure 3-7. The magnitude of these changes is comparable to the increase in stiffness of poly(ethyl methacrylate -co-methyl acrylate) doped with comparable levels of **SP** after UV exposure.[28] Photoisomerization of **SP** has also been shown to decrease the modulus of a different polymer [29], so there is no general rule as to how it affects polymer mechanical properties. The important point is that the photoinduced changes in mechanical properties tracked the **SP** mass fraction, as expected based on the adhesion results.

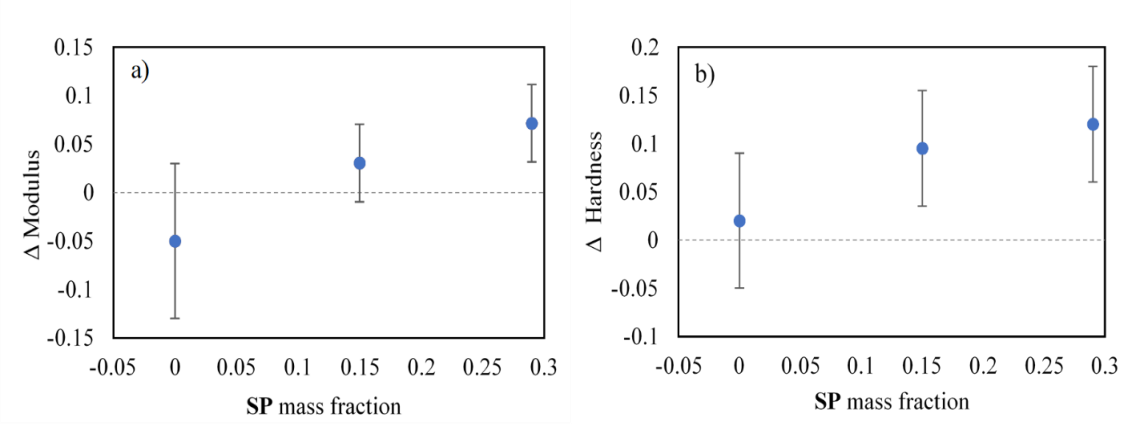

Figure 3-7: **a)** Fractional change in elastic modulus after UV exposure for different **SP** mass fractions. **b)** Fractional change in hardness after UV exposure for different **SP** mass fractions.

Table 3-3: Nanoindentation results: average modulus and hardness values with standard deviation calculated from indent maps of different mass fraction **PS**/**SP** films before and after UV exposure.

Film	Hardness (MPa)	Reduced Modulus (GPa)
PS	248 ± 11	5.99 ± 0.47
PS-UV	253 ± 16	5.69 ± 0.25
15% **SP**	252 ± 12	5.92 ± 0.20
15% **SP**- UV	276 ± 11	6.1 ± 0.20
29% **SP**	291 ± 10.	5.74 ± 0.24
29% **SP**-UV	326 ± 15	6.15 ± 0.16

If the photochromic reactions lead to an effective annealing of the polymer film, then we should see similar changes in the adhesion after thermal annealing. Consistent with this idea, we found that the shear strength of the polymer-glass bond could be increased by roughly a factor of 2 after heating at 50°C for 1 hour (Figure 3-8 a). Similarly, k_{detach} could be decreased by a factor of 20-40 after the same treatment (Figure 3-8 b). For both shear strength and delamination, the improvement due to thermal annealing was less than that generated by the photochromic reactions, even though the average temperature of the irradiated samples never rose more than 1ºC as measured by an optical thermometer. We attempted to increase the adhesion by heating **PS** films above their glass transition temperature, which is approximately 100°C.[30] After this treatment, about 40% of the films still detached quickly, but the rest remained stably attached to the glass (Figure 3-9). It appears that even after high-temperature thermal annealing, there is still some heterogeneity in the **PS** sample adhesion, while for the **PS**/**SP** films there is 100% attachment after UV exposure.

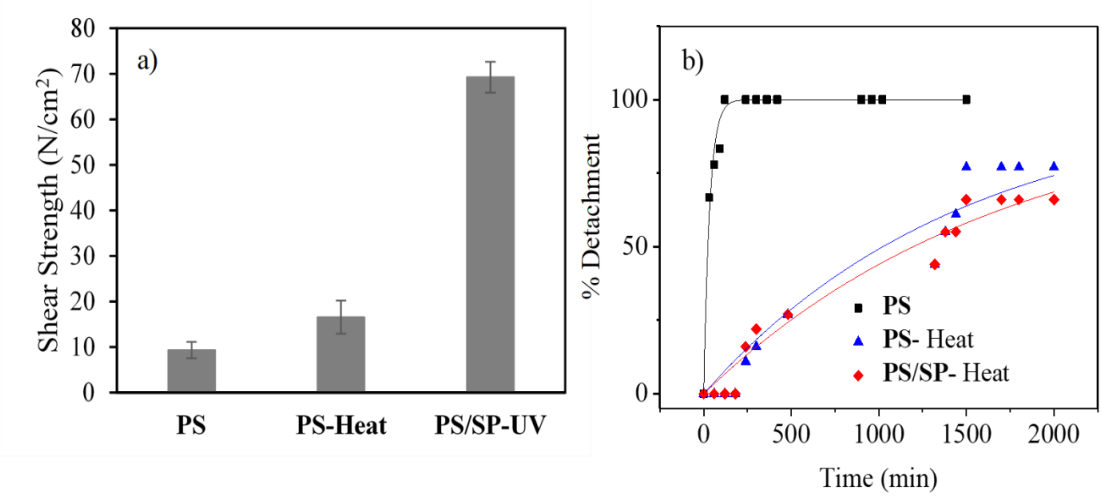

Figure 3-8: **a)** Comparison of lap-shear test results for neat **PS**, neat **PS** after heating to 50°C for 1 hour, and **PS/SP** after UV exposure. Both heating and photochromic reaction increase the adhesion, but the increase for the **PS/SP** film is at least 3 times larger. **b)** Time dependent detachment percentage for neat **PS**, neat **PS** after heating to 50°C for 1 hour, and **PS/SP** after heating to 50°C for 1 hour. For both heated films, k_{detach} was decreased by a factor of 20-40.

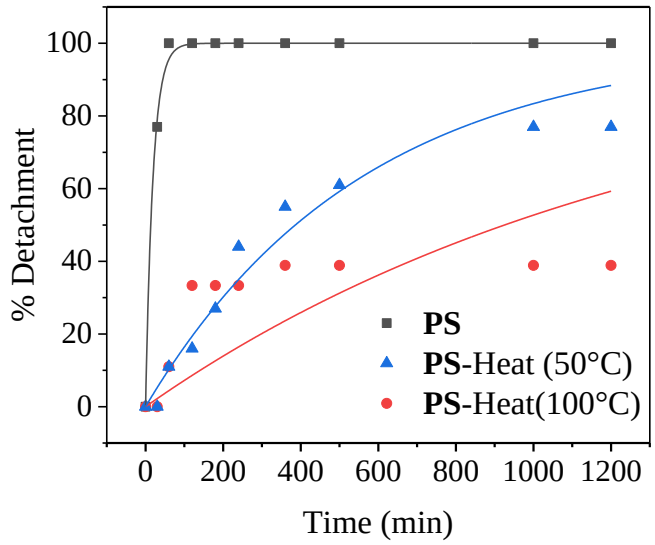

Figure 3-9: Experimental plots of the detachment percentage as a function of time. The black squares show the % detachment of neat **PS** (exponential fit yields k_{detach} = 0.05 min^{-1}), blue triangles show the % detachment of neat **PS** after heating to 50˚C for 60 min (exponential fit yields k_{detach} = 0.002 min^{-1}), and red circles show the % detachment of neat **PS** heated to 100˚C for 60 min (exponential fit yields k_{detach} = 0.0008 min^{-1}). Note that the exponential fit to the 100˚C is clearly not adequate, probably due to heterogeneity in the sample after heating.

Photochromic dopants based on azobenzene[31-32] and spiropyran[33-34] have been shown to induce photomechanical effects in amorphous polymers. Furthermore, the ability of photochromic reactions to drive spatial rearrangements and pattern formation is well established for polymer systems containing azobenzene.[35] We suspect that similar dynamics are responsible for the increased adhesion we observe. The change in adhesion clearly requires high photochrome concentrations (a 0.29 mass fraction corresponds to a

concentration of 0.89 Molar), where the glass surface sees a mixed molecular and polymer solid that is probably more fluid than a neat polymer. The physical distortion that accompanies photoisomerization, along with local heating, may be sufficient to drive rearrangements of both the polymer chains and dopant molecules. While the bulk concentration of the photochrome cannot change, it is possible that photoisomerization leads to morphology changes at the nanoscopic level, for example aggregation of the merocyanine isomer.[14, 34, 36-37] It is possible that such small-scale changes could be detected using scanning probe microscopy methods, but such measurements are beyond the scope of the present work. Finally, it should be noted that large spatial rearrangements in azobenzene-doped polymer typically required laser excitation and multiple cis-trans isomerization cycles.[38] In the present case, a single photochromic transformation cycle, initiated by lamp illumination, is sufficient to generate the nanoscale changes that modulate the adhesion.

3-3 Conclusion

The results in this chapter demonstrate that the photochromic reaction of a molecule embedded in a polymer film can affect its surface adhesion properties, as measured by shear strength and delamination in water. The size of the effect depends on the molecular structure of the photochrome and its concentration. The most dramatic results were obtained for **PS/SP** films, whose shear strength increased by a factor of 7 while the delamination rate was suppressed by at least 2 orders of magnitude after exposure to UV

light. We hypothesize that the changes in adhesion arise from localized polymer and molecular motions that eliminate void spaces and surface gaps. It is remarkable that this photochromic annealing appears to be more effective than bulk thermal annealing. Although the mechanism deserves further investigation, the demonstration of non-covalent photoinduced adhesion in polymer films is a promising step in the development of materials whose adhesive properties can be changed using light.

3-4 References

(1) Zeng, H., *Polymer Adhesion, Friction, and Lubrication*. Wiley: Hoboken, New Jersey, 2013.

(2) Gurney, R. S.; Dupin, D.; Nunes, J. S.; Ouzineb, K.; Siband, E.; Asua, J. M.; Armes, S. P.; Keddie, J. L., Switching Off the Tackiness of a Nanocomposite Adhesive in 30 s via Infrared Sintering. *ACS Appl. Mater. Interfaces* **2012,** *4*, 5442-5452.

(3) Saito, S.; Nobusue, S.; Tsuzaka, E.; Yuan, C.; Mori, C.; Hara, M.; Seki, T.; Camacho, C.; Irle, S.; Yamaguchi, S., Light-Melt Adhesive Based on Dynamic Carbon Frameworks in Columnar Liquid-Crystal Phase. *Nat. Commun.* **2016,** *7*, 12094/1-7.

(4) Goulet-Hanssens, A.; Sun, K. L. W.; Kennedy, T. E.; Barrett, C. J., Photoreversible Surfaces to Regulate Cell Adhesion. *Biomacromolecules* **2012,** *13*, 2958-2963.

(5) Blass, J.; Bozna, B. L.; Albrecht, M.; Krings, J. A.; Ravoo, B. J.; Wenz, G.; Bennewitz, R., Switching Adhesion and Friction by Light Using Photosensitive Guest-Host Interactions. *Chem. Commun.* **2015,** *51*, 1830-1833.

(6) Kadem, L. F.; Holz, M.; Suana, K. G.; Li, Q.; Lamprecht, C.; Herges, R.; Selhuber-Unkel, C., Rapid Reversible Photoswitching of Integrin-Mediated Adhesion at the Single-Cell Level. *Adv. Mater.* **2016,** *28*, 1799-1802.

(7) Zhang, J.; Ma, W.; he, X.-P.; Tian, H., Taking Orders from Light: Photo-Switchable Working/Inactive Smart Surfaces for Protein and Cell Adhesion. *ACS Appl. Mater. Interfaces* **2017,** *9*, 8498-8507.

(8) Strange, T. G.; Evans, D. F.; Hendrickson, W. A., Nucleation and Growth of Defects Leading to Dewetting of Thin Polymer Films. *Langmuir* **1997,** *13*, 4459-4465.

(9) Baxamusa, S. H.; Stadermann, M.; Aracne-Ruddle, C.; Nelson, A. J.; Chea, M.; Li, S.; Youngblood, K.; Suratwala, T. I., Enhanced Delamination of Ultrathin Free-Standing Polymer Films via Self-Limiting Surface Modification. *Langmuir* **2014,** *30*, 5126-5132.

(10) Maebayashi, M.; Matsuoka, T.; Koda, S.; Hashitani, R.; Nishio, T.; Kimura, S., Study on Polystyrene Thin Film on Glass Substrate by Scanning Acoustic Microscope. *Polymer* **2004,** *45*, 7563-7569.

(11) M.Yan; Harnish, B., A Simple Method for the Attachment of Polymer Films on Solid Substrates. *Adv. Mater.* **2003,** *15*, 244-248.

(12) Durr, H.; Bouas-Laurent, H., *Photochromism : molecules and systems*. Elsevier: New York, 1990.

(13) Berkovic, G.; Krongauz, V.; Weiss, V., Spiropyrans and Spirooxazines for Memories and Switches. *Chem. Rev.* **2000,** *100*, 1741-1753.

(14) Klajn, R., Spiropyran-Based Dynamic Materials. *Chem. Soc. Rev.* **2014,** *43*, 148-184.

(15) Irie, M.; Fukaminato, T.; Matsuda, K.; Kobatake, S., Photochromism of Diarylethene Molecules and Crystals: Memories, Switches, and Actuators. *Chem. Rev.* **2014,** *114*, 12174–12277.

(16) Freund, L. B.; Suresh, S., *Thin Film Materials: Stress, Defect Formation, and Surface Evolution*. Cambridge U. Press: Cambridge, 2003.

(17) Kook, S.-Y.; Dauskardt, R. H., Moisture-Assisted Subcritical Debondingn of a Polymer/Metal Interface. *J. Appl. Phys.* **2002,** *91*, 1293-1303.

(18) Sharratt, B. M.; Wang, L. C.; Dauskardt, R. H., Anomalous Debonding Behavior of a Polymer/Inorganic Interface. *Acta Mater.* **2007,** *55*, 3601-3609.

(19) Kwok, D. Y.; Lam, C. N. C.; Li, A.; Zhu, K.; Wu, R.; Neumann, A. W., Low-Rate Dynamic Contact Angles on Polystyrene and the Determination of Solid Surface Tensions. *Polym. Sci. Engin.* **1998,** *38*, 1675-1684.

(20) Li, Y.; Pham, J. Q.; Johnston, K. P.; Green, P. F., Contact Angle of Water on Polystyrene Thin Films: Effects of CO_2 Environment and Film Thickness. *Langmuir* **2007,** *23*, 9785-9793.

(21) Athanassiou, A.; Lygeraki, M. I.; Pisignano, D.; Lakiotaki, K.; Varda, M.; Mele, E.; Fotakis, C.; Cingolani, R.; Anastasiadis, S. H., Photocontrolled Variations in the

Wetting Capability of Photochromic Polymers Enhanced by Surface Nanostructuring. *Langmuir* **2006,** *22*, 2329-2333.

(22) Rosario, R.; Gust, D.; Hayes, M.; Jahnke, F.; Springer, J.; Garcia, A. A., Photo-Modulated Wettability Changes on Spiropyran-Coated Surfaces. *Langmuir* **2002,** *18*, 8062-8069.

(23) Wagner, N.; Theato, P., Light-Induced Wettability Changes on Polymer Surfaces. *Polymer* **2014,** *55*, 3436-3453.

(24) Wu, T.; Zou, G.; Hu, J.; Liu, S., Fabrication of Photoswitchable and Thermotunable Multicolor Fluorescent Hybrid Silica Nanoparticles Coated with Dye-Labeled Poly(N-isopropylacrylamide) Brushes. *Chem. Mater.* **2009,** *21*, 3788–3798.

(25) Park, Y. S.; Ito, Y.; Imanishi, Y., Photocontrolled Gating by Polymer Brushes Grafted on Porous Glass Filter. *Macromolecules* **1998,** *31*, 606-2610.

(26) Vlassiouk, I.; Park, C.-D.; Vail, S. A.; Gust, D.; Smirnov, S., Control of Nanopore Wetting by a Photochromic Spiropyran: A Light-Controlled Valve and Electrical Switch. *Nano Lett.* **2006,** *6*, 1013-1017.

(27) Frens, G., Depletion: A Key Factor in Polymer Adhesion. In *Adhesion Aspects of Polymer Coatings*, Mittal, K. L., Ed. Brill Academic: Zeist, The Netherlands, 2003; Vol. 2, pp 21-27.

(28) Samoylova, E.; Ceseracciu, L.; Allione, M.; Diaspro, A.; Barone, A. C.; Athanassiou, A., Photoinduced Variable Stiffness of Spiropyran-Based Composites. *Appl. Phys. Lett.* **2011,** *99*, 201905/1-.

(29) Zhang, X.; Zhou, Q.; Liu, H.; Liu, H., UV Light Induced Plasticization and Light Activated Shape Memory of Spiropyran Doped Ethylene-Vinyl Acetate Copolymers. *Soft Matter* **2014,** *10*, 3748-3754.

(30) Rieger, J., The Glass Transiton Temperature of Polystyrene: Results of a Round Robin Test. *J. Therm. Anal.* **1996,** *46*, 965-972.

(31) Tanchak, O. M.; Barrett, C. J., Light-Induced Reversible Volume Changes in Thin Films of Azo Polymers: The Photomechanical Effect. *Macromolecules* **2005,** *38*, 10566-10570.

(32) Barrett, C. J.; Mamiya, J.; Yager, K. G.; Ikeda, T., Photomechanical Effects in Azobenzene-Containing Soft Materials. *Soft Matter* **2007,** *3*, 1249-1261.

(33) Santos, E. A. G.-d. l.; Lozano-Gonzalez, M. J.; Johnson, A. F., Photoresponsive Polyurethane-Acrylate Block Copolymers. II. Photomechanical Effects in Copolymers Containing 6'-Nitro Spiropyranes and 6'-Nitro-bis-Spiropyranes. *J. Appl. Polym. Sci.* **1999,** *71*, 267-272.

(34) Athanassiou, A.; Kalyva, M.; Lakiotaki, K.; S.Georgiou; Fotakis, C., All-Optical Reversible Actuation of Photochromic-Polymer Microsystems. *Adv. Mater.* **2005,** *17*, 988-992.

(35) Cojocariu, C.; Rochon, P., Light-Induced Motions in Azobenzene-Containing Polymers. *Pure. Appl. Chem.* **2004,** *76*, 1479-1497.

(36) Cabrera, I.; Schvartsman, F.; Veinberg, O.; Krongauz, V., Photocontraction of Liquid Spiropyran-Merocyanine Films. *Science* **1984,** *226*, 341-343.

(37) Seki, T.; Ichimura, K.; Ando, E., Stable J-Aggregate Formation of Photoinduced Merocyanine in Bilayer Membrane. *Langmuir* **1988,** *4*, 1068-1069.

(38) Juan, M. L.; Plain, J.; Bachelot, R.; Royer, P.; Gray, S. K.; Wiederrecht, G. P., Stochastic Model for Photoinduced Surface Relief Grating Formation Through Molecular Transport in Polymer Films. *Appl. Phys. Lett.* **2008,** *93*, 153304/1-3.

Chapter 4: Photoinduced De-Adhesion of a Polymer Film Using a Photochromic Donor-Acceptor Stenhouse Adduct

4-1 Introduction

The ability of an organic film to adhere to an inorganic surface, like silica or a metal, can determine material properties like friction, chemical resistance, and electronic conductivity.[1] The metal-polymer interface has received considerable attention due to its importance in electronics and corrosion applications,[2-3] but the glass-polymer interface also has considerable practical importance, for example in composites.[4] Light provides a convenient and tunable noncontact way to modify the properties of the organic component via photochemistry. For example, in the case of a conductive polymer interface, photoisomerization of an organic photochromic layer can tune the interfacial barrier to charge injection.[5] In the case of adhesion, light can be used to generate covalent crosslinking between the polymer and substrate.[6-7] Photochemistry can also modulate noncovalent adhesive interactions by changing surface electrostatic properties.[8-14] In most of these examples, the photoswitching relied on the synthesis of a covalently attached surface layer of photochromic molecules, similar to what is used to modulate surface wettability. We recently showed that simpler approach, relying on the photoisomerization of photochromic dopants like spiropyran, could significantly increase adhesion between a polystyrene film and a clean silica substrate.[15] To explain this photoinduced adhesion, we hypothesized that the photoisomerization reactions could rearrange the surrounding

polymer chains, inducing nanoscale morphology changes that improved the mechanical contact between the film to the substrate.

In the covalent and noncovalent examples described above, photochemical changes lead to an increased adhesion. Using light activated photoswitches to decrease adhesion would arguably be just as useful, since it would permit the remote disassembly of structures with temporal and spatial control. One could imagine applications in fields like drug delivery, in which a capsule could be opened at a specific time and place in the body, or in manufacturing where a protective layer could be detached from a surface after it was no longer needed. Despite these potential advantageous properties, examples of light-controlled de-adhesion are not common. Branda and coworkers demonstrated photocontrolled adhesion on textured polydimethylsiloxane surfaces by taking advantage of changes in surface hydrophilicity generated by spiropyran photoisomerization.[16] Saito and coworkers showed that an anthracene-based liquid crystal could function as an adhesive at room temperature but a combination of ultraviolet (UV) light and high temperatures (200°C) could induce melting of the liquid crystal with a concomitant loss of adhesion.[17] The melting transition was initiated by photodimerization of anthracene pairs in the mesogen, permitting control by UV light, but the requirement of high temperatures probably limits the practical utility of this de-adhesion approach. The use of photoinduced thermal effects to reduce adhesion has been reported in azobenzene polymers[18] and in polymer composites.[19]

Based on our work on photochromic noncovalent adhesion in polymer films, we became interested in whether the concept of using photochemistry to modify noncovalent adhesive interactions could be applied to the problem of de-adhesion. In the previous chapter, the photoisomerizations involved bonding changes that increased the size of the photochrome, perturbing the surrounding polymer in a sort of annealing process that allowed the polymer to more closely conform to the substrate surface, increasing the mechanical adhesion.[15] We reasoned that a photoisomerization reaction that decreased molecular size might lead to the opposite effect; with the molecule pulling back from the substrate surface and lowering the adhesive forces. An additional goal was to find a photochrome that could be excited by visible rather than UV light, since visible light can penetrate more deeply into scattering environments and has less propensity to generate undesirable side reactions. A photochromic system that meets both criteria is the donor-acceptor Stenhouse adduct (**DASA**) family of molecules recently developed by Read de Alaniz and coworkers.[20-25] These photochromic molecules rely on a *cis*→*trans* photoisomerization followed by a ring-closing reaction, as outlined in Scheme 1. The detailed photophysics of this multistep transformation are still being worked out, but several generations of this scaffold have now been synthesized. The latest generation of **DASA** compounds absorb well into the near-infrared, while maintaining good isomer stability, rapid switching and high reversibility in dilute solutions.[26] Furthermore, the molecule (**DASA**) shown in Scheme 1 is somewhat unique because its isomerization produces a more compact product due to the ring-closing reaction shown in Scheme 4-2.

Calculations indicate a 12% decrease in molecular volume after photoisomerization (Table 4-1).

Table 4-1: Molecular Volume calculations. VEGA ZZ drug design software (3.1.1) was used to calculate the molecular volumes. This software uses the van der Waals radius for the calculations. Isomerized **DASA** (after light irradiation) undergoes a volume reduction of 10 Å^3, or about 12%.

	Molecular Volume
DASA (1)	84.9 Å^3
Isomerized **DASA** (2)	74.5 Å^3

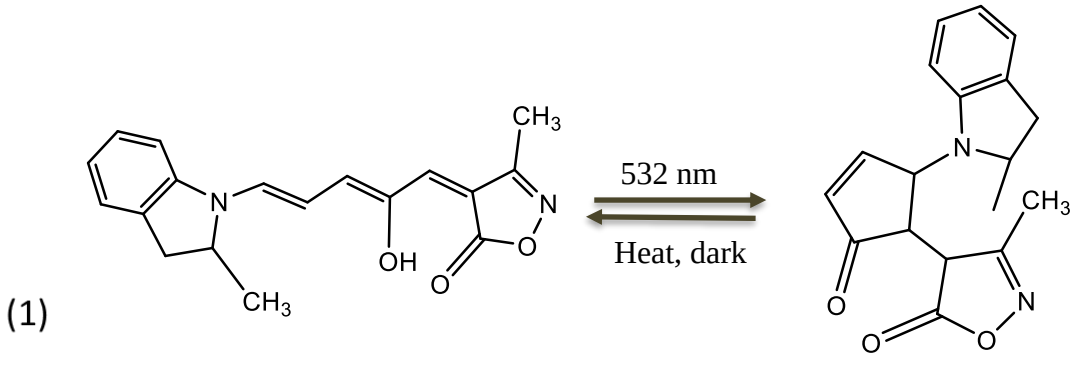

(1) (2)

Scheme 4-1: Photochromic behavior of third generation **DASA** molecule which isomerizes from the open form (1) to the closed form (2) after 532 nm irradiation

The promising attributes of the **DASA** photochromes motivated us to investigate how this photochromism affects the adhesion of polystyrene (PS) films to clean silica surfaces. Both shear and pull-off adhesive forces, as well as water delamination rates, are measured before and after irradiation. Changes in the spectroscopic properties and surface wettability are measured as well. Although it is not a particularly strong adhesive, the **DASA**/PS system does undergo photoinduced de-adhesion under ambient (room temperature) conditions. The ability to reduce polymer adhesion using visible light allows us to demonstrate the controlled release of dye molecules from a glass container, where they have been stored as a dry powder. These results demonstrate that the relatively simple approach of blending photochromic molecules in a polymer matrix can generate a new composite material with light-switchable properties.

4-2 Results and Discussion

The **DASA** molecule used in our experiments is shown in Scheme 1, which also shows the photoisomerization pathway. It is a third generation molecule that features a red-shifted absorption and improved isomer stability.[26] The absorption spectrum in solution and at high (0.08 mass fraction) loading in PS are shown in Figure 4-1. The photochromic behavior of **DASA** in dilute solution and polymer hosts has been extensively characterized.[25] Illumination at visible wavelengths leads to rapid disappearance of the absorbance, while removal of the light allows for a full recovery of the absorption on a timescale of seconds to minutes (Figure 4-1a). At the high concentrations used in our

polymer adhesion experiments, however, there are several differences (Figure 4-1b). First, the absorption lineshape is broadened and slightly shifted, indicating that intermolecular interactions affect the molecule's electronic states. More importantly, the rapid absorbance loss and facile thermal reversibility observed in dilute samples is not seen in the concentrated samples. Instead of minutes, visible light exposure times on the order of 10 hours are required to induce the absorption change, and the absorption does not recover at all on the timescale of days. This slowdown in the photochromic kinetics and loss of reversibility at high **DASA** concentrations is the subject of a separate paper.[27] However, it should be noted that the **DASA** photochromism is not reversible for the high concentration samples that show measurable changes in adhesion. Control experiments support that the lack of reversibility was not due to a photodegradation pathway. After conversion, the colorless films were redissolved in a fixed volume of CH_2Cl_2. Upon dilution, the **DASA** molecules rapidly converted back to the open form, and the visible open-form absorbance was completely recovered (Figure 4-2). This shows that high concentrations do not introduce a new irreversible photochemical pathway, but instead inhibit the previously identified cyclization pathway and its reversal.

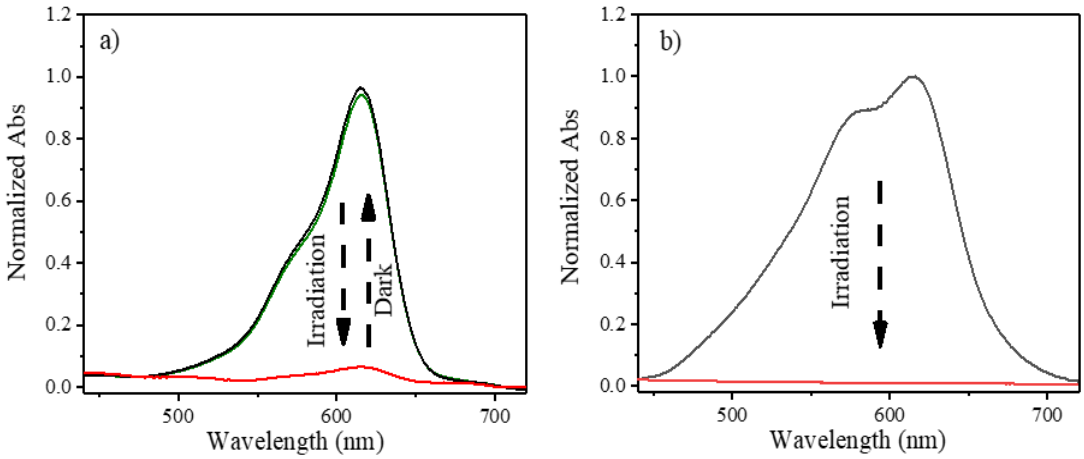

Figure 4-1: a) Normalized absorption of **DASA**/PS in dichloromethane before (black) and after laser irradiation (red). After 20 minutes, the absorption completely recovers (green), b) Normalized absorption of spin coated **DASA**/PS (black) and after 14 hours of 532 nm laser irradiation (red). Note that the red spectrum in panel a) fully recovers after a few minutes, while that in panel b) does not recover.

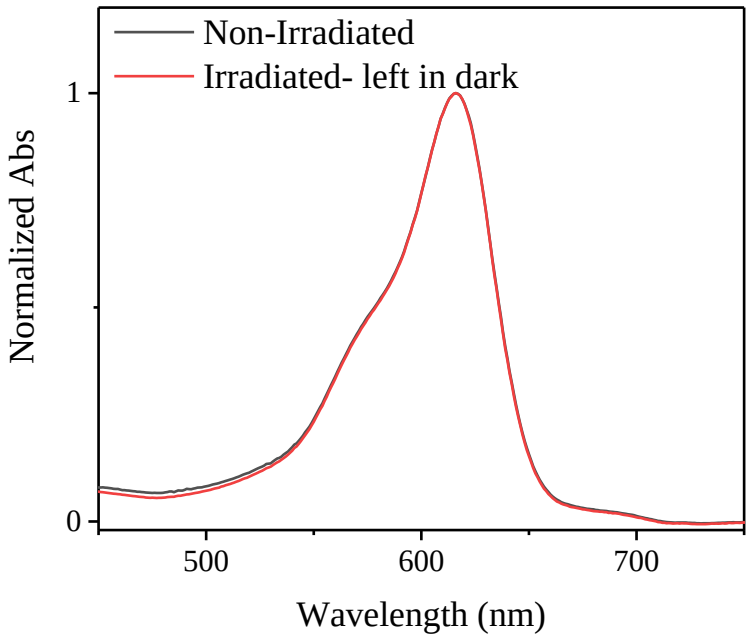

Figure 4-2: Absorption spectrum of **DASA**/PS/CH_2Cl_2 solution before depositing as a solid film (black) and the same sample after the solid film was irradiated for 14 hr to completely convert it, then redissolved in CH_2Cl_2 and finally allowed to convert back to the open form in solution (red). There is no sign of a permanent chemical change in the film.

To completely convert the **DASA** in a 0.08 mass fraction **DASA**/PS film, approximately 14 hr of exposure to 532 nm light at an intensity of 6 mW/cm^2 was required. After this period, the visible open-form **DASA** absorption completely disappeared and the blue films turned colorless. The next question was whether this color change was accompanied by a change in the adhesion properties. We used three different methods to assess polymer adhesion. First, the shear adhesion was measured as the force-per-area required to pull apart two glass slides that sandwiched a **DASA**/PS layer. In this

experiment, the force is applied parallel to the adhesive surface. The results of these measurements, before and after light exposure, are shown in Figure 4-3 for various **DASA** loadings. PS by itself is a hydrophobic, nonpolar material that only weakly adheres to the hydrophilic silica surface.[28-29] As the **DASA** concentration is increased, the adhesion force of the nonirradiated sample increases steadily. After irradiation, the shear force required to separate the slides dropped by ~30%, especially for the more concentrated samples, as shown in Figure 4-6. The shear adhesion test, in which the force is applied parallel to the polymer-glass interface, was complemented by pull-off adhesion test in which the force was applied normal to the interface. Data from this experiment is plotted in Figure 4-4, showing an even more pronounced increase in adhesion with **DASA** loading before irradiation, along with a ~20% decrease after irradiation.

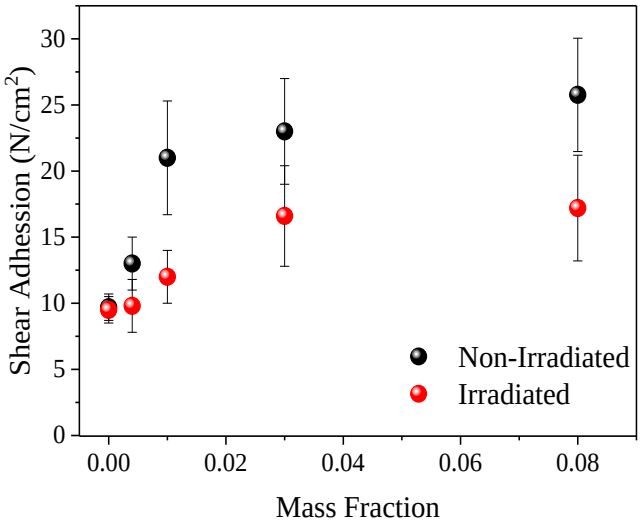

Figure 4-3: Shear adhesion measurements of **DASA**/PS thin films before (black) and after (red) 532 nm irradiation for various **DASA**/PS mass fraction samples.

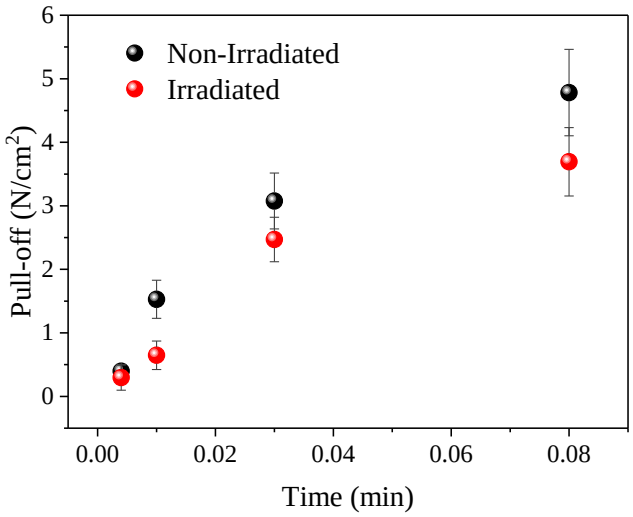

Figure 4-4: Pull-off adhesion measurements of **DASA**/PS thin films before (black) and after (red) 532 nm irradiation for various **DASA**/PS mass fraction samples.

The two force-based measures of dry adhesion were complemented by a third measurement of the polymer film delamination in water. As in our previous experiments on spiropyran/PS films,[15] the detachment of drop-cast polymer films in a stirred water environment was monitored over time. An example of the experimental results for a 0.01 mass fraction **DASA**/PS films is shown in Figure 4-8a. Before irradiation, the films were highly water resistant, with almost no detachment over the course of 24 hours. After irradiation, the films rapidly detached. The time-dependent detachment can be modeled as a first-order kinetic process, since it is believed to rely on diffusion of water into the

polymer-glass interface.[30-31] The fraction of detached films (F_{detach}) is then given by an exponential function:

$$F_{detach} = 1 - e^{-t/\tau_{detach}} \quad (1)$$

where τ_{detach} is the characteristic detachment lifetime and t is the time spent in the agitated water solution. The exponential fits are overlaid with the detachment data in Figure 4-5a, and in Figure 4-5b we plot the τ_{detach} values before and after irradiation for different **DASA** loadings. In water, PS tends to quickly delaminate from glass surfaces.[32] The addition of **DASA** increases τ_{detach} for the unirradiated samples, consistent with the data in Figures 4-6 and 4-7. After irradiation, the magnitude of the change in τ_{detach} was much greater than for the shear and pull-off adhesive force data in Figures 4-3 and 4-4 where τ_{detach} decreased by 90% for the 0.08 mass fraction sample, as compared to a 20-30% change in the adhesion force per area. Presumably, the light-induced change would be even more dramatic for higher **DASA** loadings, but above 10% mass fraction 100% photoconversion was not achieved, even after 24 hr of light exposure. Samples with higher loadings showed smaller adhesion changes because of this incomplete conversion.

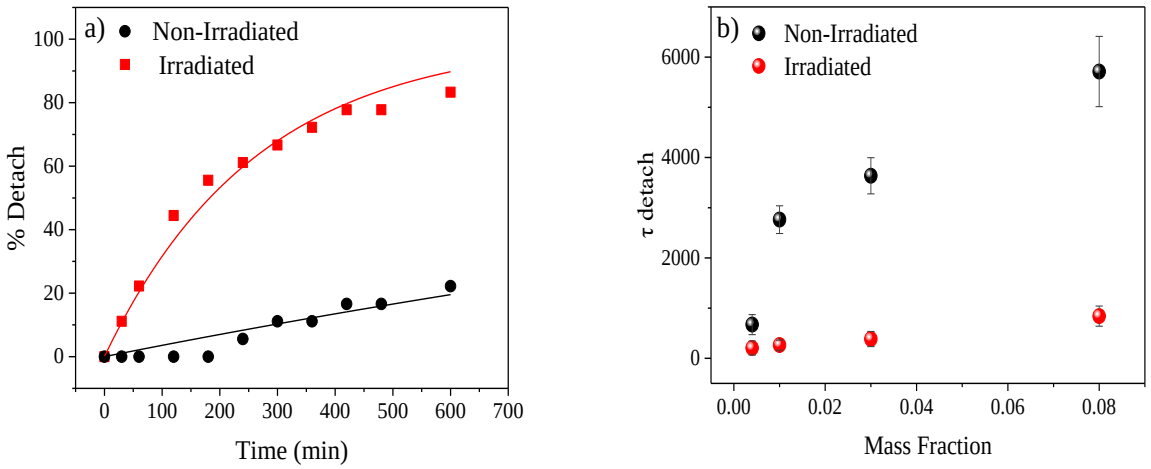

Figure 4-6: a) Time-dependent detachment percentage **DASA**/PS for mass fraction of 0.01 before (black) and after (red) 532 nm irradiation. b) τ_{detach} values for mass fractions of 0.004, 0.01, 0.03, 0.08 (red) and the values reduces significantly after irradiation (black).

To explain the previously observed photoinduced adhesion increase in **SP**/PS films, we hypothesized that the photochromic reaction resulted in localized annealing of the polymer film that enhanced the nanoscale mechanical contact between the surfaces.[15] But this type of local morphology change cannot explain the de-adhesion seen here. First, heating to 60ºC on the **DASA**/PS films resulted in increased adhesion and resistance to delamination in water (Figure 4-7), the opposite of what is observed upon exposure to light. Second, we looked for evidence of surface roughening by using atomic force microscopy (AFM) to measure the surface before and after irradiation. The AFM scans were indistinguishable (Figure 4-8) and yielded the same roughness values (1.3 ±0.4 nm and 1.1±0.2 nm) to within the experimental error.

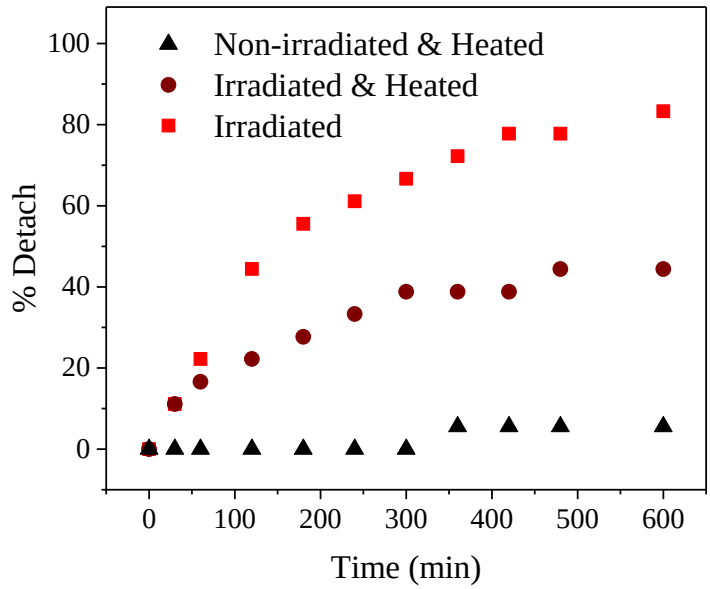

Figure 4-7: Effect of heat on the water detachment of a **DASA**/PS film with mass fraction of 0.01. Heating the irradiated (brown) and non-irradiated (black) films to 60°C does not accelerate detachment relative to the unheated, irradiated sample (red). Heating decreases the detachment rate for all samples, consistent with mechanical annealing of the polymer film.

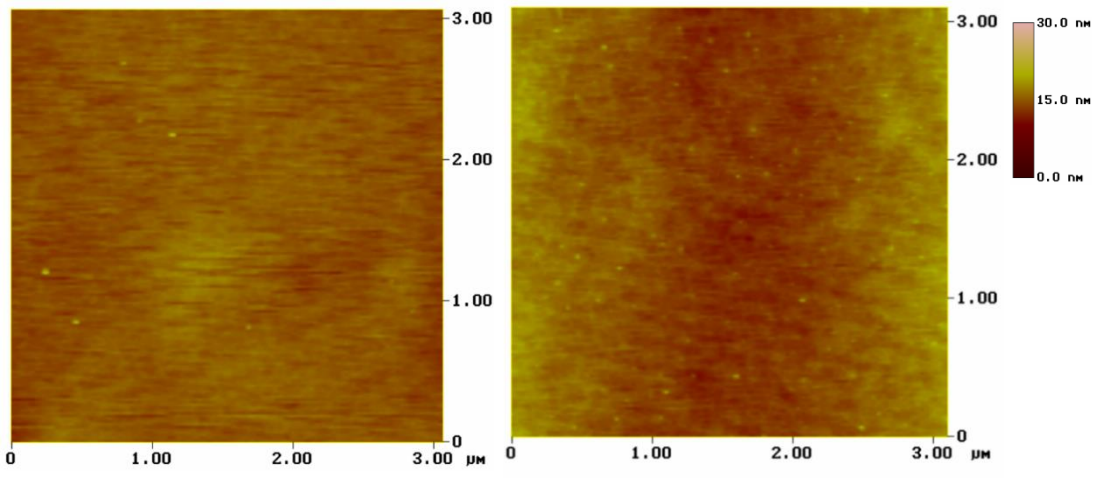

Figure 4-8: a) AFM image of a **DASA**/PS film before irradiation, with a calculated roughness of 1.1 ± 0.3 nm. b) AFM image after irradiation, with a calculated roughness of 1.3 ± 0.3 nm, indistinguishable from that of the non-irradiated film.

As mentioned above, there is no sign of irreversible photochemistry (e.g. cross-linking), since the open-form **DASA** isomer could be completely recovered after dissolution of the light-exposed film. To probe the possible role of changes in the surface chemistry, we used surface contact angle measurements. For the previously studied SP/PS films, the presence of the SP had only a small effect on the surface contact angle, with a light-induced change of 86º to 83º, as compared to 85º for neat PS. In the **DASA**/PS films, we saw similarly small changes, as summarized in Table 4-2. The 0.08 mass fraction **DASA**/PS film had an initial contact angle is 87.4º for a pH=7 water droplet, suggesting that the presence of the **DASA** makes the surface slightly more hydrophobic than PS. After irradiation, the contact angle drops to 84.8º, identical to that of neat PS to within the error.

Interestingly, the contact angle on samples before irradiation depended on the water pH. For acidic water (pH=2), the initial contact angle was significantly smaller, 84.0±0.3° versus 87.4±0.1° for pH=7. The contact angle also did not change after irradiation, to within the error, unlike the pH=7 droplet. The contact angle of neat PS film was not sensitive to pH or irradiation. These contact angle changes are smaller than for polymer films containing a high density of photochromes[33-34] but are comparable to those observed for doped polymer films.[35]

Table 4-2: Contact angle of spin-coated **DASA**/PS films on a glass substrate with water droplet at two different pH values.

	pH=2	pH=7
PS	86 ± 0.6	85.6 ± 0.7
DASA/PS	84 ± 0.3	87.4 ± 1
DASA/PS Irradiated	83.8 ± 0.3	84.8 ± 0.4

The sensitivity of the surface contact angle to pH suggested that acid-base or other types of surface-specific chemical interactions could be important. This suspicion was

reinforced by the sensitivity of the photoinduced de-adhesion to the glass cleaning procedure. Precleaning the glass slides with an acid piranha wash (H_2SO_4/H_2O_2) gave the de-adhesion results shown in Figures 2-4. When the glass was not cleaned at all, no photoinduced change is observed. When a basic piranha wash (NH_4OH/H_2O_2) was used, the photoinduced adhesion change was much smaller because the initial adhesion was much weaker, comparable to that of PS (Figure 4-9). This pH sensitivity contrasts with the lack of sensitivity to acid/base washing observed for the spiropyran/PS system where mechanical effects were dominant.[15] A second piece of evidence indicating that the adhesion change is chemical in nature was provided by an experiment in which we exposed the **DASA**/PS solution to 532 nm light before casting solid films. In solution, the photoisomerization proceeds quickly and high conversion is possible within a few minutes. The converted solution was then deposited to form a solid film containing mostly the photoisomer. These films showed the same rapid detachment in water as the irradiated films (Figure 4-10), despite the fact that they were never exposed to light in solid form. These results point to a change in **DASA**'s chemical structure as the source of the deadhesion, rather than a change in morphology of the polymer host.

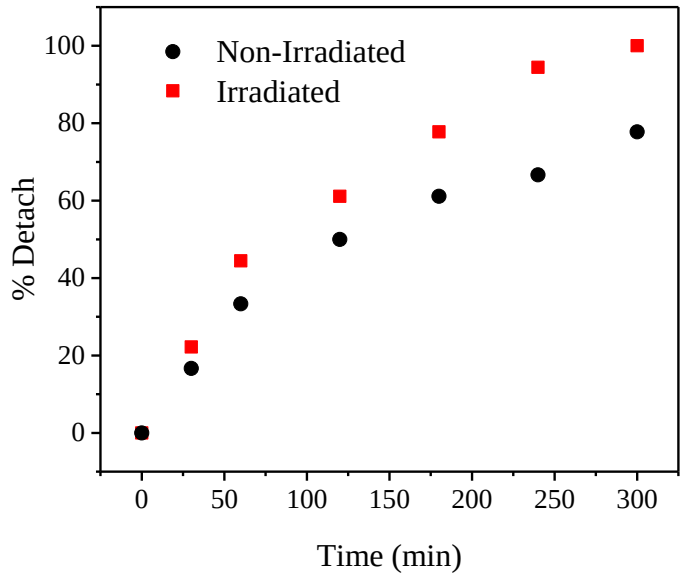

Figure 4-9: Water detachment rates for a 0.01 mass fraction **DASA**/PS film after a basic piranha wash before (black) and after irradiation (red). The initial adhesion was much weaker than for the acid wash, and no significant photoinduced change in the detachment rate was observed.

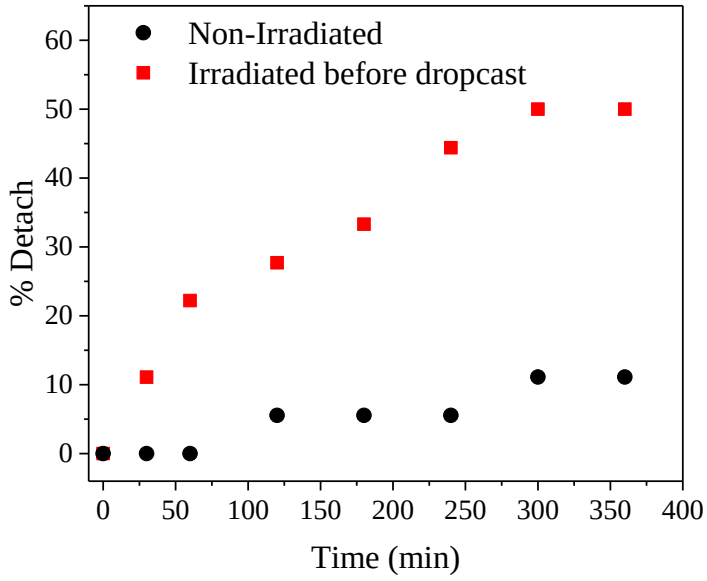

Figure 4-10: Water detachment rates for a 0.01 mass fraction **DASA**/PS film that has not been irradiated (black) and one that was irradiated to full conversion while in the CH_2Cl_2 solution before film deposition (red). The presence of the **DASA** photoisomer accelerates detachment even when it is created before the solid polymer film is formed by evaporation.

A possible mechanism for the photoinduced de-adhesion that is consistent with our observations is outlined in Figure 4-11. Given the high concentrations used, there are many **DASA** molecules located near the polymer surface. If a significant fraction exists with their tertiary amine groups oriented toward the surface, this would explain the lower contact angle observed for acidic water,[36-37] although attempts to directly quantify the nitrogen content at the surface using X-ray photoelectron spectroscopy were unsuccessful. Moreover, at the glass-polymer interface, these amines would be available to interact with surface silanol groups, forming a hydrogen-bond or proton donor complex.[38-39] The acidic

cleaning treatment should result in a higher density of protonated silanols[40-42] and thus enhanced bonding to the **DASA** amine groups.[43] The ability to support this amine-silanol interaction will depend sensitively on the surface specific orientation of the **DASA** within the PS, and this orientation would likely change after photoisomerization. For example, the photoinduced molecular-level contraction could pull the amine back into the bulk PS, disrupting the noncovalent interaction that led to stronger adhesion in the nonirradiated sample. It is also possible that photoisomerization enable the formation of hydrogen-bonded **DASA** pairs at these high concentrations. Such hydrogen-bonded pairs have been observed in crystal structures of the ring-closed form.[44] In either scenario, photoisomerization would eliminate some fraction of the amine-silanol interactions and weaken adhesion of the polymer film.

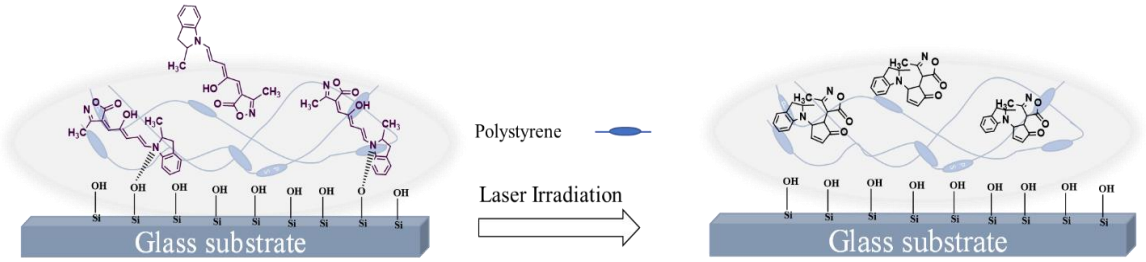

Figure 4-11: Proposed mechanism for de-adhesion of **DASA**/PS films from glass surfaces. The **DASA** photoisomerization leads to a ring-closing and molecular contraction that interferes with the amine-silanol interaction.

The small decrease in adhesion (Figures 4-4 and 4-5) is accompanied by a large change in the detachment rate in aqueous solutions (Figure 4-6). To highlight the potential

utility of the de-adhesion effect in a practical application, we hypothesized that the **DASA**/PS composite could be used as a photoswitchable release mechanism. To illustrate this application of the photochromic de-adhesion, we placed a water-soluble food dye (Allura Red) in a microscope well plate that had been precleaned using an acid piranha solution. A second precleaned glass slide was then glued to the well slide using the 0.08 mass fraction **DASA**/PS mixture and allowed to dry. The solid dye particles were completely enclosed by the two glass plates, as shown in Figure 4-12a, and remained as a dry powder after being submerged in water. Two identical assemblies were then placed in a water bath, and one irradiated with 532 nm light while the other was left in the dark. The unirradiated sample remained intact for >24 hr before the two glass plates separated and the dye was released into the surrounding water. The irradiated assembly separated after 5 hr, as shown by the sequence of images in Figure 4-12b. Eventually, the detachment of the lower glass slide leads to a sudden jump in dye concentration as measured by its absorbance (Figure 4-13). This proof-of-principle experiment demonstrates that it is possible to use a photoswitchable, water-proof adhesive to control the release of molecules into an aqueous environment.

a)

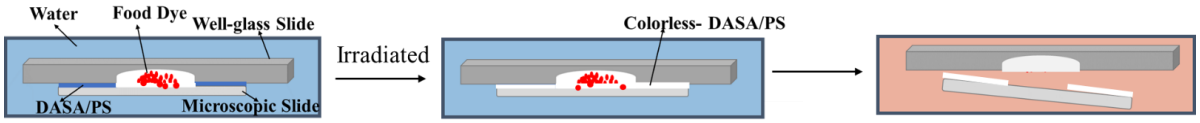

b)

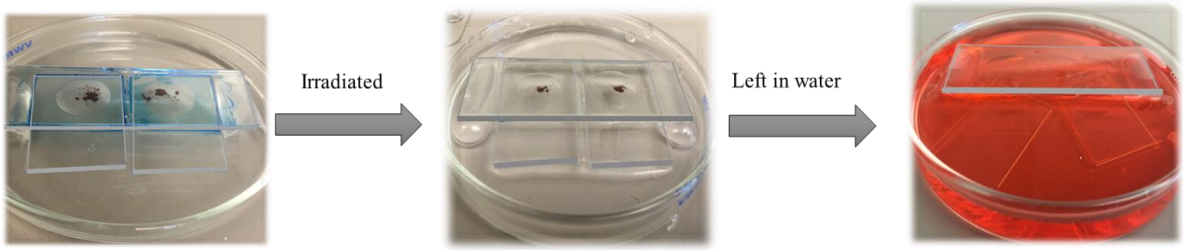

Figure 4-12: a) Schematic illustration for dye release. The solid dye particles are encapsulated between 2 glass slides which are glued together by a **DASA**/PS film. 532 nm irradiation causes the adhesion to fail and the bottom slide to drop off, releasing the dye into the surrounding water. b) Photographs of the sample before and after irradiation, and then after de-adhesion and dye release.

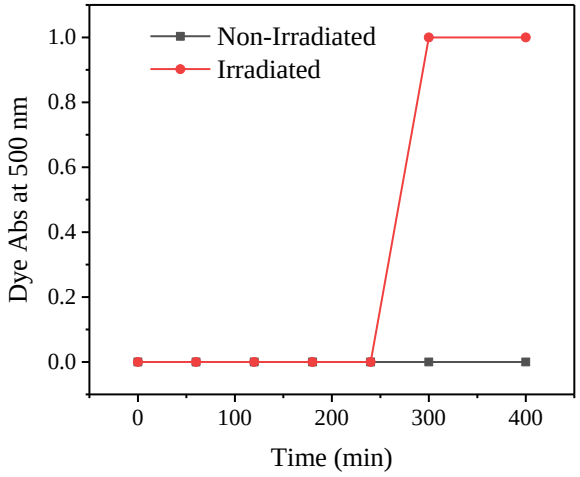

Figure 4-13: Absorption of Allura Red in water as a function of time for the irradiated (red) and non-irradiated (black) encapsulated dye samples. The jump in absorption after 4 hours represents the release of the dye after the de-adhesion of the bottom glass slide.

4-4 Conclusion

In this chapter, we have used a newly developed **DASA** photochromic molecule that enables the PS-glass adhesive bond to be significantly weakened after visible light exposure. Preliminary investigations into the physical origin of this effect suggest that molecular-level noncovalent interactions between the **DASA** photochrome and the glass surface are weakened after photoisomerization. We hypothesized that photoinduced electrocyclization of **DASA** molecules disrupts interfacial bonding interactions between the **DASA** amine groups and surface silanols. This proposed mechanism requires more experimental work to be verified. In the meantime, we demonstrated that this phenomenon can be harnessed to enable the photo-controlled release of molecules from a closed glass container into the surrounding water. These results illustrate how organic molecular photochemistry in solid matrices can lead to new and unexpected effects that may have practical applications.

4-5 References

(1) Zeng, H., *Polymer Adhesion, Friction, and Lubrication*. Wiley: Hoboken, New Jersey, 2013.

(2) Baute, N.; Jerome, C.; Martinot, L.; Mertens, M.; Geskin, V. M.; Lazzaroni, R.; Bredas, J. L.; Jerome, R., Electrochemical Strategies for Strengthening of Polymer-Metal Interfaces. *Eur. J. Inorg. Chem.* **2001**, 1097-1107.

(3) Grundmeier, G.; Stratmann, M., Adhesion and De-Adhesion Mechanisms at Polymer/Metal Interafaces: Mechanistic Understandings Based on In Situ Studies of Buried Interfaces. *Annu. Rev. Mater. Res.* **2005,** *35*, 571-615.

(4) Liu, Z.; Zhang, L.; Yu, E.; Ying, Z.; Zhang, Y.; Liu, X.; Eli, W., Modification of Glass Fiber Surface and Glass Fiber Reinforced Polymer Composites Challenges and Opportunities: From Organic Chemistry Perspective. *Curr. Org. Chem.* **2015,** *19,* 991-1010.

(5) Wang, Q.; Diez-Cabanes, V.; Dell'Elce, S.; Liscio, A.; Kobin, B.; Li, H.; Bredas, J. L.; Hecht, S.; Palermo, V.; List-Kratochvil, E. J. W.; Cornil, J.; Koch, N.; Ligorio, G., Dynamically Switching the Electronic and Electrostatic Properties of Indium-Tin Electrodes with Photochromic Monolayers: Toward Photoswitchable Optoelectronic Devices. *ACS Appl. Nano Mater.* **2019,** *2*, 1102-1110.

(6) M.Yan; Harnish, B., A Simple Method for the Attachment of Polymer Films on Solid Substrates. *Adv. Mater.* **2003,** *15*, 244-248.

(7) Vitale, A.; Trusiano, G.; Bongiovanni, R., UV-Curing of Adhesives: a Critical Review. *Rev. Adhesion Adhesives* **2017,** *5*, 105-161.

(8) Goulet-Hanssens, A.; Sun, K. L. W.; Kennedy, T. E.; Barrett, C. J., Photoreversible Surfaces to Regulate Cell Adhesion. *Biomacromolecules* **2012,** *13*, 2958-2963.

(9) Wang, N.; Li, Y.; Zhang, Y.; Liao, Y.; Liu, W., High-Strength Photoresponsive Hydrogels Enable Surface-Mediated Gene Delivery and Light-Induced Reversible Cell Adhesion/Detachment. *Langmuir* **2014,** *30*, 11823−11832.

(10) Blass, J.; Bozna, B. L.; Albrecht, M.; Krings, J. A.; Ravoo, B. J.; Wenz, G.; Bennewitz, R., Switching Adhesion and Friction by Light Using Photosensitive Guest-Host Interactions. *Chem. Commun.* **2015,** *51,* 1830-1833.

(11) Kadem, L. F.; Holz, M.; Suana, K. G.; Li, Q.; Lamprecht, C.; Herges, R.; Selhuber-Unkel, C., Rapid Reversible Photoswitching of Integrin-Mediated Adhesion at the Single-Cell Level. *Adv. Mater.* **2016,** *28*, 1799-1802.

(12) Zhang, J.; Ma, W.; He, X.-P.; Tian, H., Taking Orders from Light: Photo-Switchable Working/Inactive Smart Surfaces for Protein and Cell Adhesion. *ACS Appl. Mater. Interfaces* **2017,** *9*, 8498-8507.

(13) Lamping, S.; Stricker, L.; Ravoo, B. J., Responsive Surface Adhesion Based on Host–Guest Interaction of Polymer Brushes with Cyclodextrins and Arylazopyrazoles. *Polymer J.* **2019,** *10*, 683–690.

(14) Grzelczak, M.; Liz-Marzan, L. M.; Klajn, R., Stimuli-Responsive Self-Assembly of Nanoparticles. *Chem. Soc. Rev.* **2019,** *48*, 1342-1361.

(15) Mostafavi, S. H.; Tong, F.; Dugger, T. W.; Kisailus, D.; Bardeen, C. J., Noncovalent Photochromic Polymer Adhesion. *Macromolecules* **2018,** *51*, 2388−2394.

(16) Tannouri, P.; Arafeh, K. M.; Krahn, J. M.; Beaupré, S. L.; Menon, C.; Branda, N. R., A Photoresponsive Biomimetic Dry Adhesive Based on Doped PDMS Microstructures. *Chem. Mater.* **2014,** *26*, 4330−4333.

(17) Saito, S.; Nobusue, S.; Tsuzaka, E.; Yuan, C.; Mori, C.; Hara, M.; Seki, T.; Camacho, C.; Irle, S.; Yamaguchi, S., Light-Melt Adhesive Based on Dynamic Carbon Frameworks in a Columnar Liquid-Crystal Phase. *Nat. Comm.* **2016,** *7*, 12094/1-7.

(18) Akiyama, H.; Fukata, T.; Yamashita, A.; Yoshida, M.; Kihara, H., Reworkable Adhesives Composed of Photoresponsive Azobenzene Polymer for Glass Substrates. *J. Adhesion* **2017,** *93*, 823–830.

(19) Gurney, R. S.; Dupin, D.; Nunes, J. S.; Ouzineb, K.; Siband, E.; Asua, J. M.; Armes, S. P.; Keddie, J. L., Switching Off the Tackiness of a Nanocomposite Adhesive in 30 s via Infrared Sintering. *ACS Appl. Mater. Interfaces* **2012,** *4*, 5442-5452.

(20) Helmy, S.; Oh, S.; Leibfarth, F. A.; Hawker, C. J.; Alaniz, J. R. d., Design and Synthesis of Donor−Acceptor Stenhouse Adducts: A Visible Light Photoswitch Derived from Furfural. *J. Org. Chem.* **2014,** *79*, 11316−11329.

(21) Lerch, M. M.; Wezenberg, S. J.; Szymanski, W.; Feringa, B. L., Unraveling the Photoswitching Mechanism in Donor−Acceptor Stenhouse Adducts. *J. Am. Chem. Soc.* **2016,** *138*, 6344−6347.

(22) Mallo, N.; Brown, P. T.; Iranmanesh, H.; MacDonald, T. S. C.; Teusner, M. J.; Harper, J. B.; Ball, G. E.; Beves, J. E., Photochromic Switching Behaviour of Donor–Acceptor Stenhouse Adducts in Organic Solvents. *Chem. Commun.* **2016,** *52*, 13576-13579.

(23) Bull, J. N.; Carrascosa, E.; Mallo, N.; Scholz, M. S.; Silva, G. d.; Beves, J. E.; Bieske, E. J., Photoswitching an Isolated Donor−Acceptor Stenhouse Adduct. *J. Phys. Chem. Lett.* **2018,** *9*, 665−671.

(24) Donato, M. D.; Lerch, M. M.; Lapini, A.; Laurent, A. l. D.; Iagatti, A.; Bussotti, L.; Ihrig, S. P.; Medved, M.; Jacquemin, D.; Szymański, W.; Buma, W. J.; Foggi, P.; Feringa, B. L., Shedding Light on the Photoisomerization Pathway of Donor−Acceptor Stenhouse Adducts. *J. Am. Chem. Soc.* **2017,** *139*, 15596−15599.

(25) Lerch, M. M.; Szymanski, W.; Feringa, B. L., The (Photo)chemistry of Stenhouse Photoswitches: Guiding Principles and System Design. *Chem. Soc. Rev.* **2018,** *47*, 1910-1937.

(26) Hemmer, J. R.; Page, Z. A.; Clark, K. D.; Stricker, F.; Dolinski, N. D.; Hawker, C. J.; Alaniz, J. R. d., Controlling Dark Equilibria and Enhancing Donor−Acceptor Stenhouse Adduct Photoswitching Properties through Carbon Acid Design. *J. Am. Chem. Soc.* **2018,** *140*, 10425−10429.

(27) Lui, B. F.; Tierce, N. T.; Tong, F.; Sroda, M. M.; Luo, H.; Alaniz, J. R. d.; Bardeen, C. J., Unusual Concentration Dependence of the Photoisomerization Reaction in Donor-Acceptor Stenhouse Adducts. *submitted for publication* **2019**.

(28) Stange, T. G.; Evans, D. F.; Hendrickson, W. A., Nucleation and Growth of Defects Leading to Dewetting of Thin Polymer Films. *Langmuir* **1997,** *13*, 4459-4465.

(29) Baxamusa, S. H.; Stadermann, M.; Aracne-Ruddle, C.; Nelson, A. J.; Chea, M.; Li, S.; Youngblood, K.; Suratwala, T. I., Enhanced Delamination of Ultrathin Free-Standing Polymer Films via Self-Limiting Surface Modification. *Langmuir* **2014,** *30*, 5126-5132.

(30) Kook, S.-Y.; Dauskardt, R. H., Moisture-Assisted Subcritical Debondingn of a Polymer/Metal Interface. *J. Appl. Phys.* **2002,** *91*, 1293-1303.

(31) Sharratt, B. M.; Wang, L. C.; Dauskardt, R. H., Anomalous Debonding Behavior of a Polymer/Inorganic Interface. *Acta Mater.* **2007,** *55*, 3601-3609.

(32) Maebayashi, M.; Matsuoka, T.; Koda, S.; Hashitani, R.; Nishio, T.; Kimura, S., Study on Polystyrene Thin Film on Glass Substrate by Scanning Acoustic Microscope. *Polymer* **2004,** *45*, 7563-7569.

(33) Rosario, R.; Gust, D.; Hayes, M.; Jahnke, F.; Springer, J.; Garcia, A. A., Photo-Modulated Wettability Changes on Spiropyran-Coated Surfaces. *Langmuir* **2002,** *18*, 8062-8069.

(34) Wagner, N.; Theato, P., Light-Induced Wettability Changes on Polymer Surfaces. *Polymer* **2014,** *55*, 3436-3453.

(35) Athanassiou, A.; Lygeraki, M. I.; Pisignano, D.; Lakiotaki, K.; Varda, M.; Mele, E.; Fotakis, C.; Cingolani, R.; Anastasiadis, S. H., Photocontrolled Variations in the Wetting Capability of Photochromic Polymers Enhanced by Surface Nanostructuring. *Langmuir* **2006,** *22*, 2329-2333.

(36) Yasuda, H.; Sharma, A. K.; Yasuda, T., Effect of Orientation and Mobility of Polymer Molecules at Surfaces on Contact Angle and Its Hysteresis. *J. Polym. Sci.* **1981,** *19*, 1285-1291.

(37) Holmes-Farley, S. R.; Bain, C. D.; Whitesides, G. M., Wetting of Functionalized Polyethylene Film Having Ionizable Organic Acids and Bases at the Polymer-Water Interface: Relations Between Functional Group Polarity, Extent of Ionization, and Contact Angle with Water. *Langmuir* **1988,** *4*, 921-937.

(38) Fripiat, J. J., Silanol Groups and Properties of Silica Surfaces. In *Soluble Silicates*, ACS: 1982; Vol. 194, pp 165-184.

(39) Xu, M.; Liu, D.; Allen, H. C., Ethylenediamine at Air/Liquid and Air/Silica Interfaces: Protonation Versus Hydrogen Bonding Investigated by Sum Frequency Generation Spectroscopy. *Environ. Sci. Technol.* **2006,** *40*, 1566-1572.

(40) Tsyganenko, A. A.; Storozheva, E. N.; Manoilova, O. V.; Lesage, T.; Daturi, M.; Lavalley, J.-C., Brønsted Acidity of Silica Silanol Groups Induced by Adsorption of Acids. *Catal. Lett.* **2000,** *70*, 159-163.

(41) Brown, M. A.; Arrigoni, M.; Héroguel, F.; Redondo, A. B.; Giordano, L.; Bokhoven, J. A. v.; Pacchioni, G., pH Dependent Electronic and Geometric Structures at the Water−Silica Nanoparticle Interface. *J. Phys. Chem. C* **2014,** *118*, 29007−29016.

(42) Lowe, B. M.; Skylaris, C.-K.; Green, N. G., Acid-Base Dissociation Mechanisms and Energetics at the Silica–Water Interface: An Activationless Process. *J. Coll. Int. Sci.* **2015,** *451*, 231-244.

(43) Rosenholm, J. M.; Czuryszkiewicz, T.; Kleitz, F.; Rosenholm, J. B.; Linden, M., On the Nature of the Brønsted Acidic Groups on Native and Functionalized Mesoporous Siliceous SBA-15 as Studied by Benzylamine Adsorption from Solution. *Langmuir* **2007,** *23*, 4315-4323.

(44) Mallo, N.; Foley, E. D.; Iranmanesh, H.; Kennedy, A. D. W.; Luis, E. T.; Ho, J.; Harper, J. B.; Beves, J. E., Structure–Function Relationships of Donor–Acceptor Stenhouse Adduct Photochromic Switches. *Chem. Sci.* **2018,** *9*, 8242-8252.

Chapter 5: Heterogeneous Kinetics of Photoinduced Cross-Linking of Silica Nanoparticles with Surface-Tethered Anthracenes

5-1 Introduction

Materials that can reconfigure themselves after exposure to an external stimulus have potential applications as sensors and actuators.[1] The external stimulus can be chemical (e.g. a pH change), or physical, such as heat or the application of a magnetic field. Light is a particularly useful stimulus because it does not change the chemical composition, does not require physical contact, and has multiple degrees of freedom (intensity, polarization, and wavelength) that can be used as control parameters. One strategy to make photoresponsive materials is to surround nanoparticles (NPs) with organic molecules that can undergo photochemical reactions, for example [2+2] and [4+4] photodimerizations that create covalent cross-links between NPs [2-10], or photoisomerization reactions that change the surface properties and lead to NP aggregation. [11-18]

Previous experimental work has mostly concentrated on metal or polymer NPs whose surfaces are relatively homogeneous. Less attention has been paid to oxide NPs, but this class of materials is potentially more useful. In particular, SiO_2 can be used as an inert yet porous shell to enclose different types of cores that support a wide variety of functionalities, from plasmonic to magnetic to catalytic.[19-20] A general way to stitch together silica-coated NPs could provide a route to new types of photocontrolled, multifunctional nanomaterials.

In this chapter, we examine the ability of silica NPs decorated at the surface with anthracenes (**AN**s) to undergo photoinduced self-assembly. The anthracene [4+4] photodimerization provides a robust, spectroscopically accessible cross-linking reaction that has been successfully used to assemble gold NPs.[21-22] Our goal is to quantitatively characterize the surface coverage and cross-linking kinetics in order to develop a quantitative kinetic model that takes both intra- and interparticle reactions into account. Analysis of the extracted rate constants allows us to assess how heterogeneity leads to different types of **AN** photochemical reactions that compete with the desired cross-linking reaction. The results in this Letter confirm that surface conjugated **AN**s can be used to cross-link silica NPs, but also highlight heterogeneous behavior that likely results from a diversity of NP surface sites. This heterogeneity may complicate efforts to develop NP systems that can be rapidly reconfigured in a reproducible manner.

5-2 Results and Discussion

The procedure for preparing anthracene (**AN**) functionalized SiO_2 NPs is shown in Scheme 5-1.[23-24] The small diameter (~20 nm) of the NPs allowed the absorption spectrum of the suspension to be measured with a low scattering background (Figure 5-1). The vibronic lineshape of the **AN**-SiO_2 NPs was similar to that of 9-anthracenecarboxylic acid and the unreacted linker, indicating that the proximity of the SiO_2 does not strongly perturb the electronic structure of the aromatic core. The absorption coefficient of the linker was determined to be ε(365 nm) = 6900 $M^{-1}cm^{-1}$, allowing us to estimate the

effective concentration of **AN** in the suspension from the absorption. Since the total mass of SiO_2 NPs in the suspension was also measured, we could calculate that there were 1100 ± 200 **AN** molecules per each NP. Given a NP diameter of 20 nm, this corresponds to a surface coverage of 0.8 ± 0.1 **AN**/nm^2.

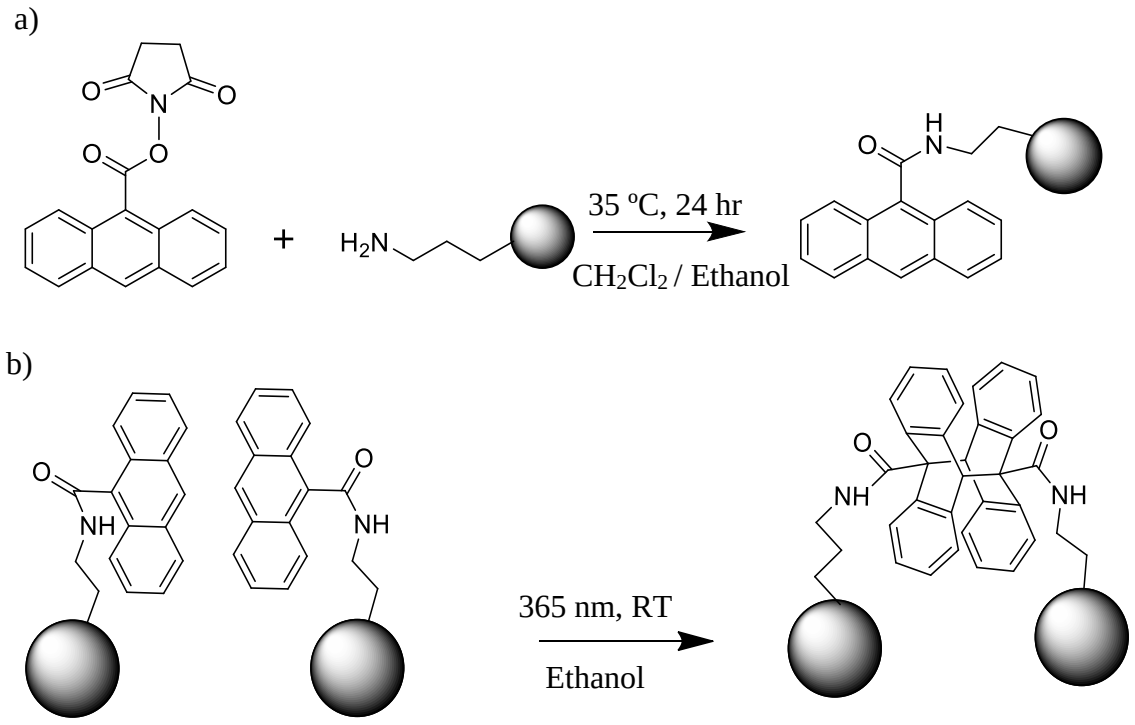

Scheme 5-1: a) Method of attaching AN to surface of propylamine-terminated SiO2 NPs. b) Photodimerization reaction conditions used for crosslinking the AN-SiO2 NPs.

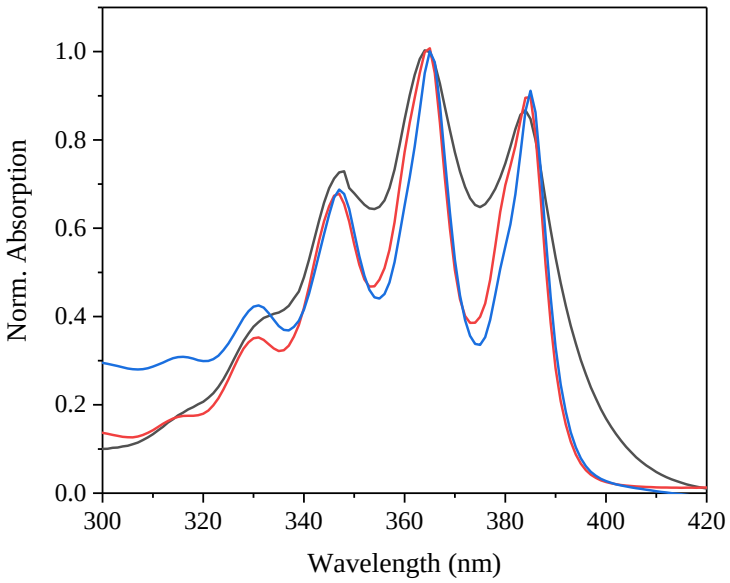

Figure 5-1: Normalized absorption spectra of the **AN** linker (black), 9 anthracene carboxylic acid (red) and the **AN**-SiO2 NPs (blue). The peaks and overall lineshapes of the three different anthracene moieties are similar, suggesting that the SiO_2 does not perturb the electronic structure of the aromatic core of the anthracene.

The presence of the tethered **AN** molecules affected the NP surface charge, as expected. Measurements of zeta potential showed a change from -30 mV for bare SiO_2 NPs to 6.2±0.5 mV for the amine-terminated SiO_2 NPs and then to 11.4 ± 1.24 mV for the SiO_2-AN NPs. This increase in the NP zeta potential is typically seen when the negatively charged siloxy surface groups are replaced by amines and then by tethered anthracenes.[25-26] The loss of surface negative charge is accompanied by a tendency to aggregate.

Dynamic light scattering measurements showed that the average particle size in the suspension was 55± 2 nm for the SiO_2-NH_2 sample and 158±7 nm for the **AN**-SiO_2 sample, suggesting that the NPs were slightly aggregated even before any photochemistry occurred.

Figure 5-2 shows the fluorescence decays for the **AN**-linker in ethanol solution and for the **AN**-SiO_2 NPs. In solution the **AN**-linker exhibited a single exponential decay with a lifetime of 3.2±0.2 ns, identical to that measured for 9-anthracenecarboxylic acid in ethanol (3.1± 0.1 ns). When bound to the NP surface, the **AN** fluorescence decay could only be fit using a biexponential function of the form $Aexp\left[-\frac{t}{\tau_A}\right] + Bexp\left[-\frac{t}{\tau_B}\right]$. The fit, overlaid with the data in Figure 5-2, yields τ_A = 1.2 ns and τ_B=7.1 ns, with the amplitude ratio A/B = 4.1. Note that this decay has both shorter and longer components than observed for the linker in solution. There is no change in the fluorescence spectrum over the course of this decay (Figure 5-2) so it must be attributed to surface-bound **AN** molecules that experience different nonradiative decay rates, presumably due to different local environments. This effect of the SiO_2 surface on the fluorescence decay has been observed for other molecules and has been taken as evidence for the heterogeneity of the SiO_2 surface.[27-29]

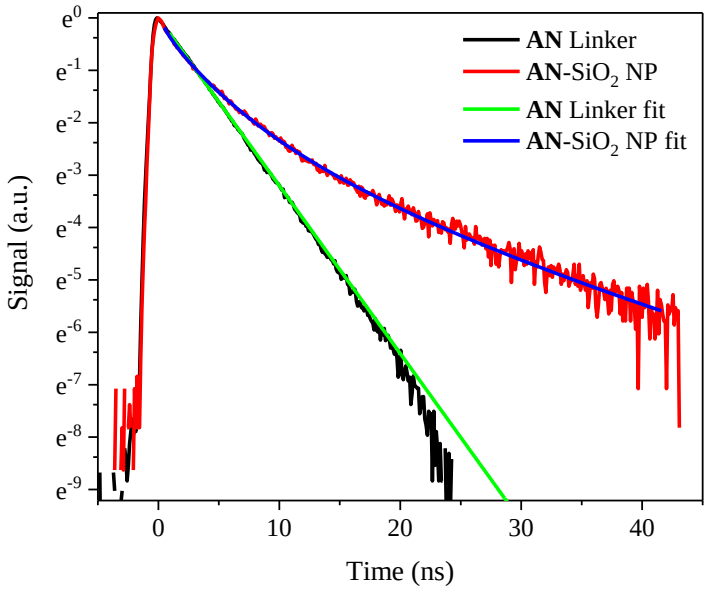

Figure 5-2: Time-resolved fluorescence measurements of the **AN** linker (black) and the **AN**-SiO_2 NPs (red) in ethanol. The **AN** linker decay can be fit with a single exponential with a lifetime of 3.2±0.2 ns (green) but the **AN**-SiO_2 decay must be fit with a biexponential decay with lifetimes of 1.2 ns and 7.1 ns.

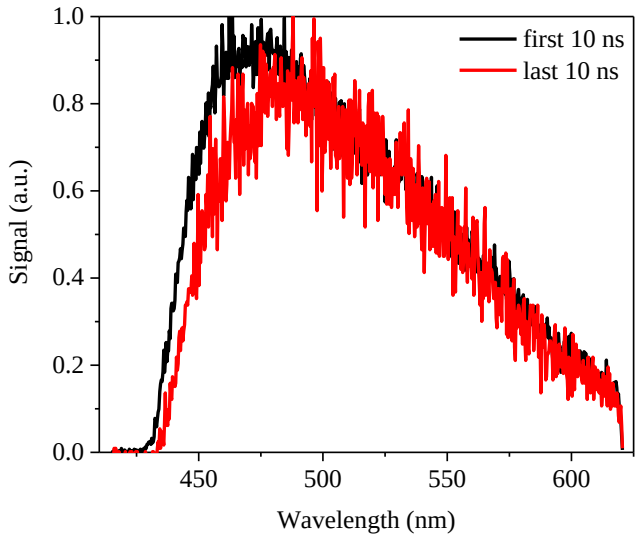

Figure 5-3: Time-resolved fluorescence spectrum integrated over the first 0-10 ns of emission (black) and 10-20 ns (red) for the **AN**-SiO_2 NPs in ethanol. There is a slight red shift for the later emission, but the overall shape of the emission remains the same during the entire decay, showing that it comes from the same **AN** species on the surface.

Given the spectroscopic evidence for different **AN** environments on the NP surface, it was important to determine whether this heterogeneity is also reflected in the cross-linking kinetics. When a suspension of NPs was exposed to 365 nm UV light, the particles agglomerated and the larger masses slowly fell out of suspension, as shown in Figure 5-4a. The resulting suspension can be deposited on a glass slide, dried, and examined using SEM (Figures 5-4b and 5-4c). Before UV irradiation, the NPs spread evenly across the glass surface. After UV irradiation, large clumps of NPs were visible, the result of NPs

becoming attached together in solution as they collide and undergo cross-linking due to intermolecular photochemical reactions.

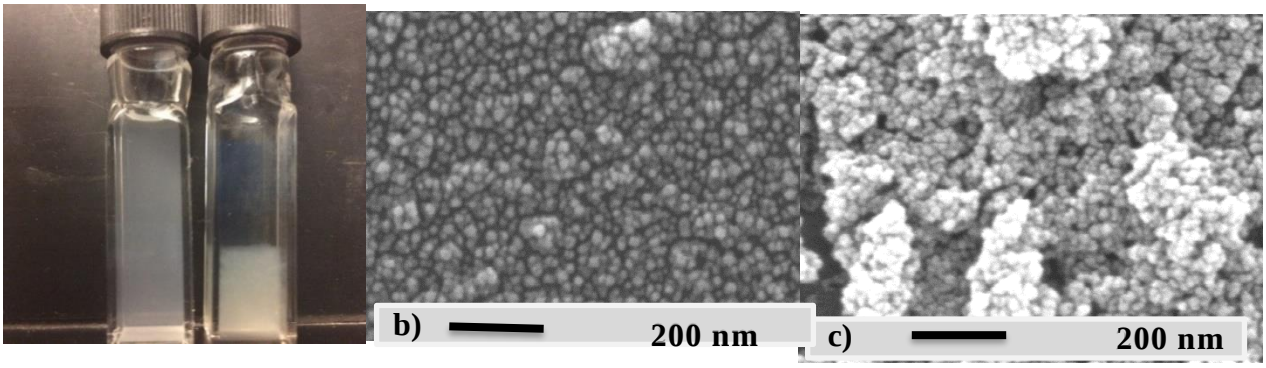

Figure 5-4: **a)** Cuvette containing an ethanol suspension of **AN**-SiO_2 NPs before (left) and after (right) 3 hours of 365 nm irradiation that causes the NPs to agglomerate and fall to the bottom of the cuvette. **b)** Scanning electron microscopy (SEM) image showing a layer of NPs before 365 nm exposure. **c)** SEM image showing the formation of large NP clusters after 365 nm exposure.

In principle, the progress of the cross-linking reaction can be followed by monitoring the disappearance of the **AN** absorption, since the loss of conjugation in the photodimer shifts its absorbance into the UV region. But to extract accurate rate information, it is important to use samples that are optically thin. Highly absorbing samples suffer from nonuniform illumination due to light attenuation, and this effect evolves as the absorbance falls during the course of the reaction. For our measurements,

we made sure the peak absorbance was less than 0.15 in order to minimize such inner filter effects. Before every absorption measurement, the sample was vigorously stirred to make sure there was a homogeneous distribution of NPs in the sample area.

In Figure 5-5, we show an example of the decay of a sample with an initial **AN** concentration N_0= 0.138 mM. After four hours of exposure to 365 nm, the **AN** absorbance has completely vanished. We can plot the absorbance (measured for the largest peak at 381 nm) versus time, and these normalized data are shown in Figure 5-6 for two different **AN** initial concentrations, N_0 = 0.138 mM and N_0 =0.012 mM. The NP decays are non-exponential, with a rapid initial decline followed by a slower component. The rate of absorption loss is concentration dependent, as expected since the cross-linking is a bimolecular reaction that proceeds more rapidly at higher **AN** (NP) concentrations.

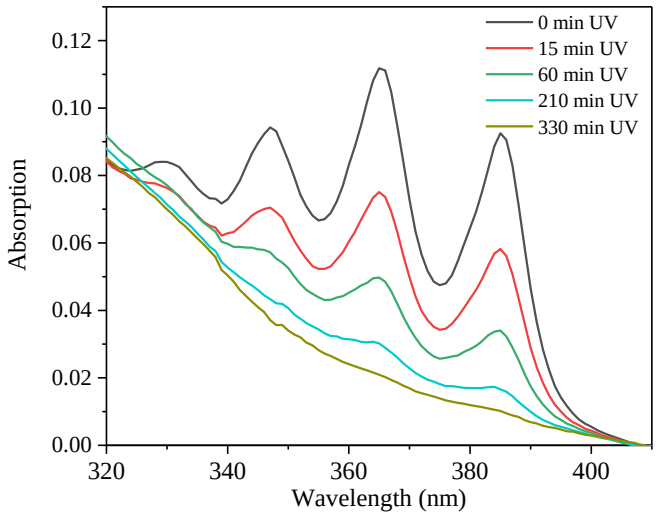

Figure 5-5: Decrease of the absorption of **AN**-SiO_2 NPs for various 365 nm exposure times. The initial **AN** concentration was N_0 = 0.138 mM.

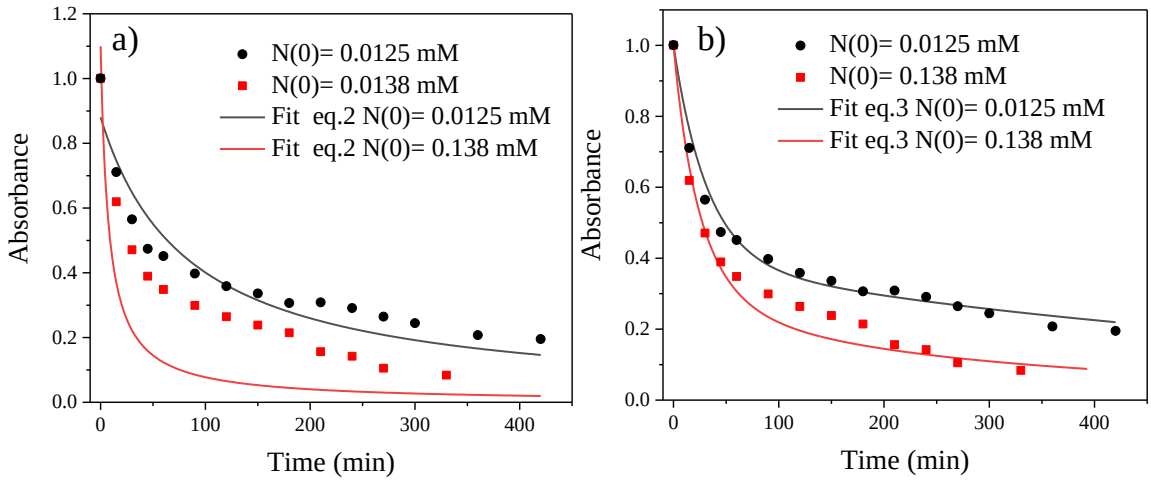

Figure 5-6: a) The time-dependent **AN**-SiO_2 NP absorption decays from Figure 4b (N_0 =0.0125 mM and N_0=0.138 mM) overlaid with fits derived using Equations (1) and (2) in the text that assume a single unimolecular decay channel with rate k_1. **b)** The time-dependent absorption decays from Figure 4b overlaid with fits derived using Equations (3) and (4) in the text that assume two different unimolecular decay channels with rates k_{1A} and k_{1B}.

In order to model the kinetics of the **AN** disappearance, we consider two processes. We take N_{NP} and N to be the concentrations of the NPs and **AN**, respectively. If we take β to be the average number of **AN** molecules per NP, we have $N=\beta N_{NP}$. We assume that the

AN molecules react as the result of interparticle NP collisions at a rate k_{coll}, leading to a second-order process. Furthermore, we assume that the surface-bound **AN** is also subject to a first-order intraparticle reaction with rate k_1. These assumptions lead to the rate equation

$$\frac{dN}{dt} = -k_1 N - k_{coll} N_{NP}^2 = -k_1 N - k_2 N^2 \qquad (1)$$

where $k_2 = \frac{k_{coll}}{\beta^2}$. Equation (1) can be solved analytically to give

$$N(t) = \frac{N_0 e^{-k_1 t}}{1 + N_0 \frac{k_2}{k_1}\left(1 - e^{-k_1 t}\right)} \qquad (2)$$

Note that the N(t) decay depends on the initial concentration N(0) due to the second order term in Equation (1). We can fit the N_0 = 0.0125 mM data in Figure 5-6a using Equation (2). Then, using the values $k_1 = 6.07\times10^7$ min^{-1} and k_2 = 956 min^{-1} obtained from this fitting, we can plot the predicted N(t) curve for N_0 = 0.138 mM. Both the low concentration fit and its high concentration prediction are overlaid with the data in Figure 5-6a. The large discrepancy between the experimental and predicted curves for N_0 = 0.138 mM shows that a single component model cannot be used to describe the data. If we drop the k_1 term and consider only the second-order k_2 term, the discrepancy becomes even larger.

To achieve agreement with experiment, the theory must take into account the fluorescence decay data that suggests there are at least two different types of **AN** bound to

the NP surface, which we denote *A* and *B*. If we assume that these populations are subject to different unimolecular decay rates k_{1A} and k_{1B}, we can write a pair of coupled rate equations:

$$\frac{dN_A}{dt} = -k_{1A}N_A - k_2N_A(N_A + N_B) \quad (3a)$$

$$\frac{dN_B}{dt} = -k_{1B}N_B - k_2N_B(N_A + N_B) \quad (3b)$$

Here we assume that type *A* and *B* **AN** molecules are equally likely to participate in the interparticle dimerization reaction. Also note that k_{1A} and k_{1B} take all intraparticle reactions into account, including dimerization of neighboring **AN**s on a single NP. This is justified by the assumption that the surface-tethered **AN**s cannot diffuse, which leads to first-order kinetics even though this is technically a bimolecular reaction. At time t=0, and given a total initial concentration N_0, we define f_A and f_B to be the initial fractions of A and B molecules, respectively.

$$N_A(0) = f_A N_0 \quad (4a)$$

$$N_B(0) = f_B N_0 \quad (4b)$$

$$f_A + f_B = 1 \quad (4c)$$

The coupled rate equations (3) can be solved numerically using a MATLAB computer program. Figure 5-6b shows the solutions for N_0 = 0.0125 mM and N_0 = 0.138 mM, with f_A = 0.6, f_B = 0.4, k_{1A} = 0.03 min^{-1}, k_{1B} = 0.001 min^{-1}, and k_2 = 100 M^{-1}min^{-1}. These

parameters do a reasonable job of reproducing the experimental decays in Figure 5-6b. The f_A/f_B ratio is 1.5, as compared to A/B=4.1 for the fluorescence decay components, so the different decomposition rates do not exactly correlate with the different fluorescence decay rates. However, it is physically reasonable to associate the more rapid fluorescence decay with a more rapid intraparticle decomposition rate, considering that specific surface interactions must give rise to both phenomena.

Our analysis suggests that a significant fraction of **AN** molecules are lost due to first-order decomposition reactions occurring on the SiO_2 surface. One obvious candidate is photodimerization of two neighboring **AN** molecules on the same particle, although the average distance between **AN** molecules (~1 nm) is substantially larger than the 0.4 nm distance required for this reaction.[30] But there is also evidence that SiO_2 can accelerate the unimolecular photo-decomposition of polycyclic aromatic hydrocarbons and **AN** in particular.[31-33] Unfortunately, there does not seem to be a well-established mechanism for the **AN** decomposition reaction on silica. Surface-mediated reactions with H_2O or O_2 are obvious candidates. From the absorption spectrum of concentrated samples after irradiation, we could identify features associated with the expected products of **AN** oxidation[34] (Figure 5-7). We suspected that the rapid loss of **AN** might be due to an oxidation reaction with O_2 molecules in the liquid but degassing the suspension resulted in an even more rapid loss of **AN** (Figure 5-8). Photoinduced aggregation was also not observed in degassed samples, suggesting that intraparticle decay processes outcompete the dimerization reaction in the absence of O_2. The ability of O_2 to suppress intraparticle

AN decomposition suggests that the **AN** triplet state may play a role in this reaction. The triplet state, which is known to undergo electron transfer reactions[35-36], has not been considered previously as a culprit in the decomposition of **AN** on SiO_2.

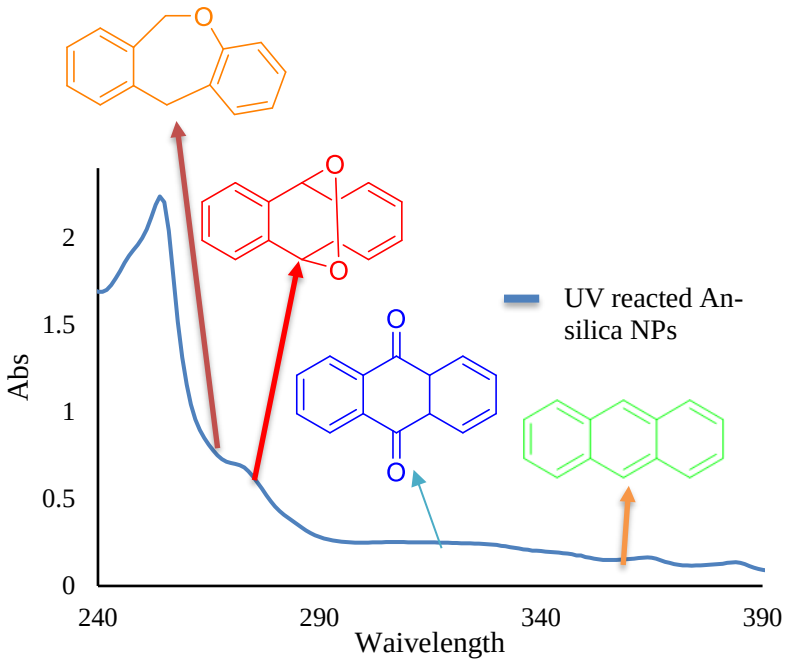

Figure 5-7: Absorption spectrum of **AN**-SiO_2 NPs after complete UV reaction. The surviving absorption features can be correlated with various oxidative products observed in Fidder et al., *J. Phys. Chem. A* **2009,** *113*, 6289–6296.

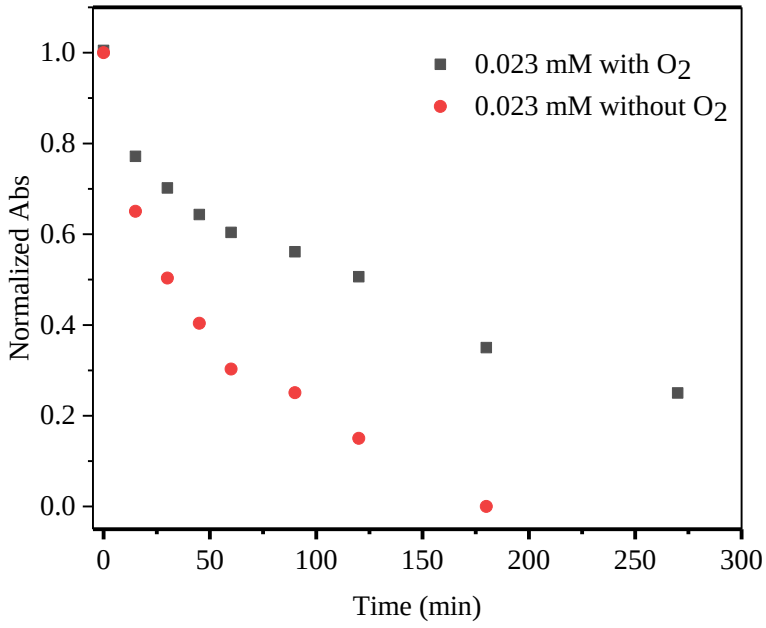

Figure 5-8: Time-dependent decay of **AN** absorption peak at 365 nm for **AN**-SiO_2 NP suspension with calculated **AN** concentration of 0.023 mM. The decay of the non-degassed suspension (black squares) is slower than that after degassing and removal of O_2. The sample was degassed by bubbling Ar gas for several minutes and then sealing the cuvette.

Finally, we analyzed the kinetics of the interparticle photodimerization cross-linking reaction. Given the rate $k_2 = 100\ M^{-1}min^{-1}$, and β=1100, we obtain the experimental $k_{coll} = 2\times10^7\ M^{-1}s^{-1}$. k_{coll} can also be calculated using the Smoluchowski bimolecular reaction rate given by[37]

$$k_{coll} = 4\pi D R_{react} \qquad (5)$$

where D is the diffusion constant of the NP and R_{react} is the reaction radius. The Stokes-Einstein equation for D is

$$D = \frac{k_B T}{6\pi\eta R} \tag{6}$$

where k_B is the Boltzmann constant, T is the temperature, η is the viscosity, and R is the particle radius. If we assume the reaction and particle radii are identical, $R = R_{\text{react}}$ and we have

$$k_{react} = \frac{2}{3}\frac{k_B T}{\eta} \tag{7}$$

Plugging in T = 298 K and η = 0.89 centipoise, we calculate k_{coll}=3.1×10^{-12} cm^3/s = 1.8×10^9 M^{-1}s^{-1}. This value is about 100× larger than the experimental k_{coll}. The lower experimental rate is not surprising, since the cross-linking reaction requires a photoexcited **AN** molecule to be correctly oriented with respect to an **AN** molecule on the other NP during the collision. This analysis shows that the NP photocross-linking reaction is far from diffusion-limited, consistent with previous results on photoinduced noncovalent aggregation.[11]

From our analysis of the NP cross-linking kinetics, it is clear that the photoinduced assembly of silica NPs provides several opportunities for improvement. First, there exist at least two different reaction pathways on the NP surface that compete with the desired interparticle dimerization. This is not too surprising: the important role of SiO_2 surface

heterogeneity has been recognized in a variety of chemical processes.[38-40] An improved knowledge of the SiO_2 surface and **AN** binding sites is probably necessary to identify chemical modifications that can prevent these side reactions. Alternatively, a more robust photochemical cross-linking agent might avoid these side reactions altogether. Second, the efficiency of the interparticle reaction after collision is estimated to be on the order of 1%. Improving interparticle reactivity, for example by lengthening the **AN** tethering chain, might improve the yield of this reaction. Elimination of the non-productive intraparticle reactions and optimization of the desired interparticle reaction should increase the photoinduced assembly rate by at least one order of magnitude.

5-3 Conclusion

From a practical standpoint, the results of this chapter demonstrate that photodimerization of surface **AN**s can be used to cross-link SiO_2 NPs. However, this reaction exhibits fairly complicated kinetic behavior, with at least two different intraparticle decomposition pathways that compete with the interparticle cross-linking photodimerization. Although SiO_2 is often considered to be chemically inert, its surface heterogeneity can provide environments that enhance the photodecomposition of surface-bound **AN**. In order to utilize the SiO_2 surface as a robust platform for organic photochemistry that leads to photoresponsive nanomaterials, a clearer understanding of how its heterogeneous nature affects photochemical reactions will be necessary. We hope that the kinetic model developed here will prove useful in analyzing future experiments.

5-4 References

(1) Balazs, A. C.; Aizenberg, J., Reconfigurable Soft Matter. *Soft Matter* **2014,** *10*, 1244-1245.

(2) Cardenas-Daw, C.; Kroeger, A.; Schaertl, W.; Froimowicz, P.; Landfester, K., Reversible Photocycloadditions, a Powerful Tool for Tailoring (Nano)Materials. *Macromol. Chem. Phys.* **2012,** *213*, 144-156.

(3) Yuan, X.; Fischer, K.; Schartl, W., Reversible Cluster Formation of Colloidal Nanospheres by Interparticle Photodimerization. *Adv. Func. Mater.* **2004,** *14*, 457-463.

(4) Yuan, X.; Fischer, K.; Schartl, W., Photocleavable Microcapsules Built from Photoreactive Nanospheres. *Langmuir* **2005,** *21*, 9374-9380.

(5) Yuan, X.; Schnell, M.; Muth, S.; Schartl, W., Cluster Formation and Rheology of Photoreactive Nanoparticle Dispersions. *Langmuir* **2008,** *24*, 5299-5305.

(6) Zhou, J.; Sedev, R.; Beattie, D.; Ralston, J., Light-Induced Aggregation of Colloidal Gold Nanoparticles Capped by Thymine Derivatives. *Langmuir* **2008,** *24*, 4506-4511.

(7) Pocoví-Martínez, S.; Parreno-Romero, M.; Agouram, S.; Perez-Prieto, J., Controlled UV-C Light-Induced Fusion of Thiol-Passivated Gold Nanoparticles. *Langmuir* **2011,** *27*, 5234–5241.

(8) Chung, J. W.; Lee, K.; Neikirk, C.; Nelson, C. M.; Priestley, R. D., Photoresponsive Coumarin-Stabilized Polymeric Nanoparticles as a Detectable Drug Carrier. *Small* **2012,** *8*, 1693-1700.

(9) Roth, P. J.; Theato, P., Covalent Attachment of Gold Nanoparticles to Surfaces and Polymeric Substrates Using UV Light. *Macromol. Chem. Phys.* **2012,** *213*, 2550−2556.

(10) Chen, Y.; Wang, Z.; Hea, Y.; Yoon, Y. J.; Jung, J.; Zhang, G.; Lin, Z., Light-Enabled Reversible Self-Assembly and Tunable Optical Properties of Stable Hairy Nanoparticles. *Proc. Nat. Acad. Sci.* **2018,** *115*, E1391-E1400.

(11) Zhou, C.; Zhao, Y.; Jao, T.-C.; Wu, C.; Winnik, M. A., Effect of Concentration on the Photoinduced Aggregation of Polymer Nanoparticles. *J. Phys. Chem. B* **2002,** *106*, 9514-9521.

(12) Bell, N. S.; Piech, M., Photophysical Effects between Spirobenzopyran-Methylmethacrylate-Functionalized Colloidal Particles. *Langmuir* **2006,** *22*, 1420-1427.

(13) Klajn, R.; Bishop, K. J. M.; Grzybowski, B. A., Light-Controlled Self-Assembly of Reversible and Irreversible Nanoparticle Suprastructures. *Proc. Nat. Acad. Sci.* **2007,** *104*, 10305–10309.

(14) Kimoto, A.; Iwasaki, K.; Abe, J., Formation of Photoresponsive Gold Nanoparticle Networks via Click Chemistry. *Photochem. Photobiol. Sci.* **2010,** *9*, 152–156.

(15) Kohntopp, A.; Dabrowski, A.; Malicki, M.; Temps, F., Photoisomerisation and Ligand-Controlled Reversible Aggregation of Azobenzene Functionalised Gold Nanoparticles. *Chem. Commun.* **2014,** *50*, 10105--10107.

(16) Shiraishi, Y.; Shirakawa, E.; Tanaka, K.; Sakamoto, H.; Ichikawa, S.; Hirai, T., Spiropyran-Modified Gold Nanoparticles: Reversible Size Control of Aggregates by UV and Visible Light Irradiations. *Appl. Mater. Interfaces* **2014,** *6*, 7554−7562.

(17) Lan, Y.; Wu, Y.; Karas, A.; Scherman, O. A., Photoresponsive Hybrid Raspberry-Like Colloids Based on Cucurbit[8]uril Host–Guest Interactions. *Angew. Chem. Int. Ed.* **2014,** *53*, 2166 –2169.

(18) Zhao, H.; Sen, S.; Udayabhaskararao, T.; Sawczyk, M.; Kučanda, K.; Manna, D.; Kundu, P. K.; Lee, J.-W.; Král, P.; Klajn, R., Reversible Trapping and Reaction Acceleration within Dynamically Self-Assembling Nanoflasks. *Nat. Nanotech.* **2016,** *11*, 82-88.

(19) Andres; Guerrero-Martınez; Perez-Juste, J.; Liz-Marzan, L. M., Recent Progress on Silica Coating of Nanoparticles and Related Nanomaterials. *Adv. Mater.* **2010,** *22*, 1182–1195.

(20) Wang, X.; Feng, J.; Bai, Y.; Zhang, Q.; Yin, Y., Synthesis, Properties, and Applications of Hollow Micro-/Nanostructures. *Chem. Rev.* **2016,** *116*, 10983−11060.

(21) Smith, A. R.; Watson, D. F., Photochemically Triggered Assembly of Composite Nanomaterials through the Photodimerization of Adsorbed Anthracene Derivatives. *Chem. Mater.* **2010,** *22,* 294–304.

(22) Zhou, Q.; Zhang, B.; Han, D.; Chen, R.; Qiu, F.; Wu, J.; Jiang, H., Photo-Responsive Reversible Assembly of Gold Nanoparticles Coated with Pillar[5]arenes. *Chem. Commun.* **2015,** *51*, 3124--3126.

(23) Mazur, M.; Blanchard, G. J., Oxidative Transformations of Surface-Bound Perylene. *Langmuir* **2005,** *21*, 1441-1447.

(24) Nakamura, M.; Shono, M.; Ishimura, K., Synthesis, Characterization, and Biological Applications of Multifluorescent Silica Nanoparticles. *Anal. Chem.* **2007,** *70*, 6507-6514.

(25) Bagwe, R. P.; Hilliard, L. R.; Tan, W., Surface Modification of Silica Nanoparticles to Reduce Aggregation and Nonspecific Binding. *Langmuir* **2006,** *22*, 4357-4362.

(26) Graf, C.; Gao, Q.; Schütz, I.; Noufele, C. N.; Ruan, W.; Posselt, U.; Korotianskiy, E.; Nordmeyer, D.; Rancan, F.; Hadam, S.; Vogt, A.; Lademann, J. r.; Haucke, V.; Rühl, E., Surface Functionalization of Silica Nanoparticles Supports Colloidal Stability in Physiological Media and Facilitates Internalization in Cells. *Langmuir* **2012,** *28*, 7598−7613.

(27) Liu, Y. S.; Ware, W. R., Photophysics of Polycyclic Aromatic Hydrocarbons Adsorbed on Silica Gel Surfaces. 1. Fluorescence Lifetime Distribution Analysis: An Ill-Conditioned Problem. *J. Phys. Chem.* **1993,** *97*, 5980-5986.

(28) Wang, H.; Harris, J. M., Origins of Bound-Probe Fluorescence Decay Heterogeneity in the Distribution of Binding Sites on Silica Surfaces. *J. Phys. Chem.* **1995,** *99*, 16999-17009.

(29) Roy, D.; Piontek, S.; Walker, R. A., Surface Induced Changes in Coumarin Solvation and Photochemistry at Polar Solid/Liquid Interfaces. **2011,** *13*, 14758–14766.

(30) Ramamurthy, V.; Venkatesan, K., Photochemical Reactions of Organic Crystals. *Chem. Rev.* **1987,** *87*, 433-481.

(31) Zingg, S. P.; Sigman, M. E., Influence of an SiO_2/Cyclohexane Interface on the Photochemistry of Anthracene. *Photochem. Photobio.* **1993,** *57*, 453-459.

(32) Dabestani, R.; Ellis, K. J.; Sigman, M. E., Photodecomposition of Anthracene on Dry Surfaces: Products and Mechanism. *J. Photochem. Photobiol. A* **1995,** *86*, 231-239.

(33) Mazur, M.; Blanchard, G. J., Photochemical and Electrochemical Oxidation Reactions of Surface-Bound Polycyclic Aromatic Hydrocarbons. *J. Phys. Chem. B* **2004,** *108*, 1038-1045.

(34) Fidder, H.; Lauer, A.; Freyer, W.; Koeppe, B.; Heyne, K., Photochemistry of Anthracene-9,10-endoperoxide. *J. Phys. Chem. A* **2009,** *113*, 6289–6296.

(35) Hsiao, J.-S.; Webber, S. E., Triplet-State Electron Transfer from Anthracene and Pyrene Covalently Bound to Polyelectrolytes In Aqueous Solution. *J. Phys. Chem.* **1992,** *96*, 2892-2901.

(36) Worrall, D. R.; Williams, S. L.; Wilkinson, F., Electron Transfer Reactions of Anthracene Adsorbed on Silica Gel. *J. Phys. Chem. B* **1997,** *101*, 4709-4716.

(37) Mun, E. A.; Hannell, C.; Rogers, S. E.; Hole, P.; Williams, A. C.; Khutoryanskiy, V. V., On the Role of Specific Interactions in the Diffusion of Nanoparticles in Aqueous Polymer Solutions. *Langmuir* **2014,** *30*, 308-317.

(38) Morrow, B. A.; McFarlan, A. J., Surface Vibrational Modes of Silanol Groups on Silica. *J. Phys. Chem.* **1992,** *96*, 1395-1400.

(39) Kholin, Y.; Zaitsev, V., Quantitative Physicochemical Analysis of Equilibria on Chemically Modified Silica Surfaces. *Pure Appl. Chem.* **2008,** *80*, 1561–1592.

(40) Schrader, A. M.; Monroe, J. I.; Sheil, R.; Dobbs, H. A.; Keller, T. J.; Li, Y.; Jain, S.; Shell, M. S.; Israelachvili, J. N.; Han, S., Surface Chemical Heterogeneity Modulates Silica Hydration. *Proc. Nat. Acad. Sci.* **2018,** *115*, 2890–2895.

Chapter 6 Conclusion and future work

This dissertation studied light-responsive adhesion by embedding photochromic molecules in polymers and photo-induced dimerization to cross link silica nanoparticles.

6-1 Conclusions

The results in the first study demonstrated that photoswitching a molecule embedded in a polymer film can affect properties of the polymer at the interface, including surface adhesion. The adhesion changes were measured by delamination in water and lap shear adhesion tests. Molecular structure of the photochrome and its concentration dictate the types and strength of the adhesion. Two minutes of UV irradiation to spiropyran embedded polystyrene showed the most dramatic results, increasing the lap shear strength by a factor of 7 and suppressing the delamination rate by at least 2 orders of magnitude. We hypothesized that the polymer localization and molecular motion forced the polymer strands to fill the surface voids, and this is the main reason for the adhesion. Our results demonstrated that photochromic annealing created stronger adhesion compared to bulk thermal annealing.

In our second study, the focus was on de-adhesion. We used our previous findings on the adhesion project to engineer photo-induced de-adhesion. For this purpose, newly developed **DASA** photochromic molecule embedded in polystyrene and adhesion measurements illustrated that visible light exposure significantly weakened adhesive bonds. The pull-off adhesion, lap shear, and water delamination tests were used to illustrate

de-adhesion. Calculations showed that after a photochromic reaction, the **DASA** molecular volume is reduced. This phenomenon may disrupt non-covalent interactions between the silanols and amines in photochromic molecules. The photo-induced de-adhesion method can be used as a light-controlled release of encapsulated molecules.

Although these methods are very promising in controlling adhesion and de-adhesion remotely, they also come with some disadvantages that we tried to address in our current and future works. For instance, initial studies showed that spiropyran-polystyrene adhesion to a surface increased significantly after UV irradiation. The main problem with this system was that it was almost irreversible. In the **DASA** project, the results prove a decrease in adhesion strength, but the main problem was that it happened only after many hours of irradiation (up to 10 hours) and this system did not show any reversibility.

Addressing the reversibility, we decided to mix **DASA** and **SP** together using lower concentrations than used in chapters 3 and 4. Using the **DASA-SP** mixture was promising because they react with 2 different wavelengths to increase and decrease adhesion. This potentially could help induce a stronger and faster deadhesion. UV irradiation should be able to increase the adhesion by only reacting with SP, but UV irradiation would not have any interaction with **DASA** at all. On the other hand, both merocyanine and **DASA** react with visible light (532 nm), and from previous experiments, we illustrated that in both cases adhesion decreased. The results of this experiment are illustrated in figures 6-1 and 6-2. Use of a relatively high concentration of photochromic molecules impacted reversibility and irradiation times, which is shown in chapters 3 and 4. It means that the higher the

concentration of photochromes, the harder it is to reverse the photochromic reaction. Because **DASA** and **SP** have synergistic effects on one another, the mixture system needs a lower concentration of each molecule to show the optimum effect and this helps to significantly reduce the irradiation time needed to see the desired effect.

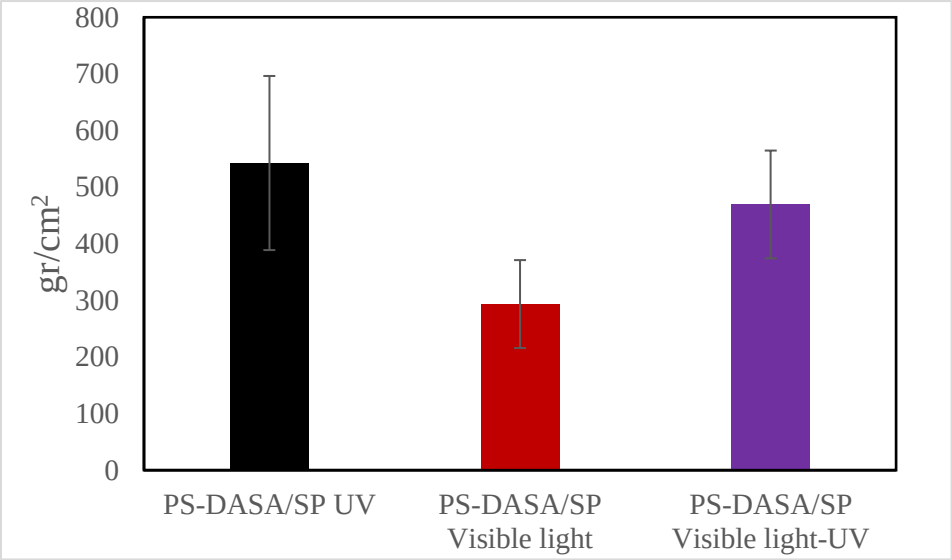

Figure 6-1: Pull-off Adhesion Measurement: UV exposure increased adhesion initially (black); laser (532 nm) irradiation decreased the adhesion (red); UV exposure shows reversibility in adhesion and increased adhesion (purple).

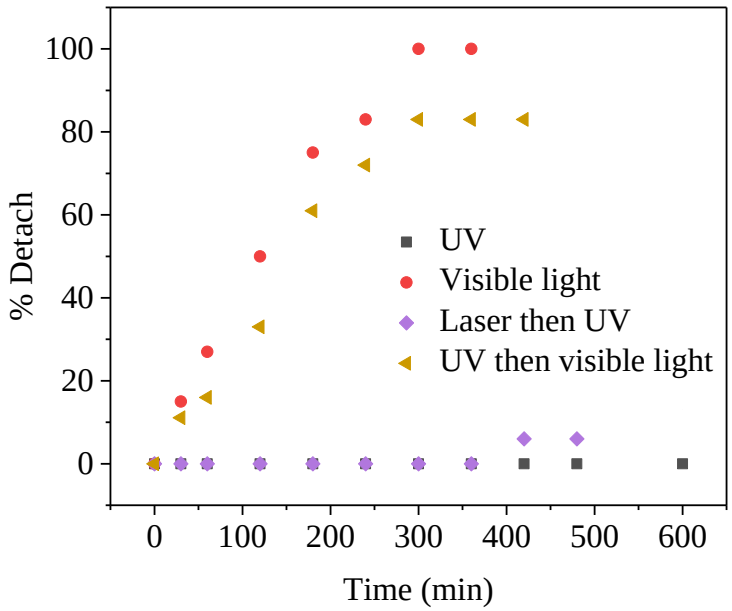

Figure 6-2: Water detachment measurements; UV irradiated (black) showed strong adhesion to substrate; laser (532 nm) irradiation accelerated 100% detachment over 2 hours; laser irradiation followed by UV exposure (purple) illustrated high adhesion and also reversibility of the **DASA-SP** mixture; UV and then laser irradiation showed a decrease in adhesion (brown)

6-2 Effect of polymer on adhesion

6-2-1 Zeonex (ZX)- Cyclic Olefin Polymers (COPs)

An other approach to address the reversibility and long irradiation time was to change to a polymer that has a higher glass-transition temperature (T_g), and hydrophobicity. One hypotheses for the adhesion mechanism was that photochromic reactions induced local softening at the interface and made the polymer physically adhere to the glass. A higher T_g may make this mechanism unsuccessful by showing higher resistance to local softening.

Also, a polymer with higher hydrophobicity may have less adhesion to a polar surface. Using a polymer with higher hydrophobicity would reduce the polymer impact on adhesion and would only allow the adhesion from photochromes and not the polymer itself.

Zeonex (ZX) is a relatively new polymer with low water absorption, good optical transparency in the near UV range, easy device fabrication, high resistance to chemicals including polar solvents (in contrast to other polymers used for lab-on-a-chip applications), and high biological inertness that makes it suitable for biomedical applications. This polymer is found in some applications, such as DNA analysis, blood analysis, microchips, and microfluidics.[1–3]

Zeonex has no UV absorption in the irradiation range for the samples. It also has a much higher T_g (150 ºC) and hydrophobicity than polystyrene. Local heating based on photoswitching may have less effect on this polymer than polystyrene.

The pull-off adhesion test of ZX-**SP** showed a significant increase in adhesion after UV irradiation and a decrease in adhesion after visible light irradiation. The experiments were done for mass fraction of 11%. Water detachment results were also very promising and illustrated a big improvement of detachment. Before any irradiation, the polymer detached within in 15 minutes, while after UV irradiation, zero detachments were observed. ZX-**SP** showed a good reversibility in adhesion. Laser irradiation for short time (1 hour) brought adhesion back to the initial state, and the ZX-**SP** fully detached in 10 minutes.

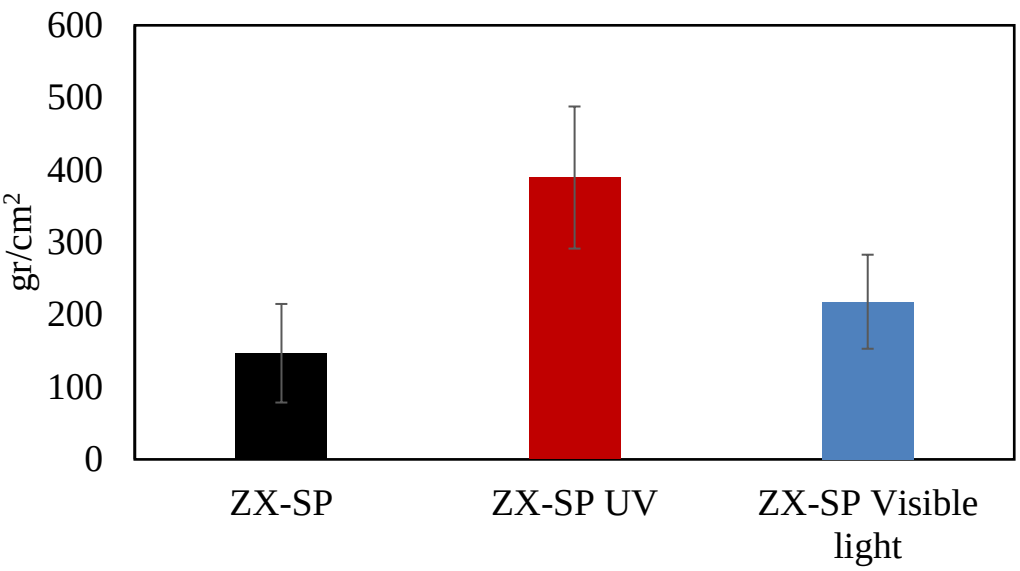

Figure 6-3: Results for pull-off adhesion testing for ZX-**SP**; Initially polymer presented very low adhesion with a cleaned glass substrate (black); UV irradiation significantly increased the adhesion (red); laser irradiation reduced the adhesion and showed reversibility of the adhesion (blue).

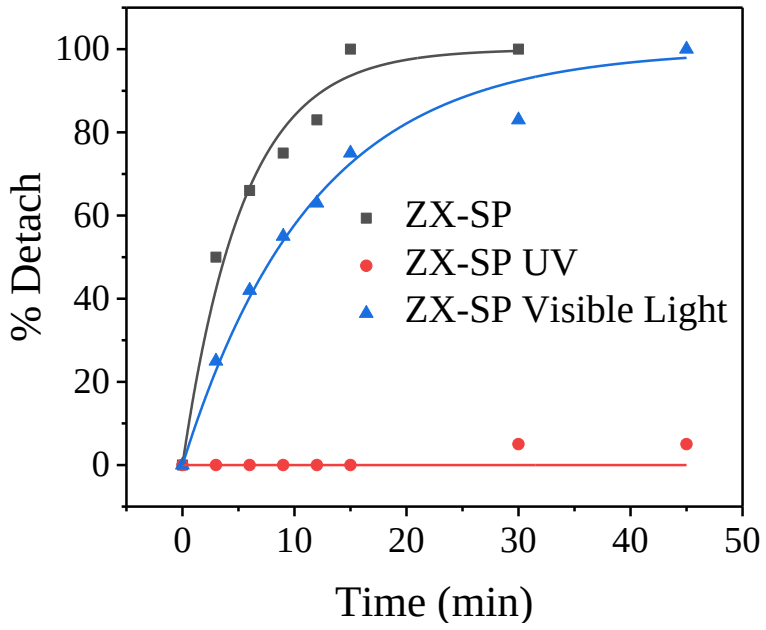

Figure 6-4: Water detachment results for ZX-**SP**. Initially polymer-photochrom showed a very insignificant adhesion to surface (black); UV irradiation significantly increased the adhesion (red); laser irradiation reduced the adhesion to the initial state (blue).

6-3 Effects of silinols on adhesion

6-3-1 Effects of glass types on adhesion

Another issue to address in future work is to confirm our proposed mechanisms. Knowing the actual mechanism will help us to engineer a stronger adhesive with better reversibility. In previous chapters, some mechanisms were proposed, such as polar-polar interactions and physical adhesion. Polar-polar interactions might be the main reason for observed effects, but there was a need to increase the certainty about the mechanisms.

As discussed in the introduction, there are three kinds of glass with various amounts of silianols on the surface. Measurements showed that by increasing the concentration of silanols on the surface, adhesion also increased. Soda-Lime has the lowest silanol concentration and also the minimum amount of adhesion compared to other glass types. Quartz has the highest adhesion of PS-SP with 99% SiO_2 concentration. These results illustrated the direct relation between silanol concentration and polymer adhesion.

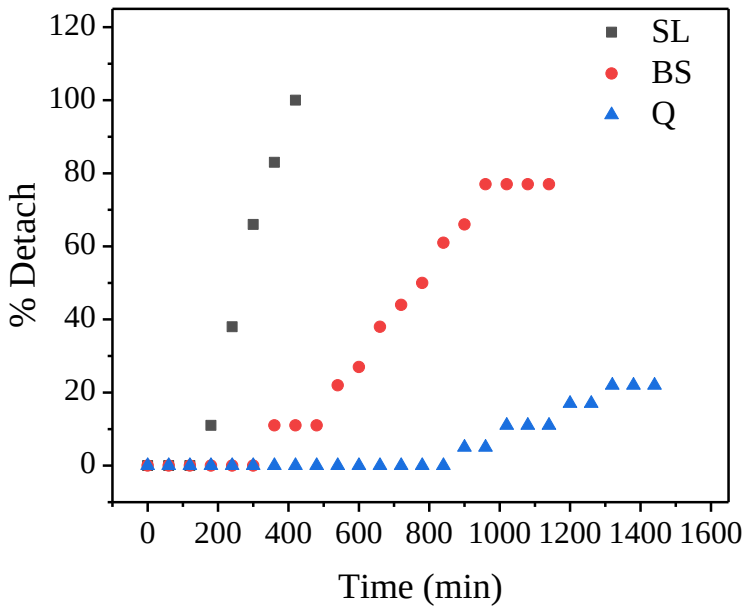

Figure 6-3 PS-DASA (1%) **SP** (13%) was drop cast on 3 different types of glass, including SL (soda-lime), BS (boro-silicate), and Q (quartz). Samples were irradiated by a laser (532 nm) in-situ in stirred water and detachment was monitored over time.

6-3-2 Adhesion on a heated substrate

Chapter 2 discussed how extreme heat (250 ºC) can reduce the concentration of silanols on a glass surface and make it more hydrophobic since heating causes evaporation and condensation of silanol functional groups. Two pieces of Quartz (99% SiO_2) glass substrate were washed with piranha solution and then with DI water and left to dry. One of the glass slides was heated to 250 ºC for 4 hours and then left to cool down to room temperature. Then, both slides were covered with polymer islands drop-cast using PS-**SP/DASA**, put in stirred water, and monitored for detachment over time. As illustrated in figure 6-4, lowering concentration of silanols decreased adhesion of polymer to surface.

This experiment revealed the role of silanols in the adhesion mechanism.

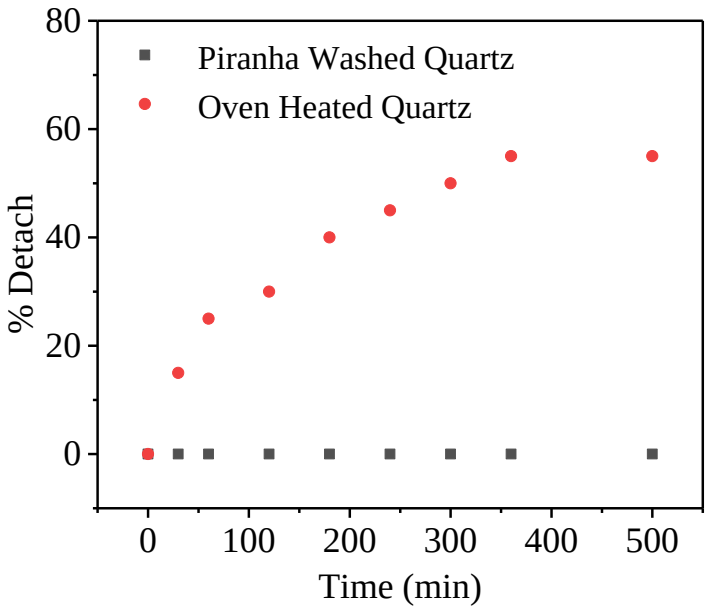

Figure 6-4: Adhesion of **PS-DASA/SP** on piranha-washed quartz (black) and heated quartz (red). Heating the substrate and decreasing the concentration of silanols led to a significant decrease in adhesion.

6-4 Covalent adhesion

Other than non-covalent adhesion, we studied photo-induced covalent adhesion. Photodimerization of **AN** ligands on SiO_2 NPs can be used to covalently attach nanoparticles together. Surprisingly, UV exposure to **AN**-bound NPs showed a complicated kinetic behavior by initiating both the bimolecular and unimolecular reaction simultaneously. Chapter five suggests that surface heterogeneity of SiO_2 provided a favorable environment for **AN** photodecomposition which limited the efficiency of the

cross-linking of the nanoparticles. The role of SiO_2 to accelerate the mechanism for unimolecular pathways is still unclear, and there is need for further study.

For higher efficiencies, we need to address the photo-induced decomposition of **AN** by trying different derivatives of anthracene or novel molecules and also using variety of core-shell nanoparticle systems like gold that has minimum effect on dimerization moieties.

After developing a highly efficient reversible photo dimerization system with a minimum photo induced unimolecular pathways, we will be able to assemble them into complex shapes using external magnetic force or laser trapping. After assembly, ultraviolet light can initiate photochemical reactions that cross-link the nanoparticles together into a desired structure. This structure can then be translated or rotated by a magnetic field. Afterwards, it can be disassembled by breaking the covalent bonds between the nanoparticles. The nanoparticles can then be recycled to form new structures.

References

1. Van Midwoud, P. M., Janse, A., Merema, M. T., Groothuis, G. M. M. & Verpoorte, E. Comparison of biocompatibility and adsorption properties of different plastics for advanced microfluidic cell and tissue culture models. *Anal. Chem.* **84**, 3938–3944 (2012).

2. Bernard, M. *et al.* Biocompatibility assessment of cyclic olefin copolymers: Impact of two additives on cytotoxicity, oxidative stress, inflammatory reactions, and hemocompatibility. *J. Biomed. Mater. Res. - Part A* **105**, 3333–3349 (2017).

3. Yamazaki, M. Industrialization and application development of cyclo-olefin polymer. in *Journal of Molecular Catalysis A: Chemical* vol. 213 81–87 (2004).